素子材料特論
第2授業

Li-ion電池負極(I)

1. Li-ion電池および負極
2. 黒鉛系負極

Bonding Hybridization	Allotropes	Derived and Defective Forms
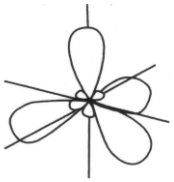 **SP^3**	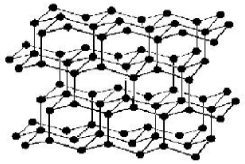 **Cubic diamond**	 Diamond-like Carbon
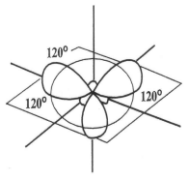 SP^2	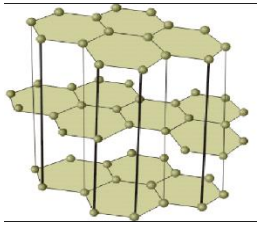 **Hexagonal graphite**	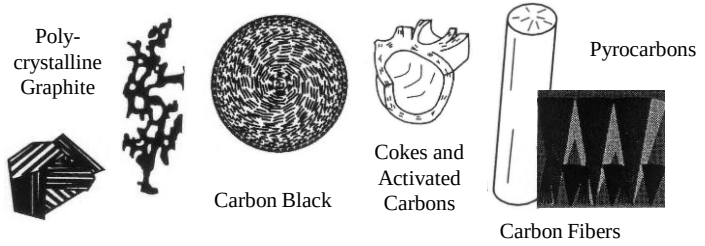 Poly-crystalline Graphite; Carbon Black; Cokes and Activated Carbons; Pyrocarbons; Carbon Fibers
 $SP^{2+\varepsilon}$ rehybridization	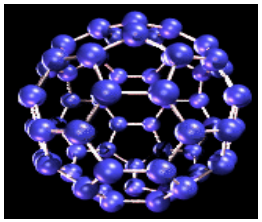 **Fullerene**	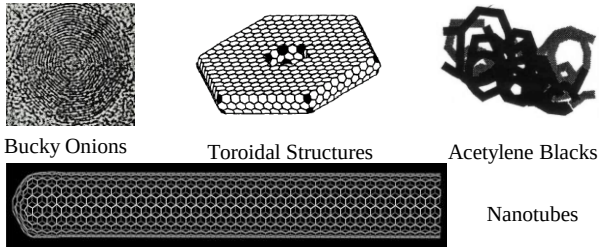 Bucky Onions; Toroidal Structures; Acetylene Blacks; Nanotubes
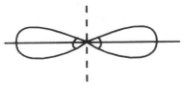 SP^1	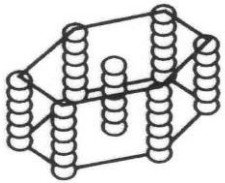 **Carbyne**	Ref.) Bourrat, X. Structure in Carbons and Carbon Artifacts. In: *Sciences of Carbon Materials.* Marsh, H.; Rodriguez-Reinoso, F., Eds., Universidad de Alicante, **2000**. pp1-97.

Carbon Allotropes

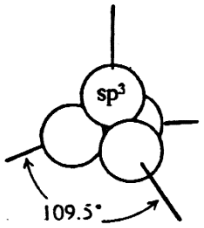

sp³ 混成軌道

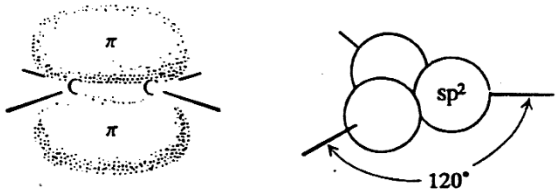

sp² 混成軌道

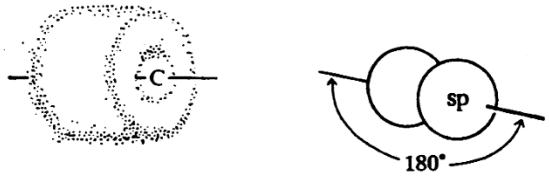

sp 混成軌道

π軌道の概形　　σ軌道を球で表した時の配置

(a)　　(b)

図-1　炭素の混成軌道

表-1　各種炭素－炭素結合の結合解離エネルギーと結合距離[1)]

化合物	結合解離エネルギー (kcal/mol)	結合距離 (Å)
H_3C-C_3H	88	1.53
$H_2C=C_2H$	163	1.34
$HC\equiv CH$	198	1.21

表-2　炭素同素体の種類[3)]

結合の種類	配位数	炭素同素体
sp	2	カルビン（ポリイン, クムレン）
sp^2	3	グラファイト（六方晶, 菱面体晶）
		フラーレン（C_{60}, C_{70}, バッキイチューブなど）
sp^3	4	ダイヤモンド（立方晶, 六方晶, 菱面体晶*）
		ダイヤモンド多形体（6H, bc-8*など）
		ダイヤモンドライクカーボン（DLC）, i-カーボン
イオンまたは	6	単純立方晶*, β-スズ型*
金属的	8	体心立方晶*
	12	面心立方晶*, 六方最密充填*

* 実!

表-4　Ⅳ族 sp^3 立方晶体の性質[6)]

性　質	ダイヤモンド	β-SiC	Si
格子定数（Å）	3.567	4.358	5.430
密度（g/cm^3）	3.515	3.216	2.328
熱膨張率（$\times10^{-6}$/℃）	1.1	4.7	2.6
融点（℃）	4000	2540	1420
バンドギャップ（eV）	5.45	3.0	1.1
キャリア移動度（$cm^2/(V\cdot S)$）			
電　子	2200	400	1500
ホール	1600	50	600
熱伝導率（W/(cm・K)）	20	5	1.5
硬度（kg/mm^2）	10000	3500	1000

Molecular structures of graphite

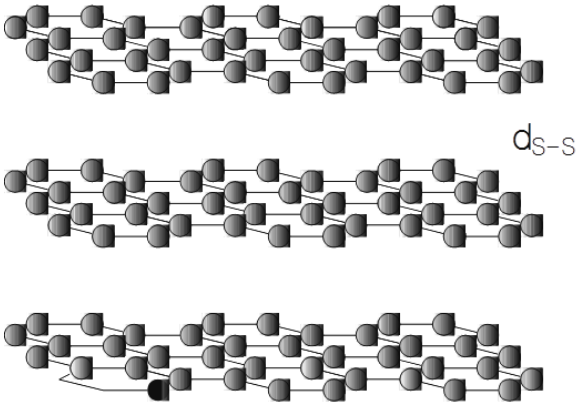

(a) Basic Structure of Graphite

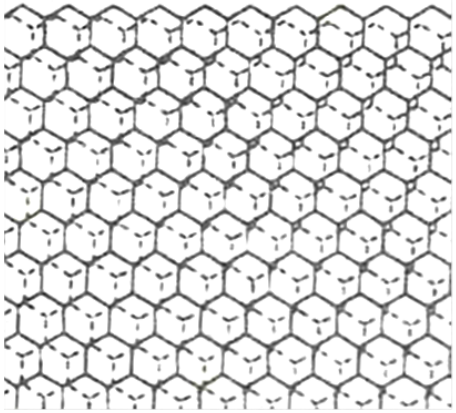

(b) Turbostratic structure (low crystallinity)

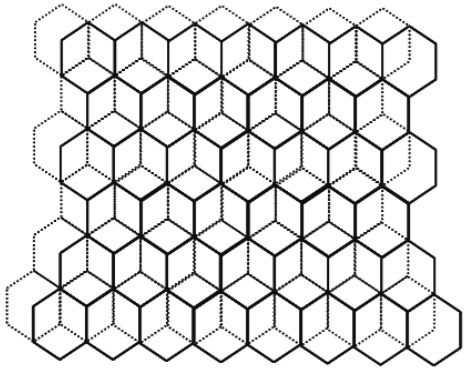

(C) Graphitic structure (high crystallinity)

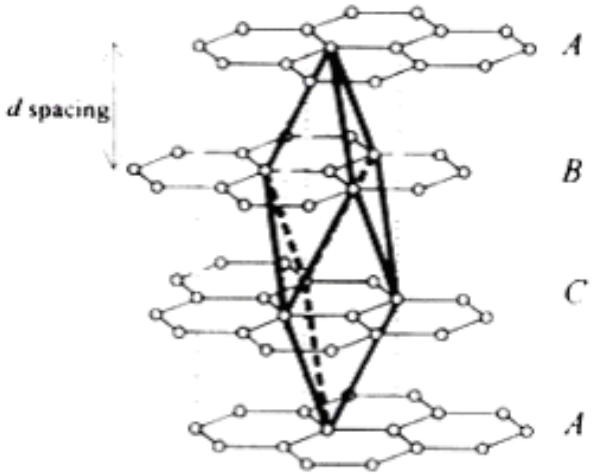

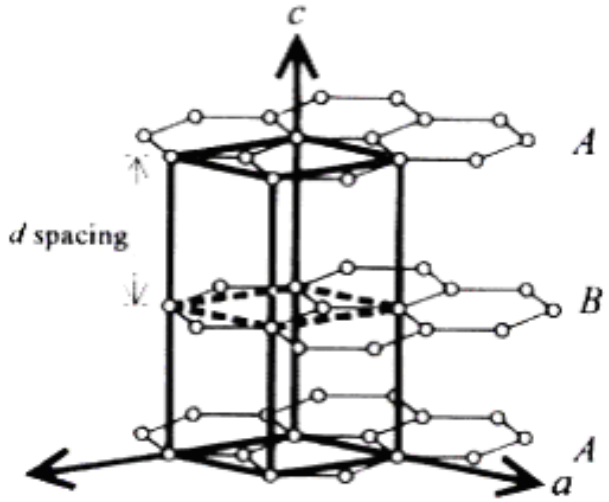

Characteristics of carbons

- **Thermal stability**
- **High thermal and electric conductivities**

  SWNT, Diamond : 4000 W/mK, K-11

  carbon fiber: 1100 W/mK
- **Small heat expansion**
- **High thermal shock properties**
- **High chemical stability**
- **Abrasion and lubricant properties**
- **High mechanical properties**

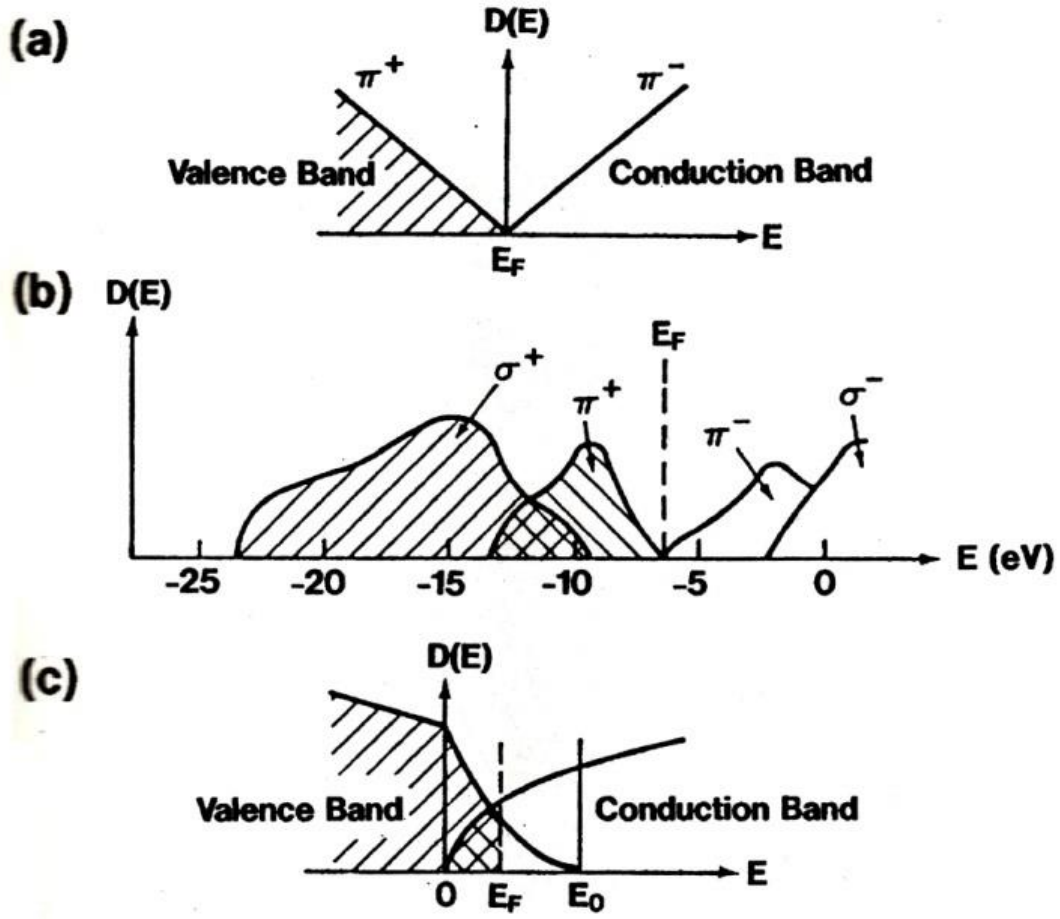

電子の状態密度$D(E)$のエネルギーE依存：2次元黒鉛に対するフェルミエネルギーE_F近傍のπ電子の電子状態状態分布(a)，黒鉛の全エネルギー領域における電子状態分布密度分布(b)，および黒鉛のE_F近傍のπ電子の状態密度分布(c)

Carbon is key element for Batteries !!

①Li-ion

[High capacity]

(+) : LiCoO2
(-) : Carbon(Graphite)
Conductor :Carbon

②Dry Battery

[Cheap]
[Easy Available]

(+) : MnO2
(-) : Zn
Conductor :Carbon

③Ni-MH

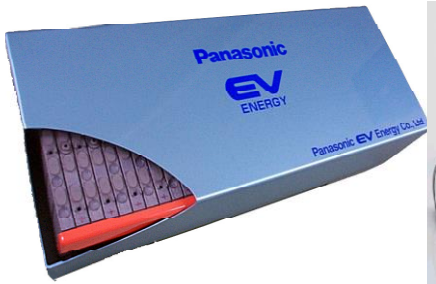

[High power]
[Total balance]

(+) : $\underline{(Ni\text{-}Co\ )(OH)_2}$
(-) : $\underline{Mm(Ni\text{-}Mn\text{-}Al\text{-}Co)_5}$
substrate:Nickel and Carbon

Applications and necessity of Li-ion battery

Energy storage system in smart grid

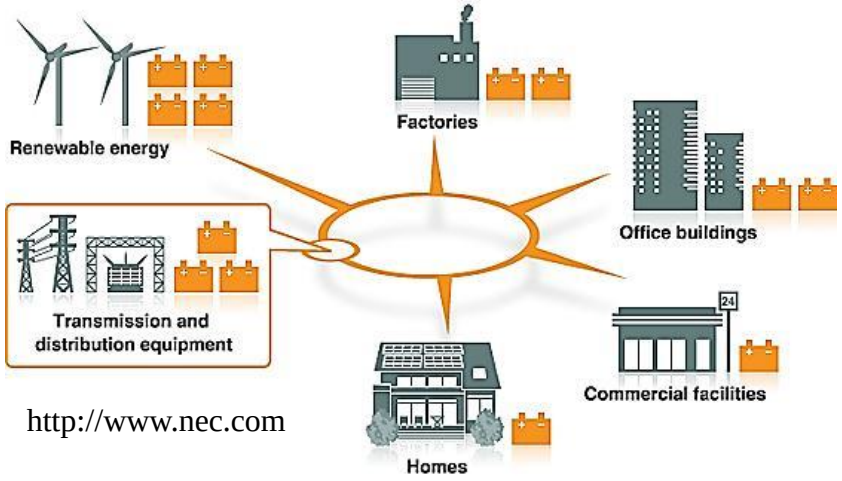

http://www.nec.com

Power source of electric vehicles

ICE

< Toyota Camry >

Electric motor

< Toyota RAV4 EV >

Energy density of various rechargeable batteries

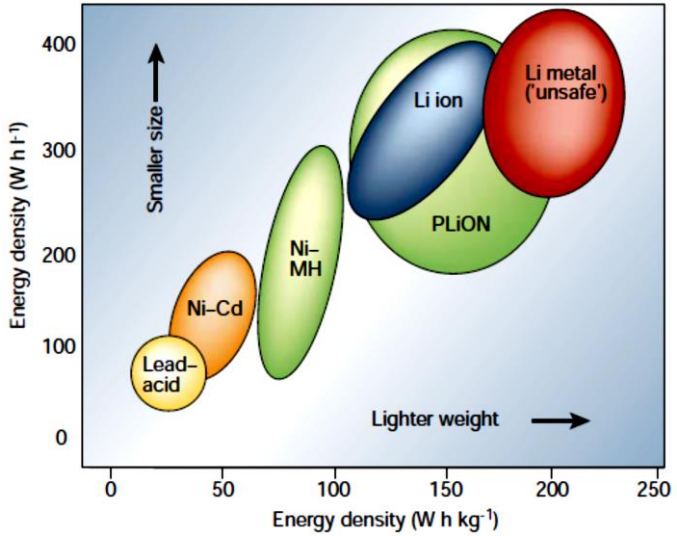

J.M. Tarascon, M. Armand, Nature 414 (2001) 359.

Li-ion battery is paid much attention as power sources of ESS and electric vehicles in a variety of rechargeable batteries.

ICE : Internal combustion engine, ESS : Energy storage system

Global market and requirements of Li-ion battery

Global market of Li-ion battery in ESS

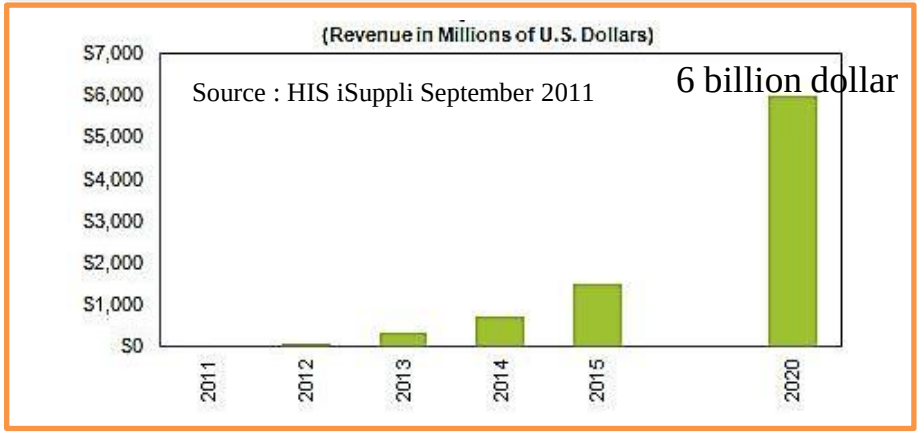

Source : HIS iSuppli September 2011

6 billion dollar

Global market of Li-ion battery in EV

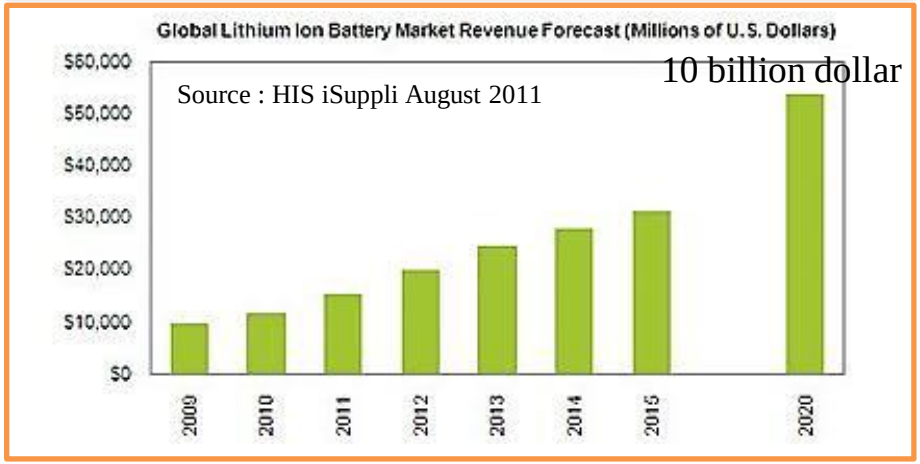

Source : HIS iSuppli August 2011

10 billion dollar

Requirements of Li-ion battery as power sources of ESS and EV

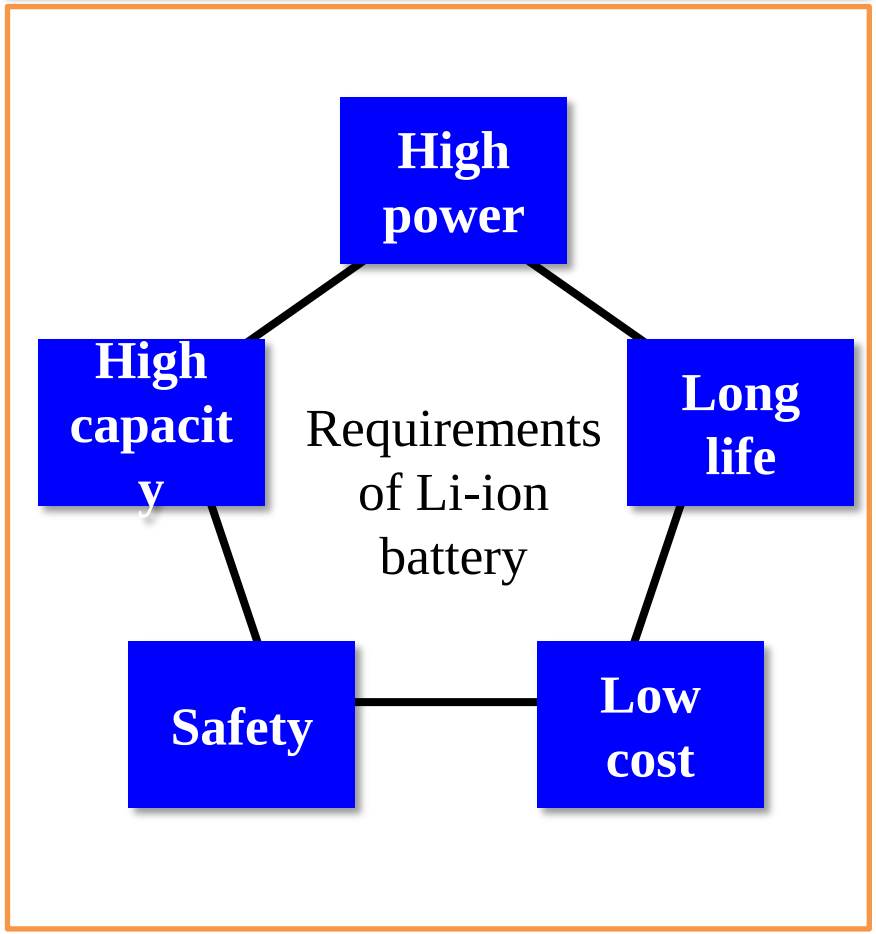

Carbon Electrode for Li-ion Battery

- **Graphite electrode is currently established.**
  - Low cost with cheaper natural graphite
  - Limited capacity less than 372 mAh/g
  - Limited power density

Larger power density for hybrid vehicle

➔ Glassy carbon with small crystalline unit (Low Cond.)

Thinner carbon nanofiber

Larger capacity

➔ Glassy carbon with large inner surface

Si or Sn family (Large volumetric change at Ch/Disc)

⇨ **Functional nano-composites**

Roles of Carbon for Anode of Li-ion Batteries

- Anodic Electrode to Hold Reduced Li-ion
  Intercalation → Graphite
  Surface Electron Transfer into Sealed Void
  → Carbon
- Electron Conductive Material
  Anodic Carbon and Cathodes Material
- Expansion Moderation
  Holding and Release of Ion Is Accompanied with Volumetric Charge
  Larger Capacity per Volume → Larger Expansion

電池負極物質

- 電池の中で還元剤として機能

自身が酸化（イオン化）し、電解質に溶解することで負極は負に帯電する。活量=1の水溶液中、標準状態における標準水素電極に対するその電位は標準電極電位E0と呼ばれ、元素ごとで表に示す異なる値を取る。

E0 = - ΔG/nF (イオン化傾向、真空中で陽イオンになりやすさ)

表1　代表的な金属元素の標準電極電位と第1イオン化エネルギーの相関

電極	放電反応	ギブスエネルギー	標準電極電位	イオン化エネルギー
Li	$Li \rightarrow Li^+ + e^-$	−293.31 kJ/mol	− 3.045 V	520 kJ/mol
K	$K \rightarrow K^+ + e^-$	−283.27 kJ/mol	− 2.925 V	419 kJ/mol
Ca	$Ca \rightarrow Ca^{2+} + 2e^-$	−553.58 kJ/mol	− 2.866 V	590 kJ/mol
Na	$Na \rightarrow Na^+ + e^-$	−261.9 kJ/mol	− 2.714 V	496 kJ/mol
Mg	$Mg \rightarrow Mg^{2+} + 2e^-$	−454.8 kJ/mol	− 2.363 V	738 kJ/mol
Al	$Al \rightarrow Al^{3+} + 3e^-$	−485 kJ/mol	− 1.662 V	578 kJ/mol
Zn	$Zn \rightarrow Zn^{2+} + 2e^-$	−147.06 kJ/mol	− 0.763 V	906 kJ/mol
Fe	$Fe \rightarrow Fe^{2+} + 2e^-$	−78.9 kJ/mol	− 0.44 V	759 kJ/mol
H	$H \rightarrow H^+ + e^-$	0 kJ/mol	0 V	1,312 kJ/mol
Cu	$Cu \rightarrow Cu^{2+} + 2e^-$	65.49 kJ/mol	0.337 V	745 kJ/mol
Ag	$Ag \rightarrow Ag^+ + e^-$	77.1 kJ/mol	0.7991 V	731 kJ/mol

地殻中の各元素の存在比

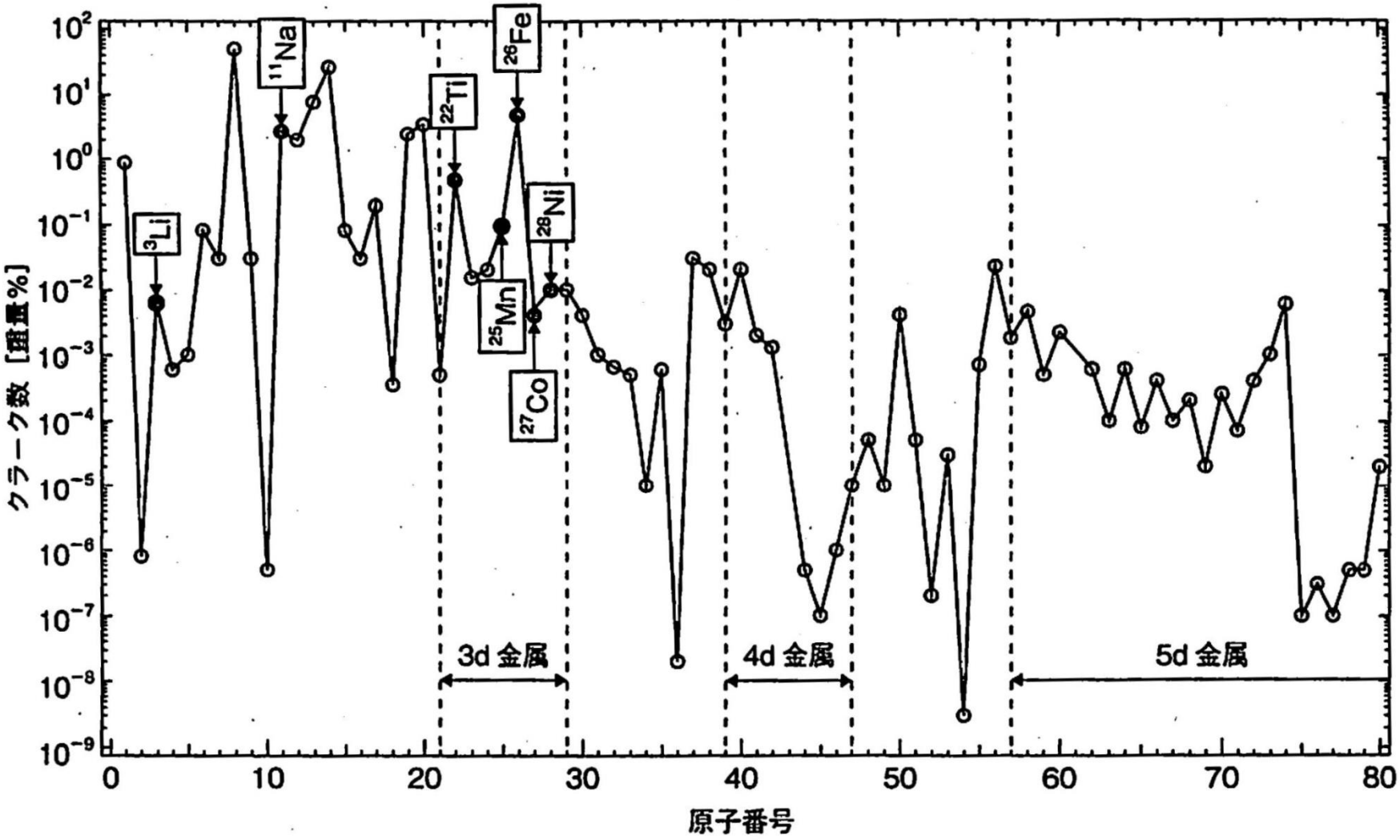

Li2次電池における負極材の研究動向

1. Li金属負極:

- 還元力の強さが仇となり、殆どの電解液を還元分解してしまう問題点あり。
- 還元の際、Dendrite結晶状として還元
- モリエナジー（カナダ）1989年、NTT形態で内部短絡事故

2. Carbon電極

- 1991年SONYが採択、Li-ion電池化、世界初
- C6Li, 372 mAh/g

3. Si, Sn系、チタニア系、バナディウム系…

Li-ion Battery Road

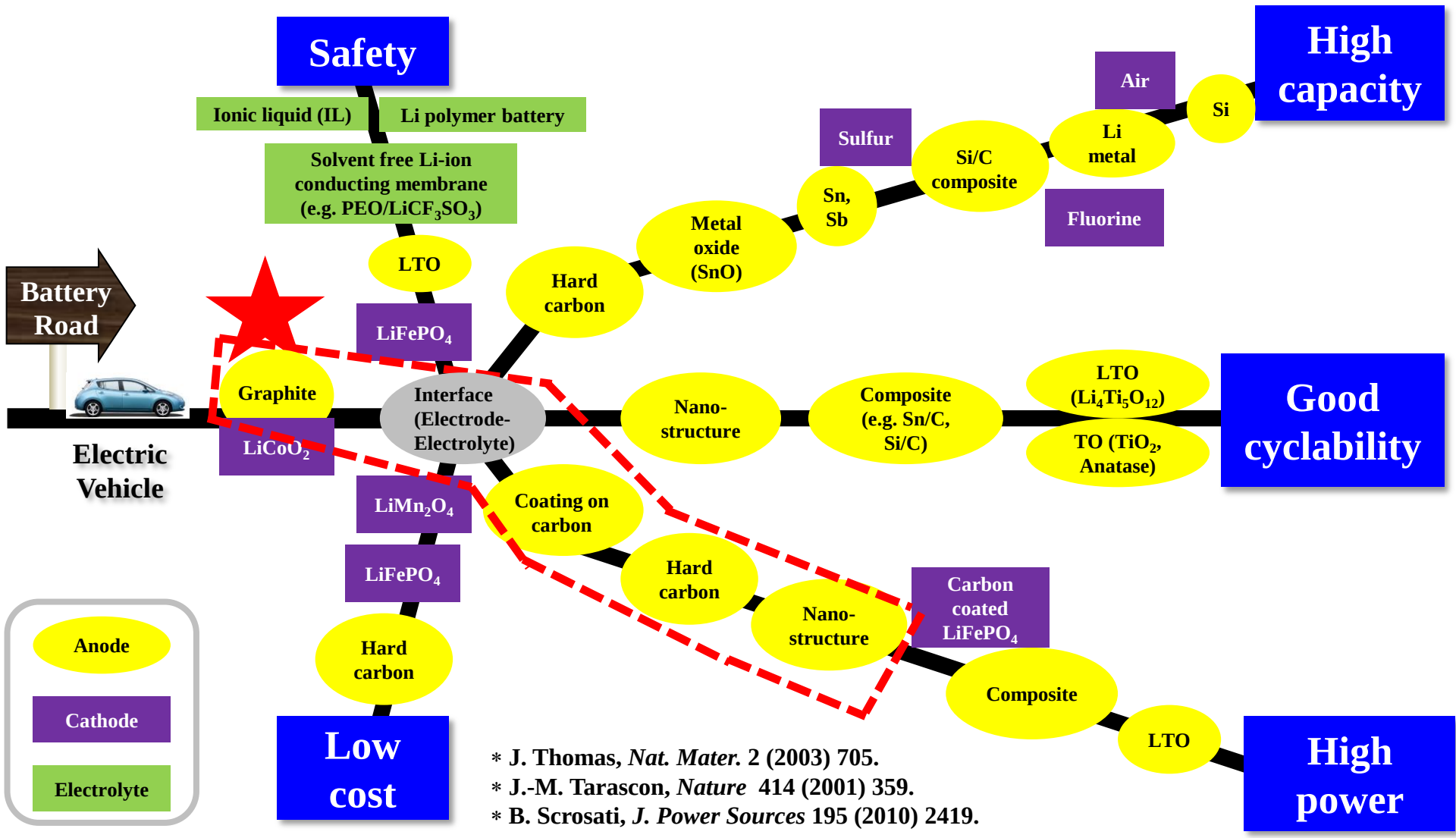

* J. Thomas, *Nat. Mater.* 2 (2003) 705.
* J.-M. Tarascon, *Nature* 414 (2001) 359.
* B. Scrosati, *J. Power Sources* 195 (2010) 2419.

Ch./Dis. Principle of Li-ion 2nd Batteries

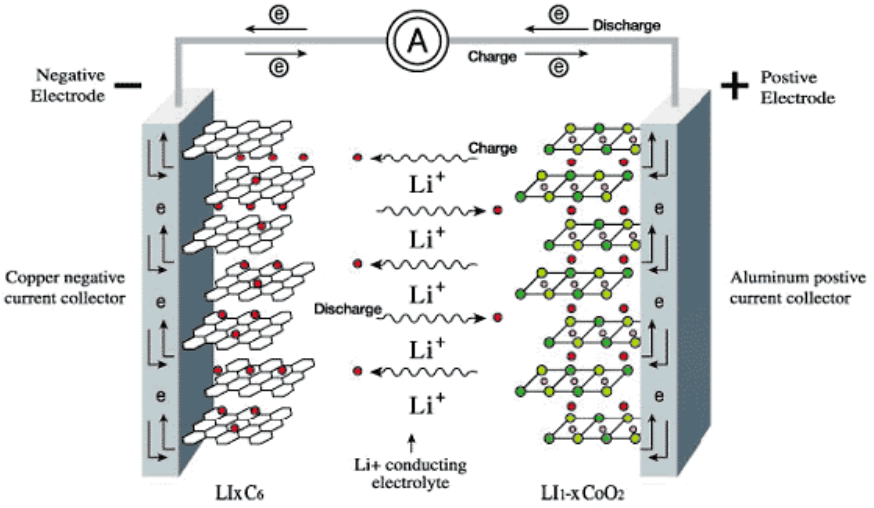

Anodic Materials for Li-ion 2nd Batteries

	Carbon	Si alloys	Li alloys
Theoretical Cap.(mAh/g)	372 (LiC_6)	4200 ($Li_{4.4}Si$)	3860
Present Stage	Commercialized	Developing	Developing
Merit	Low Cost Good Cycle Life Good Chemical Stability	High Capacity	High Capacity
De-merit	Low Rate Capability	High Volume Expansion ⇒ Bad Cycle	Strong Reaction ⇒ Bad Cycle & Thermal Stability
Materials	Graphite, Soft/Hard carbon	-	-
User	Sanyo, Matsushita, STC, A&T Battery, Shin-Kobe, GS, Moli, Mitsubishi, Sony, SDD, Hitachi Maxcel, LG Chem.	-	-

Characteristics and materials of 2nd Batteries

Ref. KISTI, Materials for 2nd Batteries (2004/06)

		Ni-Cd	Ni-MH	Li-ion	Li polymer
Cathodic material		NiOOH	NiOOH	LiMO2	LiMO2
Anodic material		Cd	MH	Carbon	Carbon
Electrolyte		KOH/H2O	KOH/H2O	LiX/Organic Solution	LiX/Polymer electrolyte
Operating voltage(V)		1.2	1.2	3.6	3.6
Cycle		1000	1000	1200	1000
Self discharge rate (%/month)		-	20~25	< 10	≪ 10
Environmental pollutant		Yes	Yes	No	No
Energy density	Per weight (Wh/kg)	-	65	120	100
	Per volume (Wh/L)	160	240	280	220
Manufacturing company		Sanyo, Toshiba	Matsushita, Sanyo, Toshiba	Sony, Sanyo, Matsushita	Valence, Ultralife

Mechanism of charge & discharge

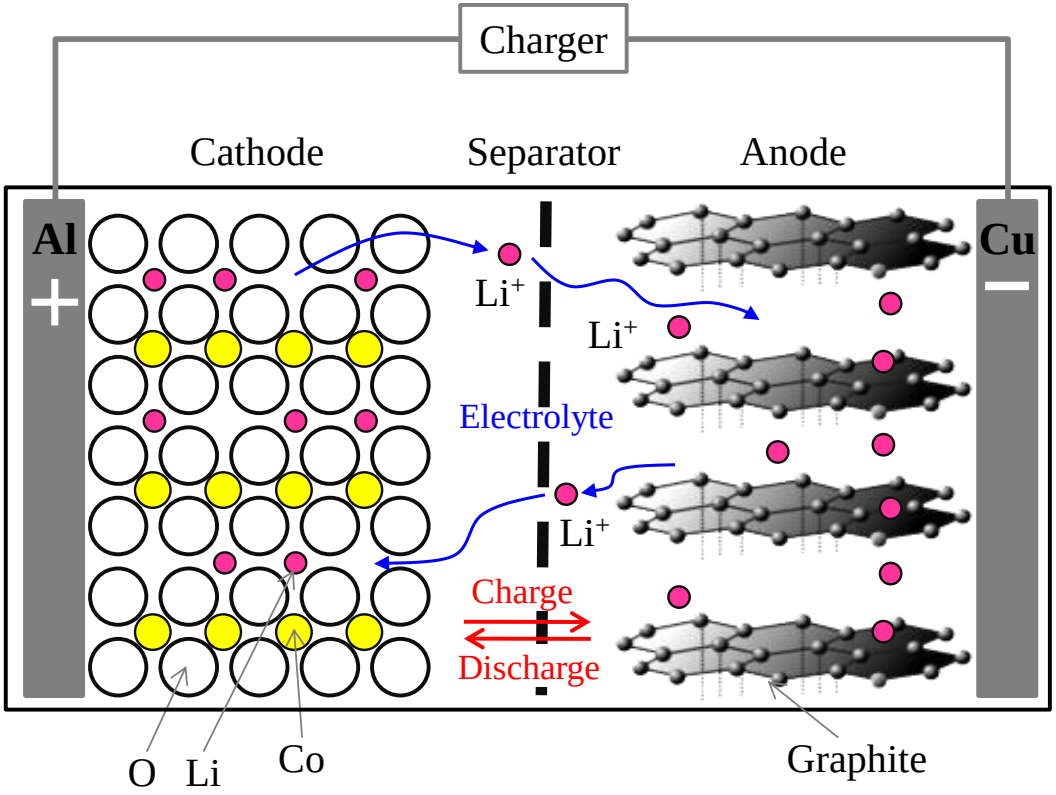

Cathode : $LiCoO_2 \leftrightarrow CoO_2 + Li^+ + 2e^-$

Anode : $C_6 + Li^+ + e^- \leftrightarrow LiC_6$

Overall : $LiCoO_2 + C_6 \leftrightarrow CoO_2 + LiC_6$

Carbon materials of LIB

	Precursor	Advantages	Disadvantages
Graphite (over 2800°C)	Natural / Artificial graphite MCMB, Needle cokes VGCF	Low discharge potential (≈ 0.2V) Long cycle life	Low discharge capacity (372 mAh/g) Poor rate performance High cost
Soft Carbon Graphitizable carbon (600~800°C)	MCMB Meso phase pitch Green cokes	High capacity (700~1000mAh/g) Low cost	High discharge potential (≈ 1.0V) High irreversible capacity Poor cycle stability
Hard Carbon Non-graphitizable carbon (1000~1400°C)	Thermosetting polymer Glassy carbon, Coal Organic material Stabilized isotropic pitch	High capacity (400~700mAh/g) High rate performance Low discharge potential (≈ 0.1V) Low cost	Large irreversible capacity

Characteristics of Carbon Material

HTT ↔ Resistance

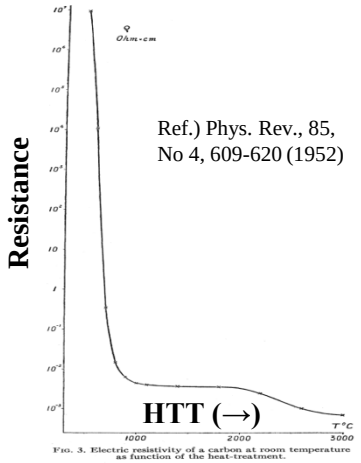

Fig. 3. Electric resistivity of a carbon at room temperature as function of the heat-treatment.

Ref.) Phys. Rev., 85, No 4, 609-620 (1952)

Li content ↔ d-spacing

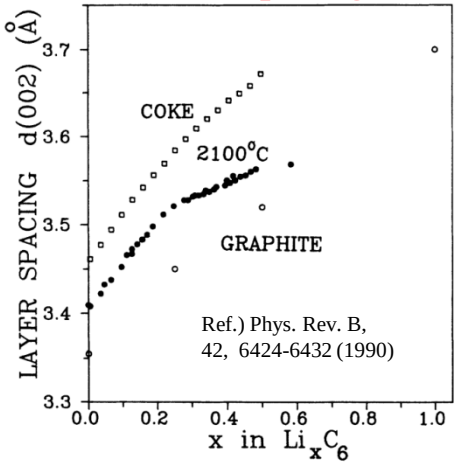

Ref.) Phys. Rev. B, 42, 6424-6432 (1990)

HTT ↔ Capacity

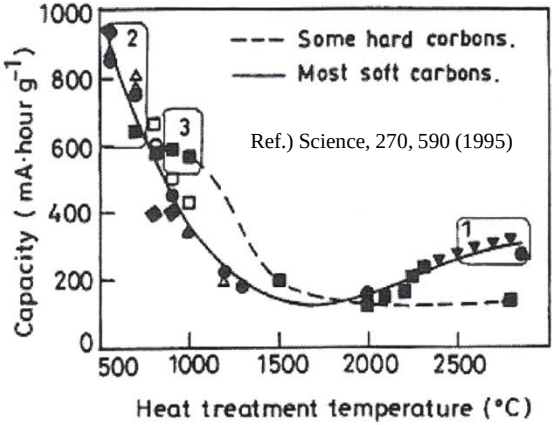

Ref.) Science, 270, 590 (1995)

Structural mechanism of carbon

Ref.) Proc. R. Soc. A209 (1951) 196-218

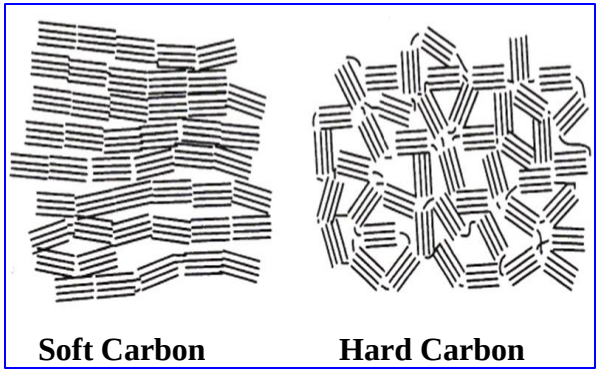

Franklin model

Ref.) Report of Kyushu Univ. 12 (1) (1998) 45-57

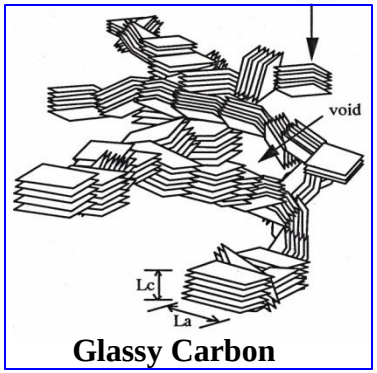

Mochida model

Charge-Discharge Profile

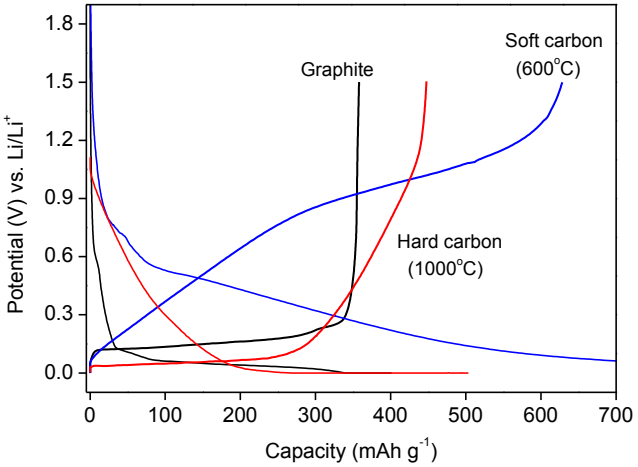

Lithium Ion Battery, Electrode

Lithium ion insertion sites of carbon

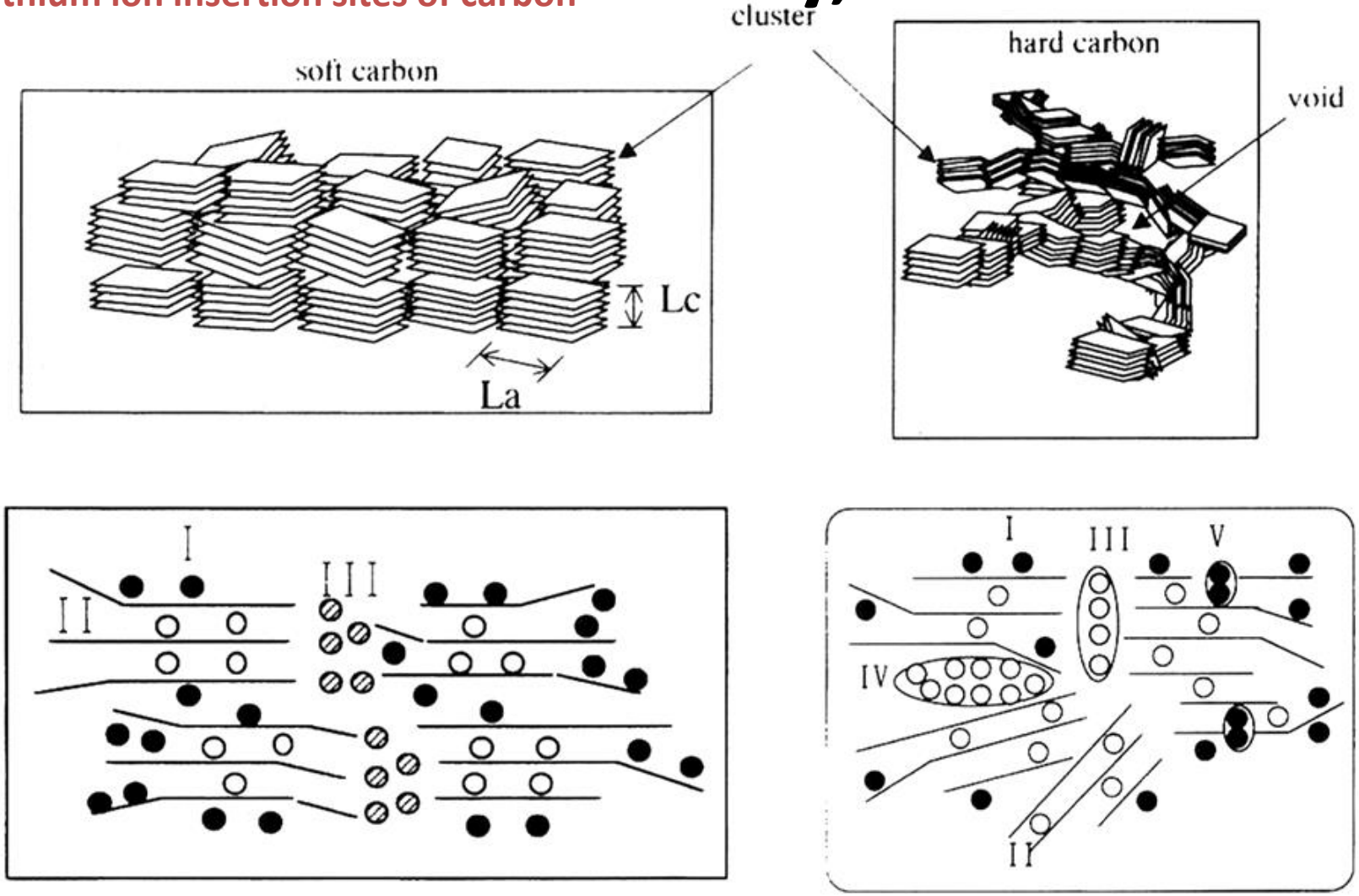

- Larger Capacity : Energy Density
- Larger Rate : Power Density
- Safety : Stable Forms of Reduced Alkaline Ion
- Lowest Unusable Ion

  → Complete Electrode Material

  Carbon Is Always A Key Material.

Typical Properties of Synthetic Graphites

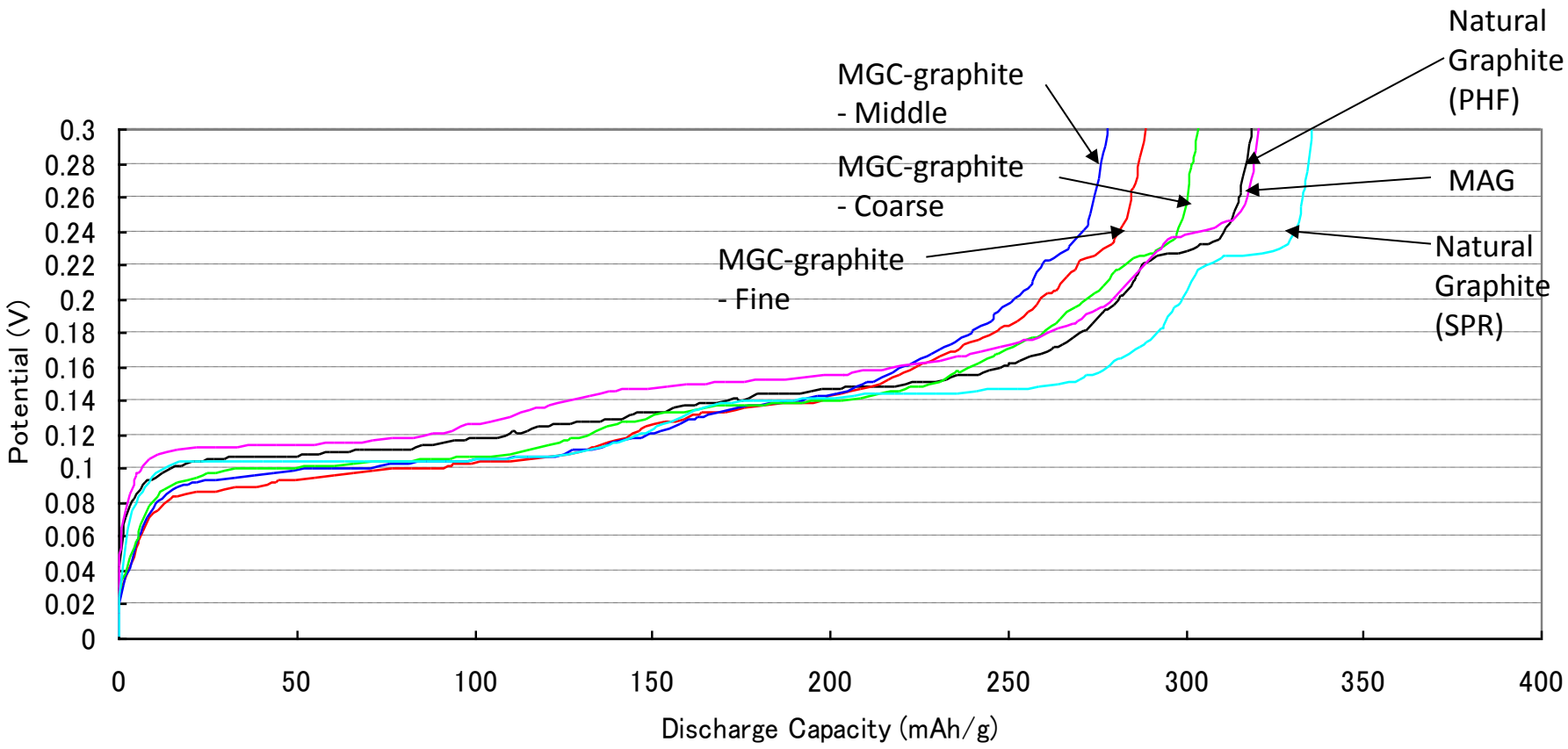

GraphiteとGraphene

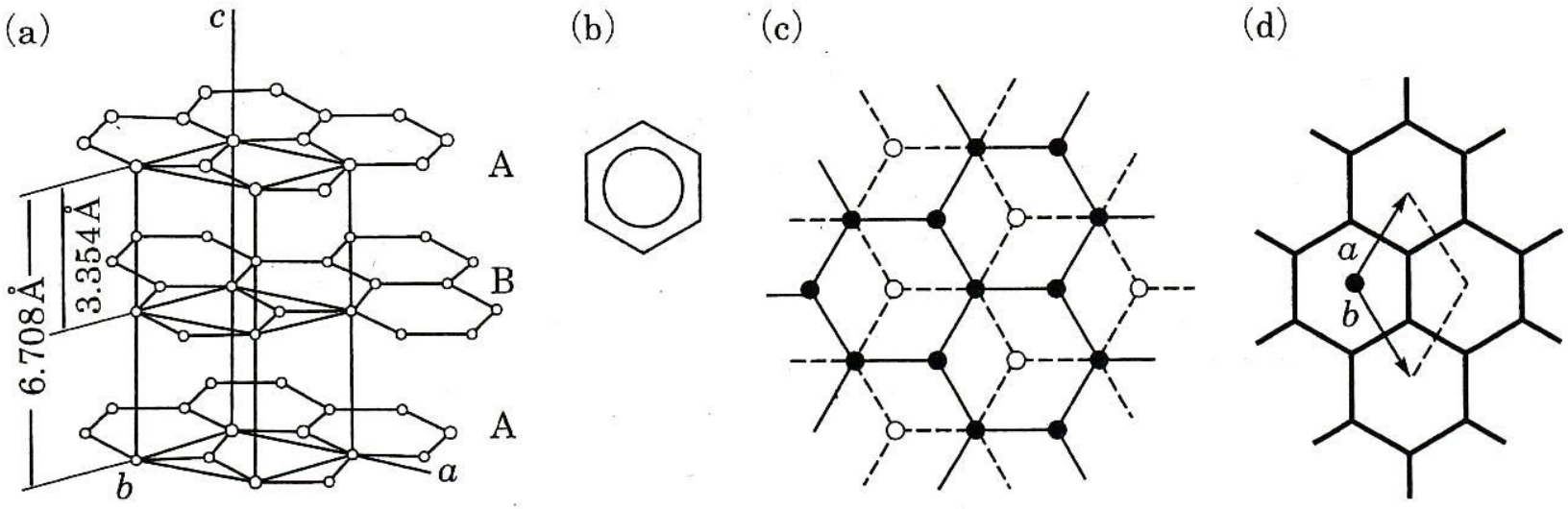

図4.2　グラファイトの構造

(a) グラファイトの結晶構造．ABA 様式で積層している．(b) ベンゼン．(c) c 軸方向の上方から 2 枚面の重なりを見たもの．●が上の面の炭素原子で，○が下の面の炭素原子を表す．(c) ab 面の構成．単一の ab 面（グラフェン面）だけなら，単位セルは菱形の部分で，2 個の炭素原子を含む．ab 面の並進長さは，$|a|=|b|=2.462$ Å.

炭素の結晶構造パラメータ

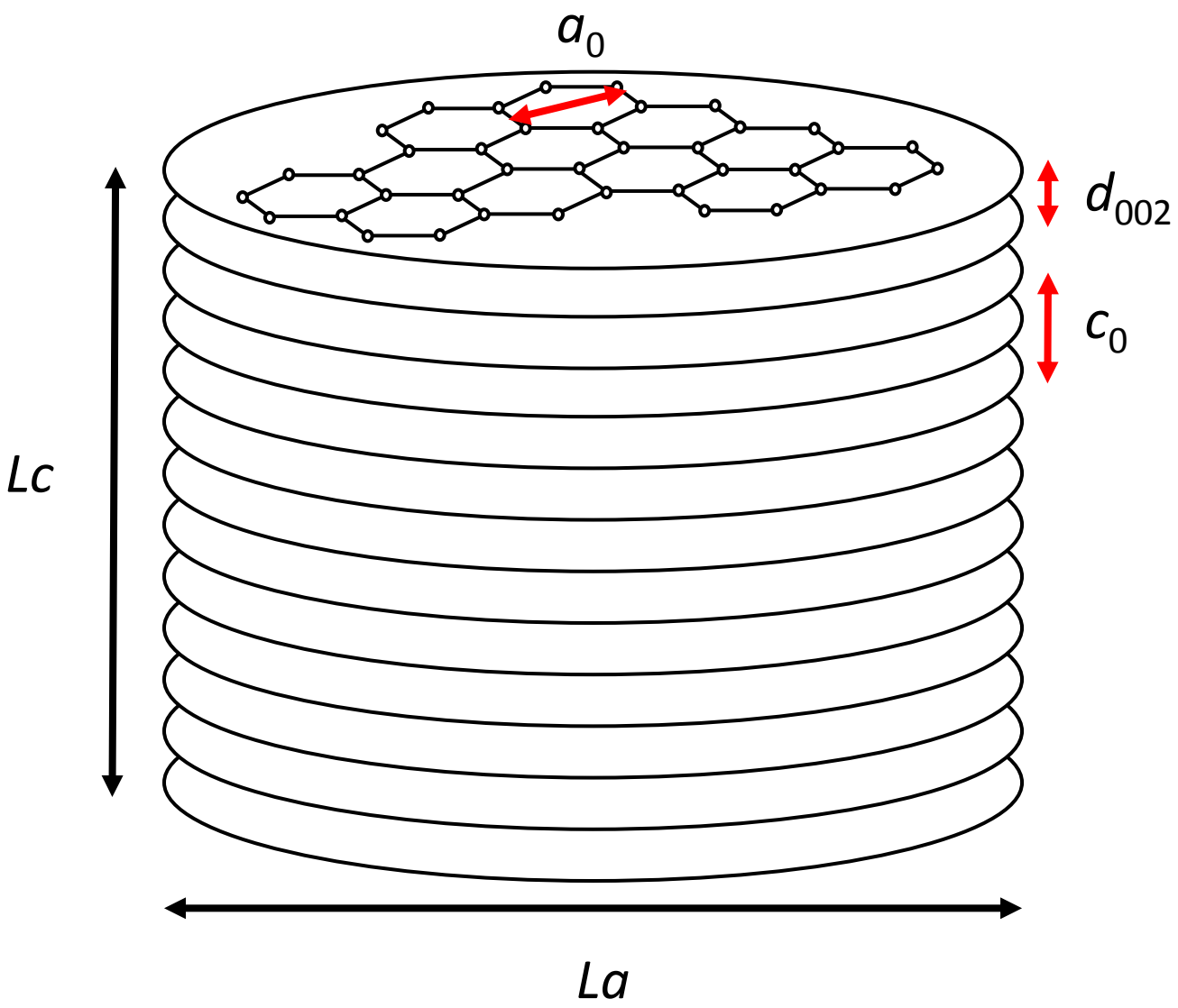

結晶面と面間隔の関係

(002)面と$d_{(002)}$

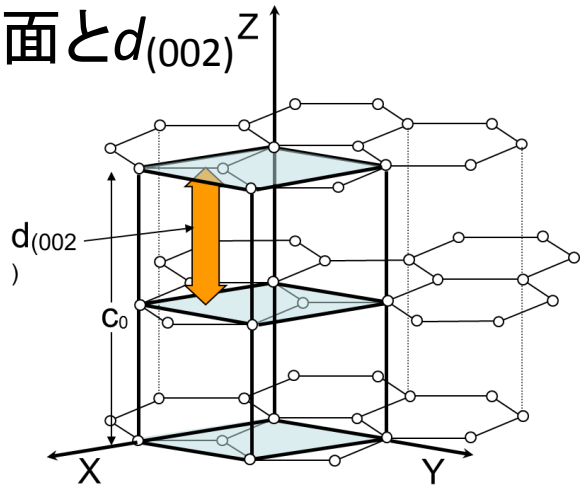

(110)面と$d_{(110)}$

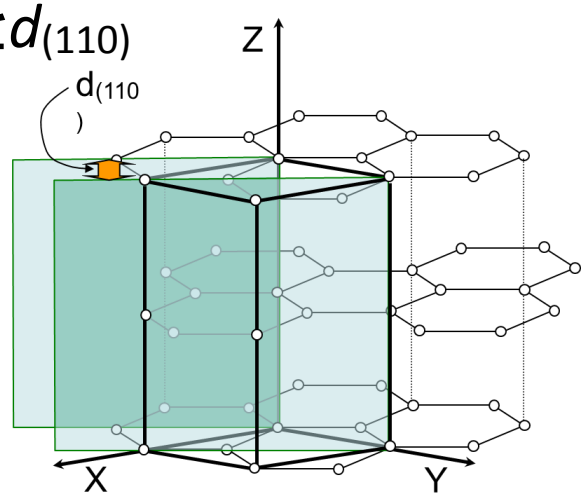

(112)面と$d_{(112)}$

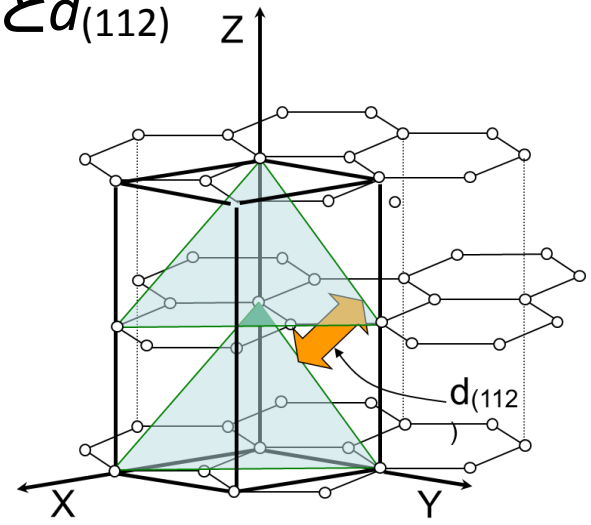

Graphiteの構造

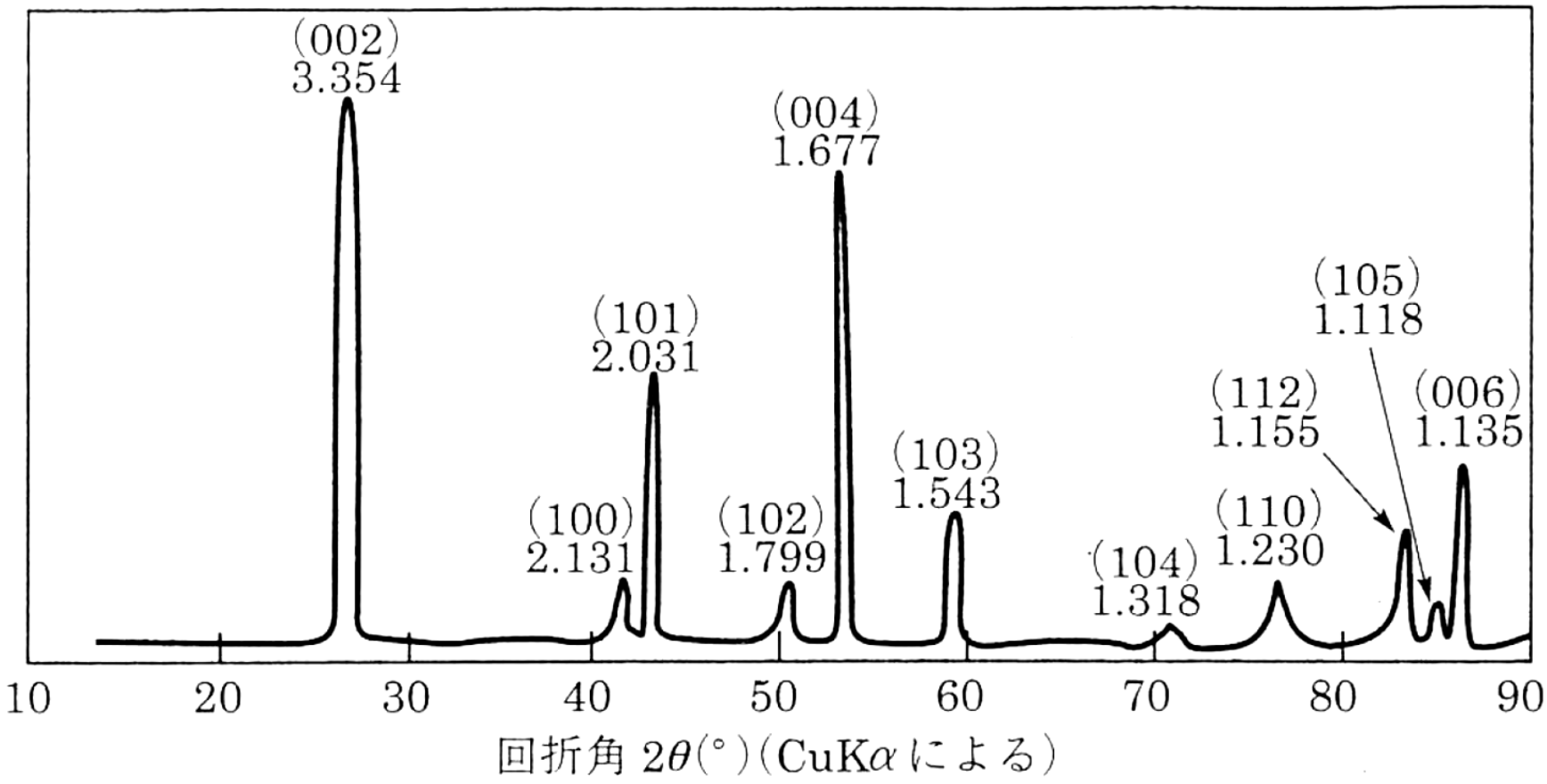

図4.4　グラファイトのX線回折パターン

黒鉛の電子構造

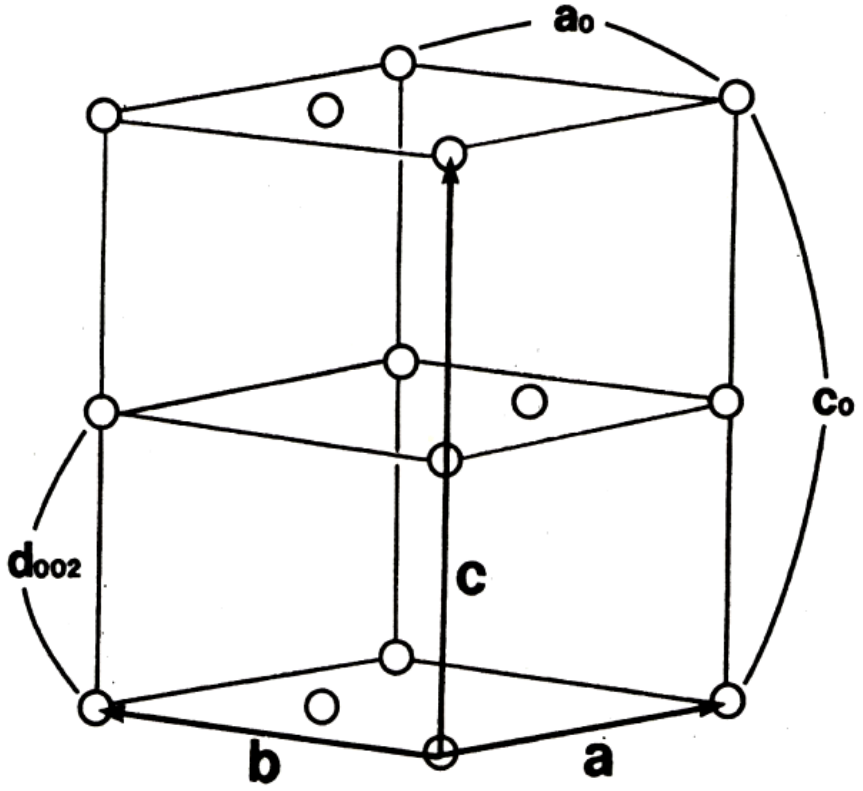

最隣接原子間距離：0.1421nm
第2隣接原子間距離：0.2461nm
層間距離：0.3354nm

黒鉛結晶の単位格子と格子定数a_0,c_0および基本格子ベクトル***a,b,c***

Lithium Ion Battery, Electrode

Lithium ion insertion sites of carbon

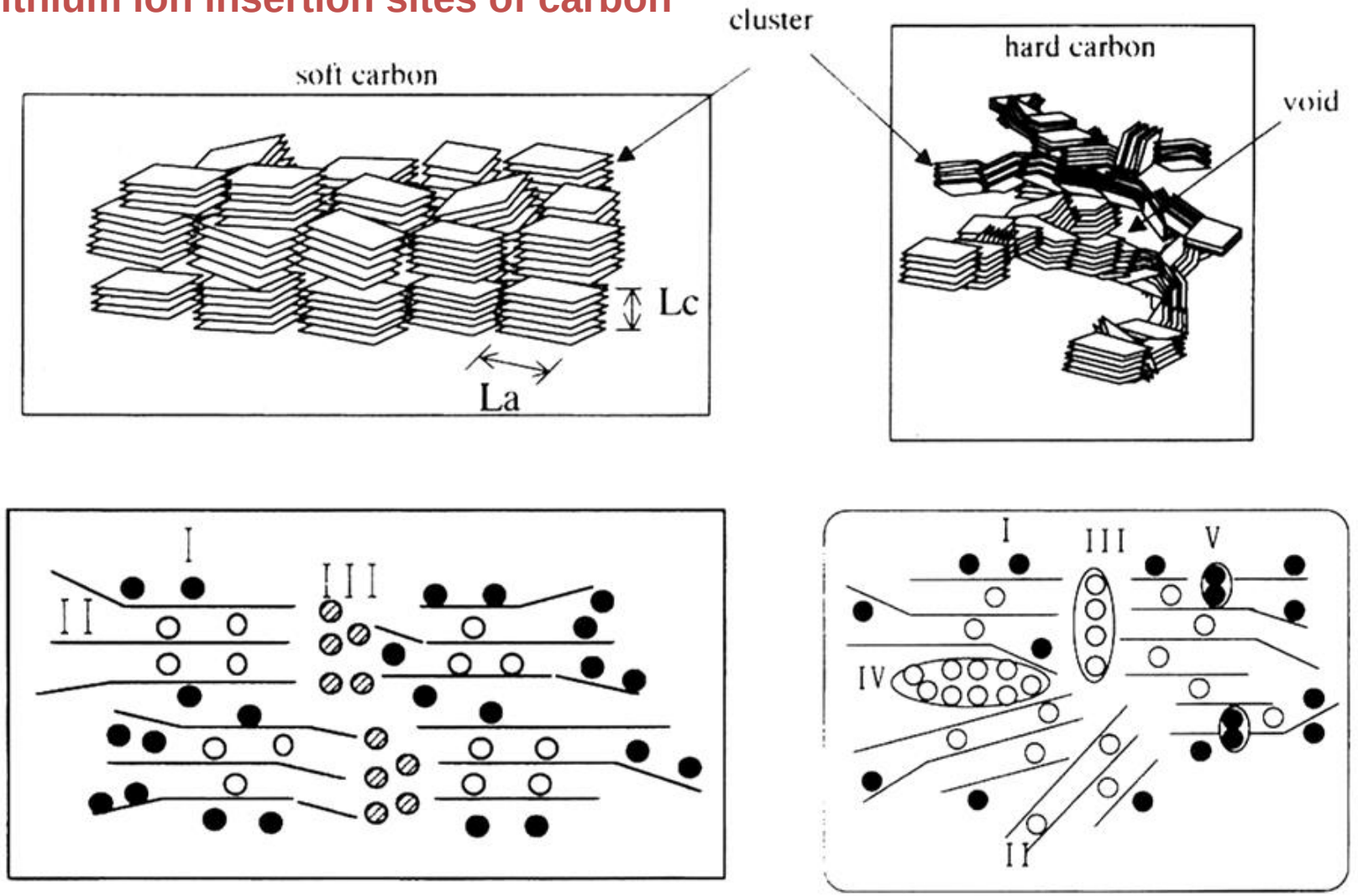

Graphiteの反応性

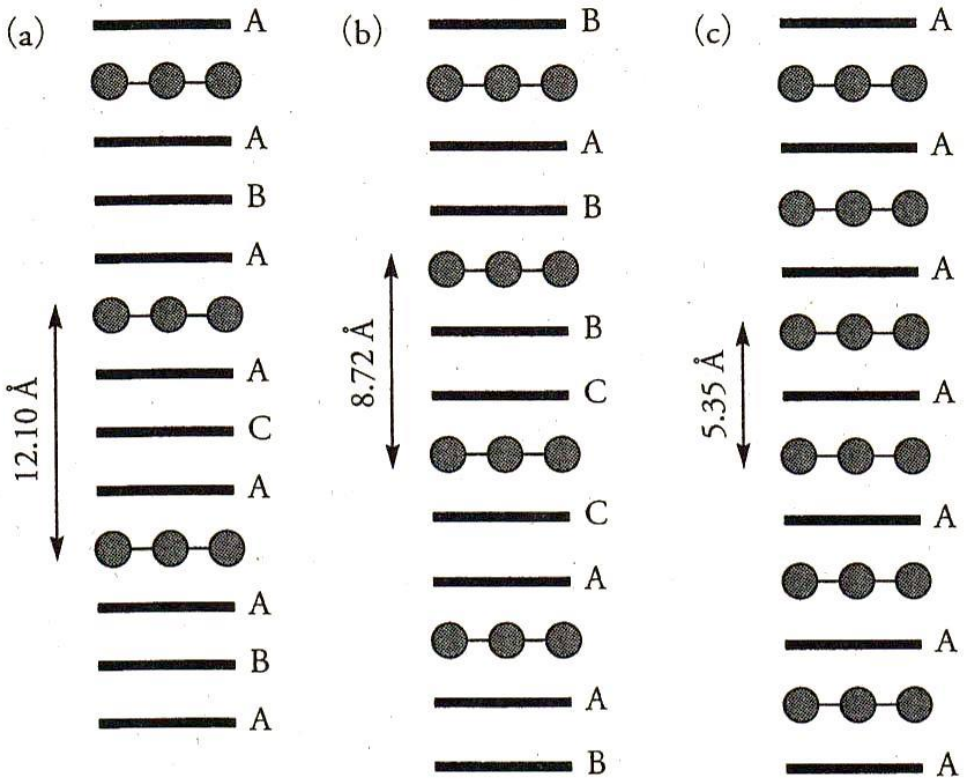

図4.6　カリウムをインターカレートとしたGICのステージ構造

実線はグラファイトの *ab* 面で，A，B，Cはその積層様式．灰色の丸印はカリウム原子．
(a) KC_{36}（ステージ3），(b) KC_{24}（ステージ2），(c) KC_{8}（ステージ1）．

GICでは、HOバンドの頂上から電子が引き抜かれることによって正孔が注入されたり、LUバンドの底に余剰電子が与えられたりするので、フェルミ状態の密度が増加して導電性が上がる。

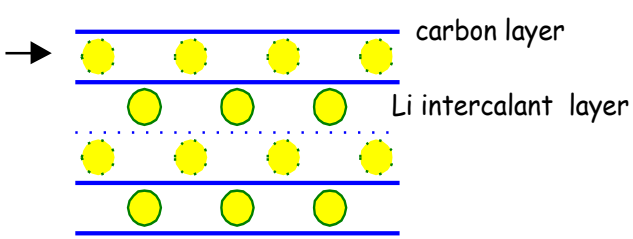

LiC_6, LiC_9 - stage 1
: A type of superlattice

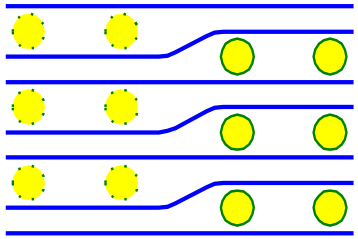

LiC_{12} - stage 2

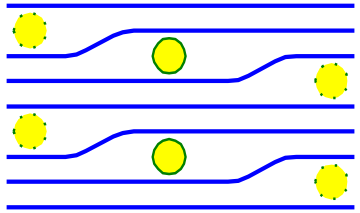

LiC_{18} - stage 3

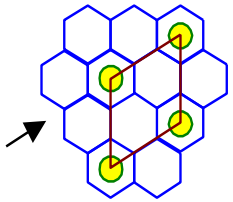

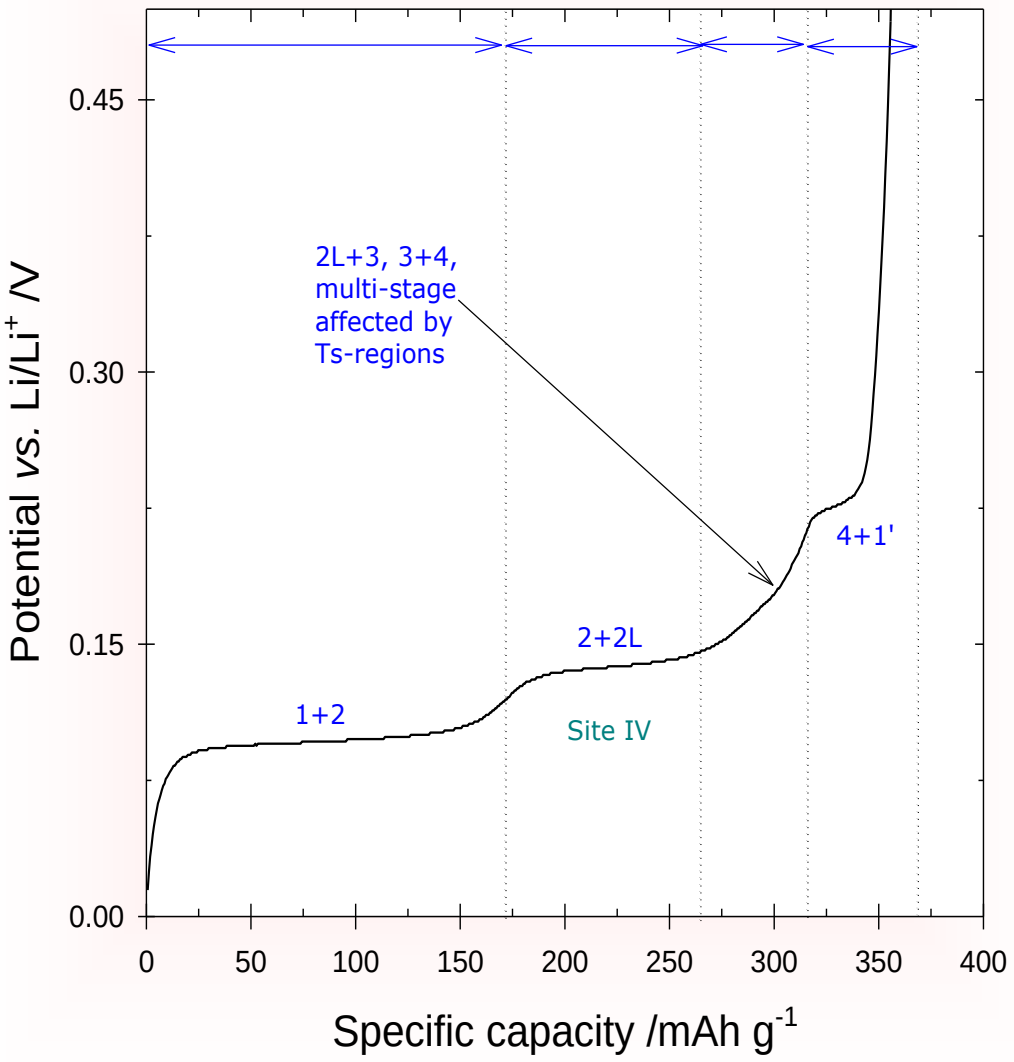
0.45
0.30
0.15
0.00
0
50
100
150
200
250
300
350
400
Potential vs. Li/Li+ /V
Specific capacity /mAh g-1
2L+3, 3+4,
multi-stage
affected by
Ts-regions
4+1'
2+2L
1+2
Site IV

Voltammetric behavior of grpahite

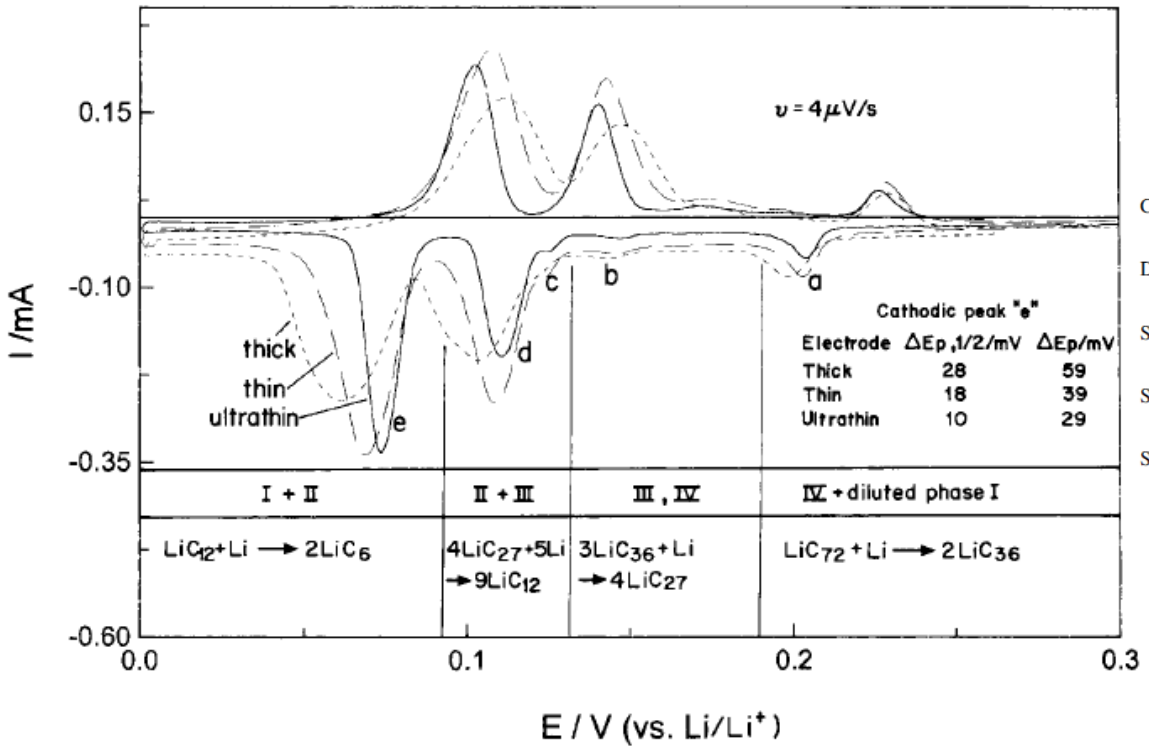

$C_6 + 0.083Li^+ + 0.083e^- \rightleftharpoons Li_{0.083}C_6$ Diluted stage I, Li_xC_6, $x \leq 0.083$

Diluted stage I $Li_{0.083}C_6 + 0.083e^- + 0.083Li^+ \rightleftharpoons Li_{0.166}C_6$ stage IV

Stage VI $Li_{0.166}C_6 + 0.056e^- + 0.056Li^+ \rightleftharpoons Li_{0.222}C_6$ Stage III

Stage III $Li_{0.222}C_6 + 0.278e^- + 0.278Li^+ \rightleftharpoons Li_{0.5}C_6$ Stage II

Stage II $Li_{0.5}C_6 + 0.5e^- + 0.5\,Li^+ \rightleftharpoons LiC_6$ Stage I

Fig. 1. Typical voltammetric behavior of graphite electrodes at a very slow scan rate, $v = 4$ μV/s in EC-DMC 1:3/$LiAsF_6$ solution. (Graphite flakes, KS-6, Timcal). Ultrathin, thin and thick electrodes correspond to submicronic (0.16 mg/cm^2, see preparation procedure in Refs. [5,9]), 10 microns (3.3 mg/cm^2), and 140 μm (12 mg/cm^2), respectively. The current for the thin and ultrathin electrodes was normalized with that of the thick electrodes according to their mass ratios in order to have the 3 CV on the same scale. The electrode area was 2.4 cm^2 for the thin and the ultrathin, and ≈0.2 cm^2 for the thick electrode.

Design and Its Thermal Change of Aromatic Stacking

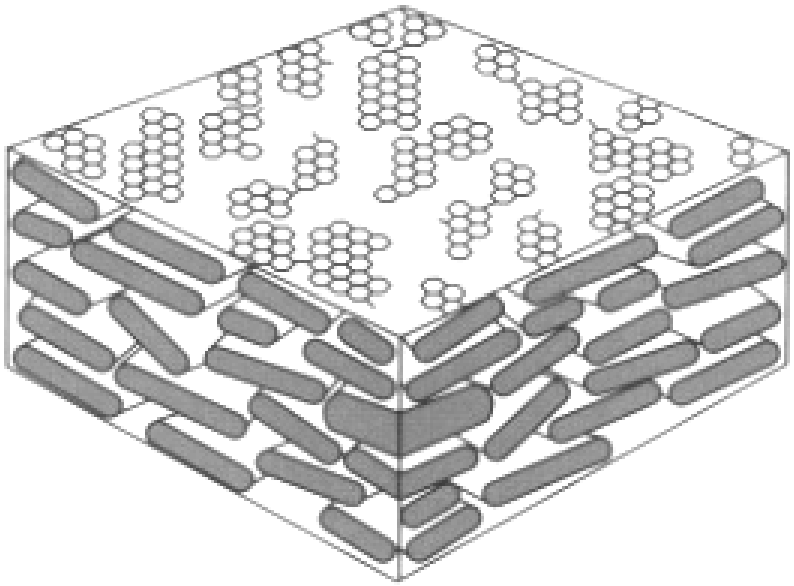

Molecular Models

Spider Wedge Stacking of mesophase pitch
(Zimmer et al. Advances in Liquid Crystal, New York, 1982, 5)

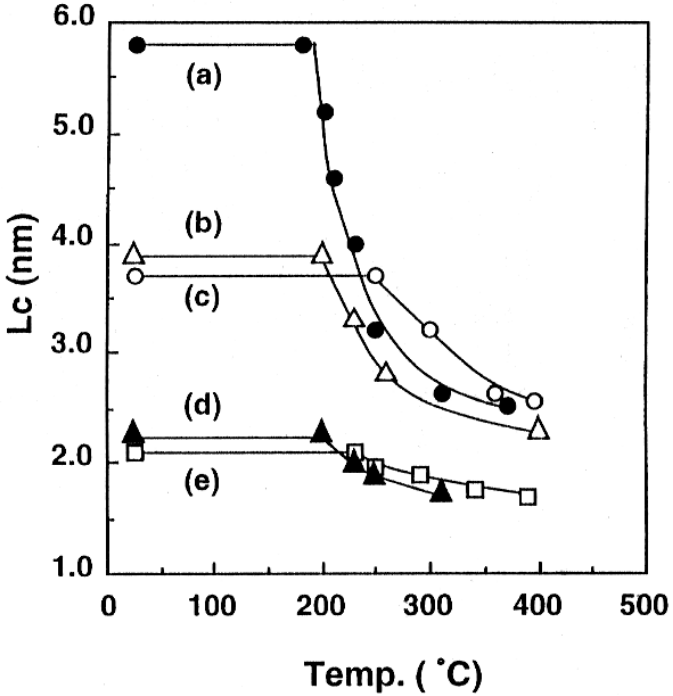

Melt-XRD analysis

Change in Lc of mesophase pitch at higher temperature; (a) methylnaphthalene-derived pitch; (b) petroleum-derived mesophase pitch; (c); coal tar derived-mesophase pitch; (d) naphthalene-derived mesophase pitch; (e) anthracene-derived mesophase pitch
(Korai et al. Carbon, 1992, 30, 1019)

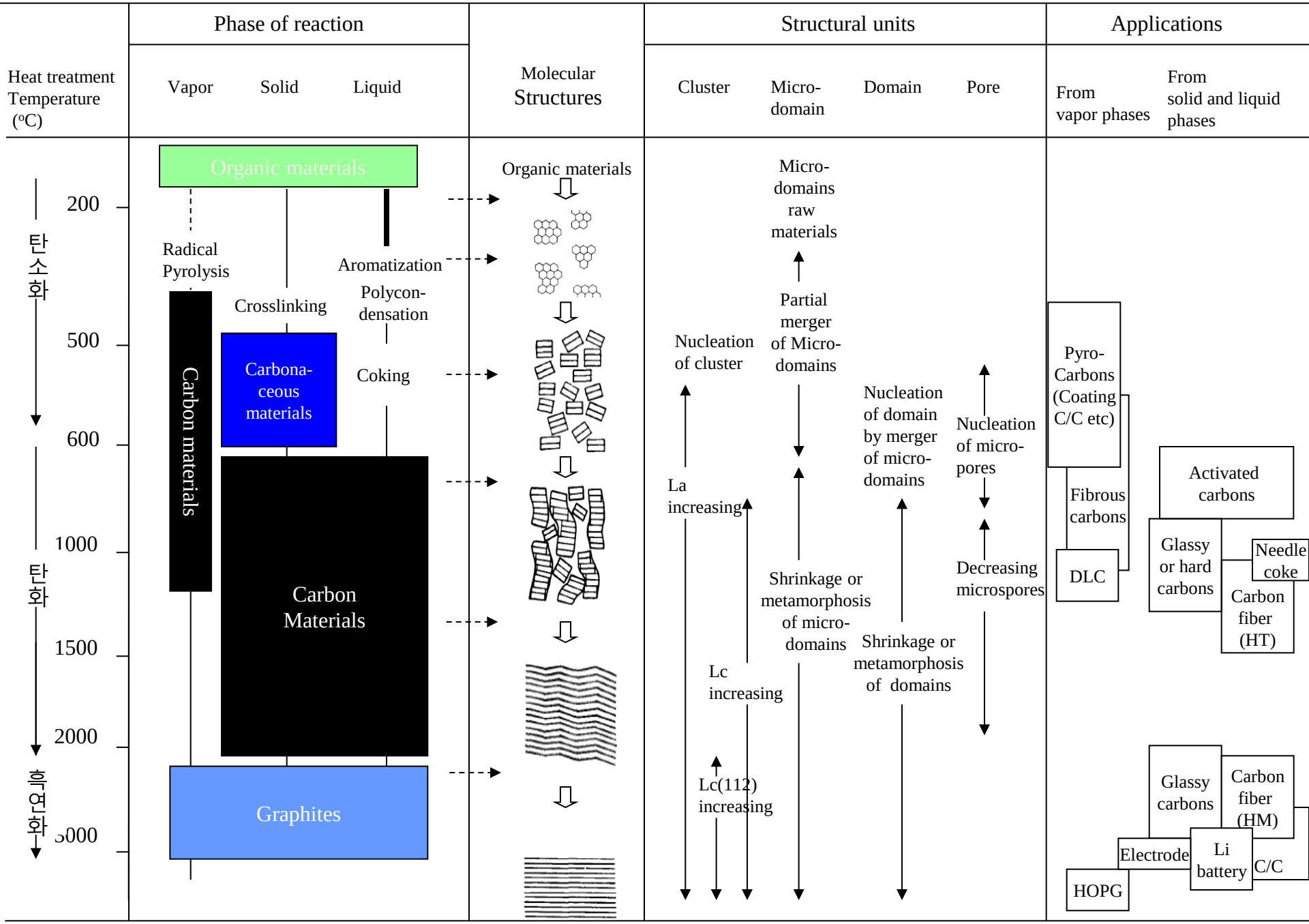
Phase of reaction
Vapor
Solid
Liquid
Molecular Structures
Structural units
Cluster
Micro-domain
Domain
Pore
Applications
From vapor phases
From solid and liquid phases
Heat treatment Temperature (°C)
200
500
600
1000
1500
2000
3000
탄소화
탄화
흑연화
Organic materials
Radical Pyrolysis
Crosslinking
Aromatization
Polycon-densation
Coking
Carbon materials
Carbona-ceous materials
Carbon Materials
Graphites
Organic materials
Micro-domains raw materials
Partial merger of Micro-domains
Nucleation of cluster
La increasing
Lc increasing
Lc(112) increasing
Shrinkage or metamorphosis of micro-domains
Nucleation of domain by merger of micro-domains
Shrinkage or metamorphosis of domains
Nucleation of micro-pores
Decreasing microspores
Pyro-Carbons (Coating C/C etc)
Fibrous carbons
DLC
Activated carbons
Glassy or hard carbons
Needle coke
Carbon fiber (HT)
Glassy carbons
Carbon fiber (HM)
Electrode
Li battery
C/C
HOPG

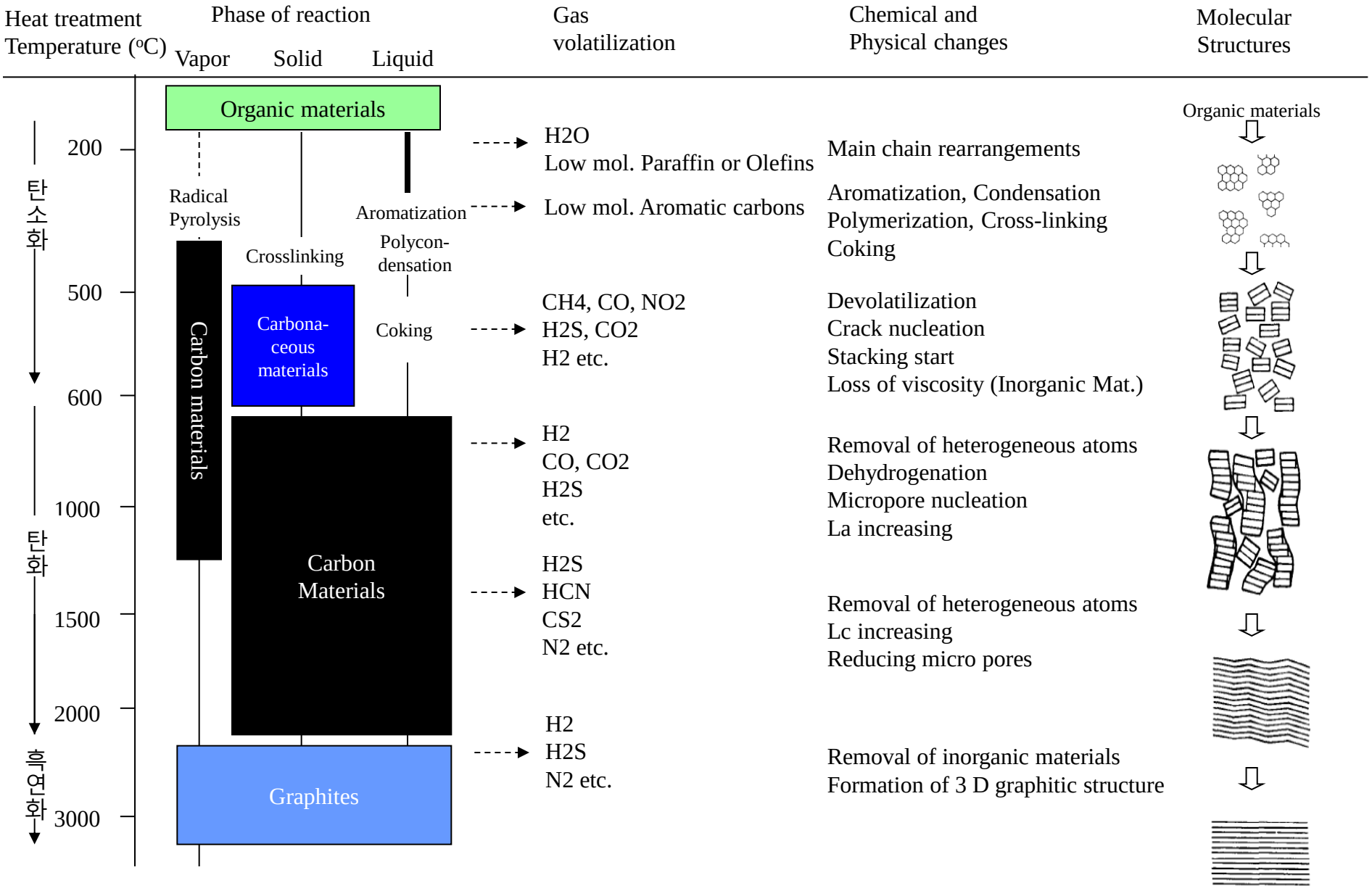
Heat treatment Temperature (°C)
Phase of reaction
Vapor
Solid
Liquid
Gas volatilization
Chemical and Physical changes
Molecular Structures
Organic materials
200
500
600
1000
1500
2000
3000
탄소화
탄화
흑연화
Radical Pyrolysis
Aromatization
Crosslinking
Polycon-densation
Coking
Carbon materials
Carbona-ceous materials
Carbon Materials
Graphites
H2O
Low mol. Paraffin or Olefins
Low mol. Aromatic carbons
CH4, CO, NO2
H2S, CO2
H2 etc.
H2
CO, CO2
H2S
etc.
H2S
HCN
CS2
N2 etc.
H2
H2S
N2 etc.
Main chain rearrangements
Aromatization, Condensation
Polymerization, Cross-linking
Coking
Devolatilization
Crack nucleation
Stacking start
Loss of viscosity (Inorganic Mat.)
Removal of heterogeneous atoms
Dehydrogenation
Micropore nucleation
La increasing
Removal of heterogeneous atoms
Lc increasing
Reducing micro pores
Removal of inorganic materials
Formation of 3 D graphitic structure
Organic materials

Franklin's Models of Carbon Structures

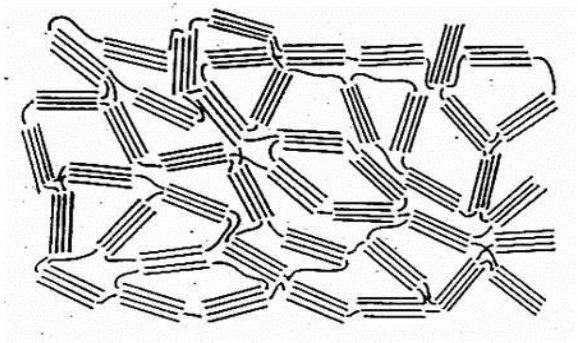

(a) Non-Graphitizing (Isotopic)

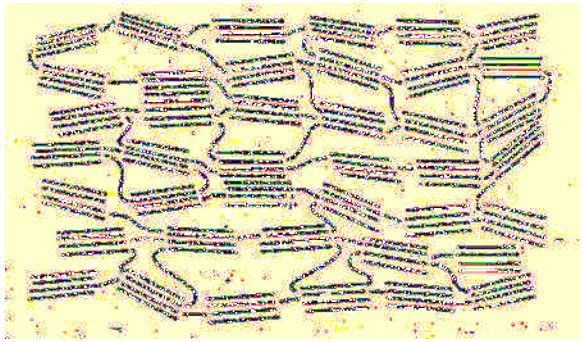

(b) Partially Graphitizing

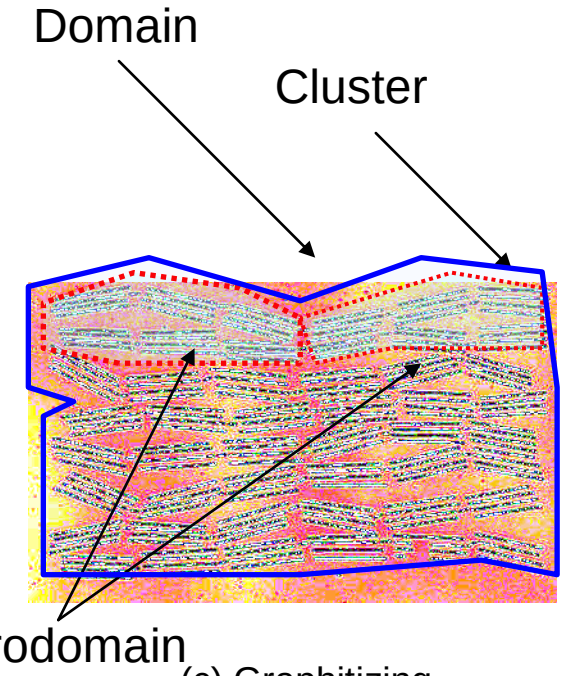

(c) Graphitizing

有機物の加熱による変化

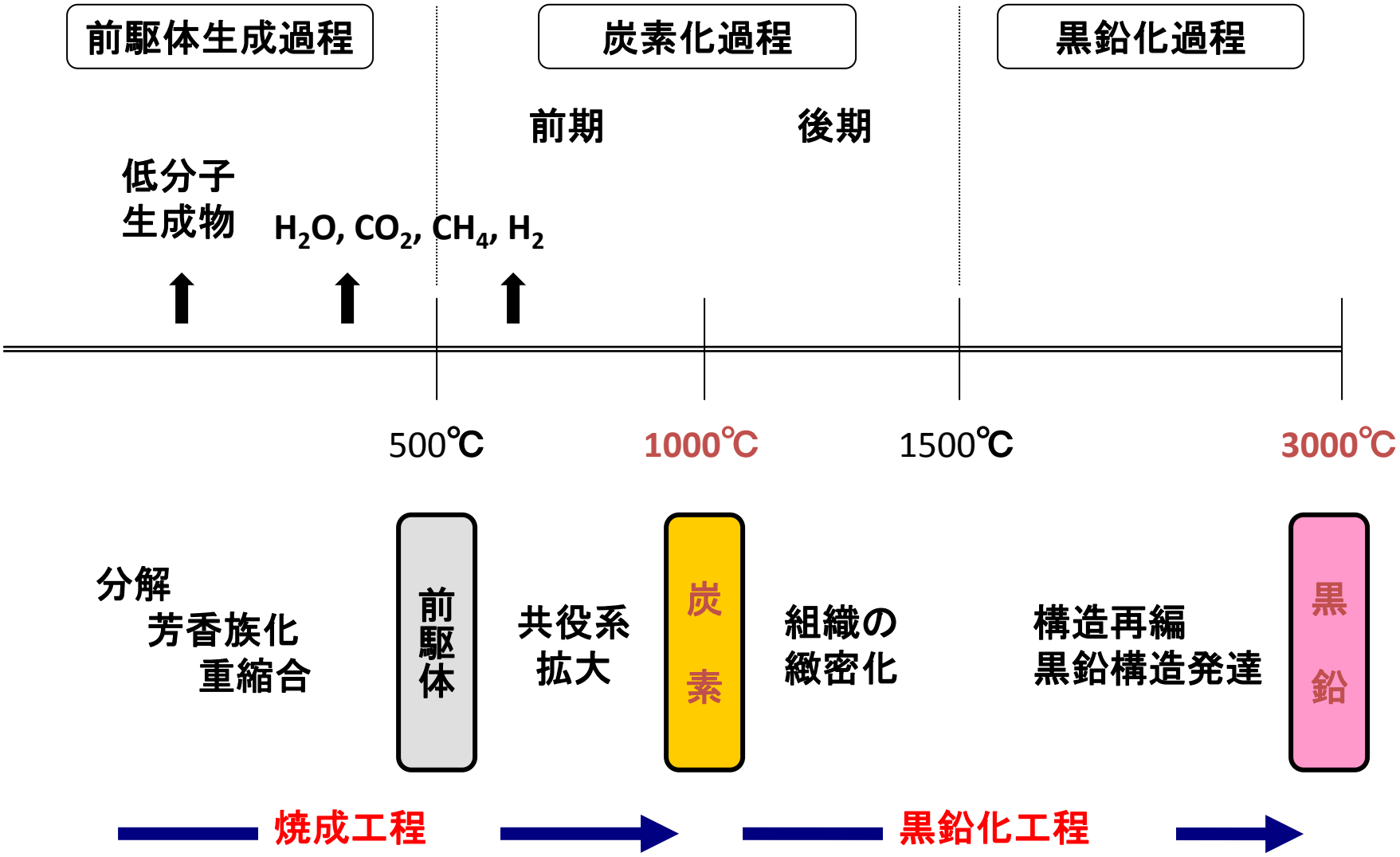

熱処理温度による結晶構造変化

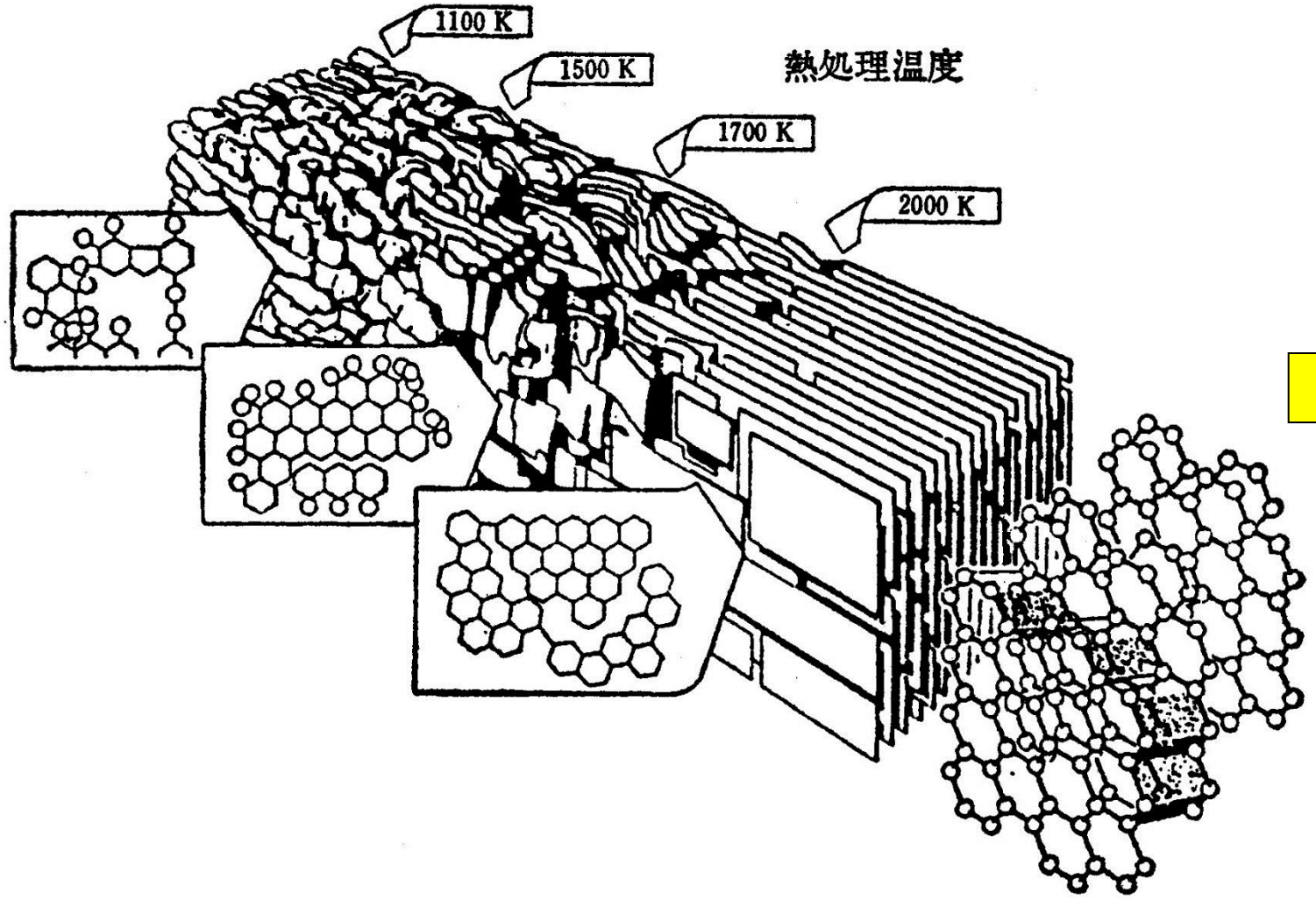

Structure of Needle Coke

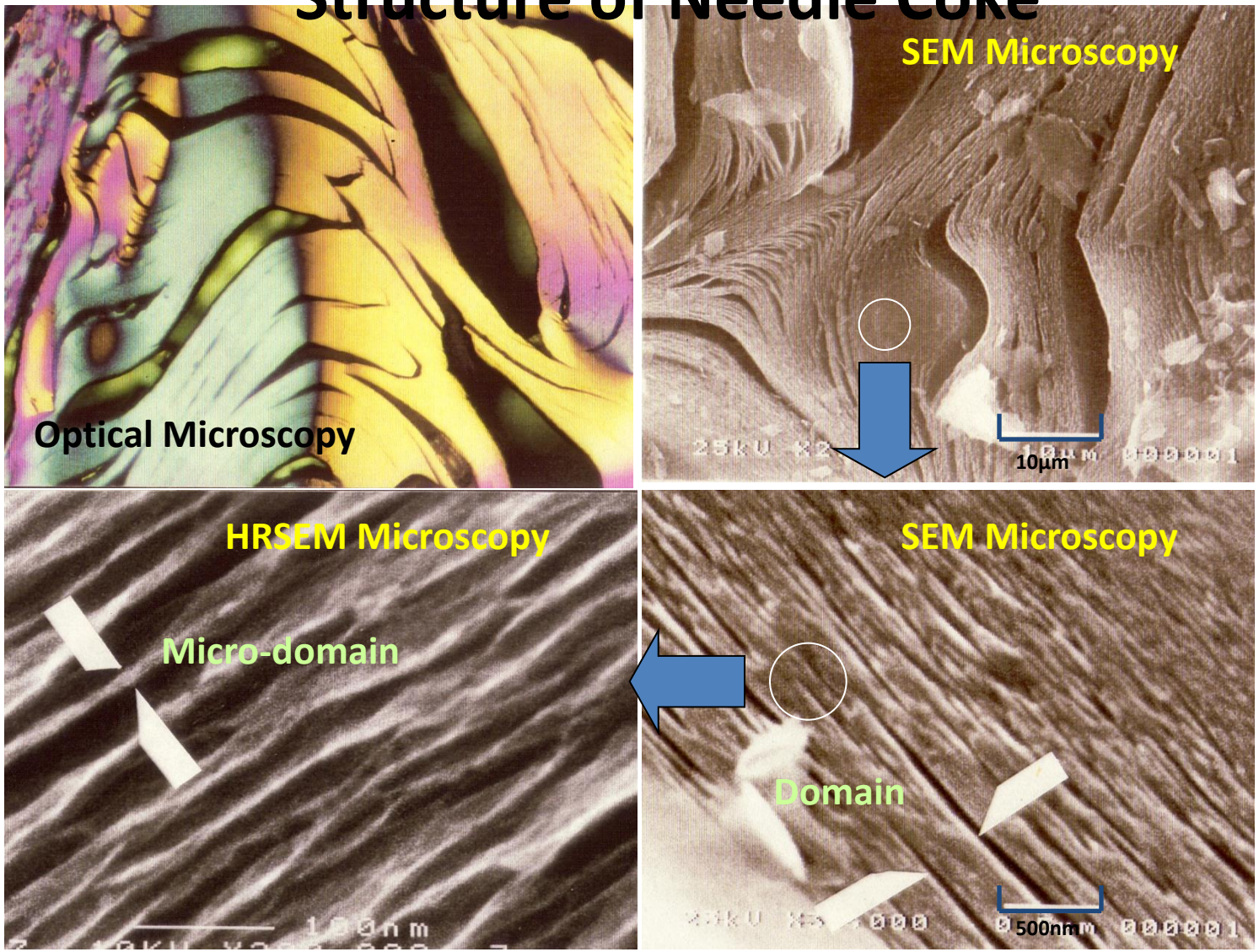

Nanoscopic Structure of Mesophase Pitch Based Carbon Fiber

Problem : Low Compressive Strength > Restriction of CFRP Application

Factor: Size and Distribution of Micro-domain

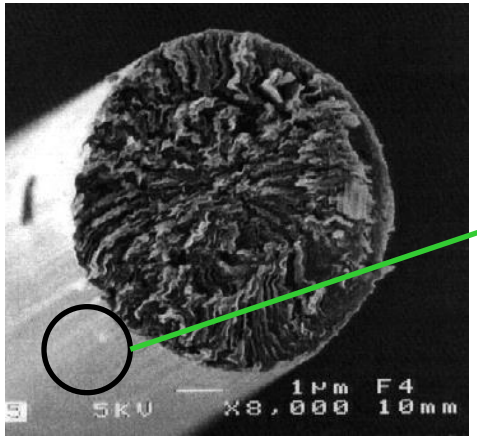

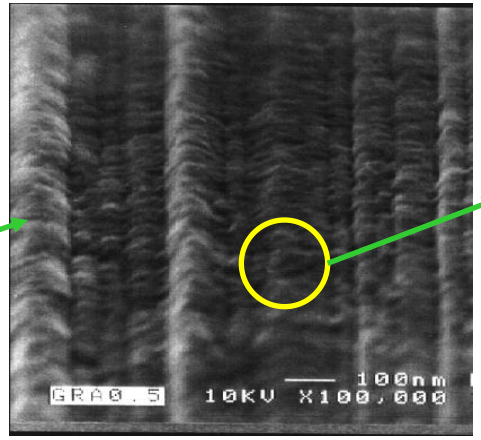

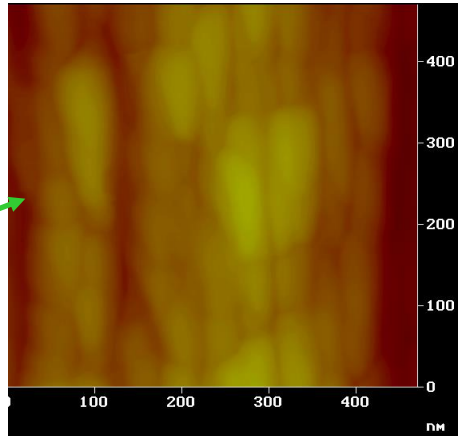

Pleat Structure > Homogeneous / Small > Increasing Compressive Strength

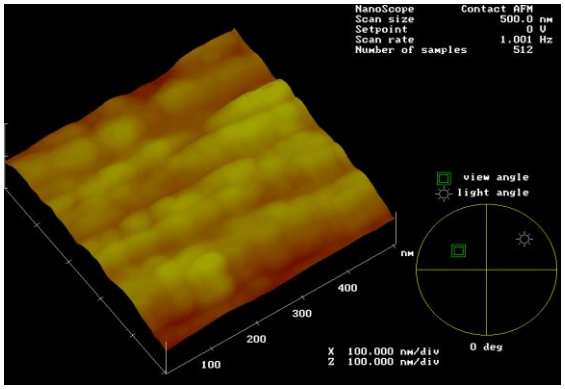

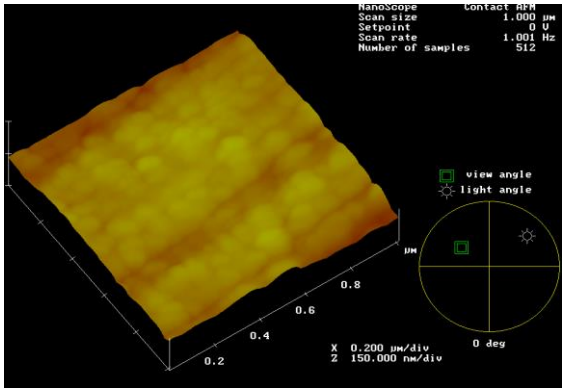

Molecular alignment theories of MCMB (Old Theories)

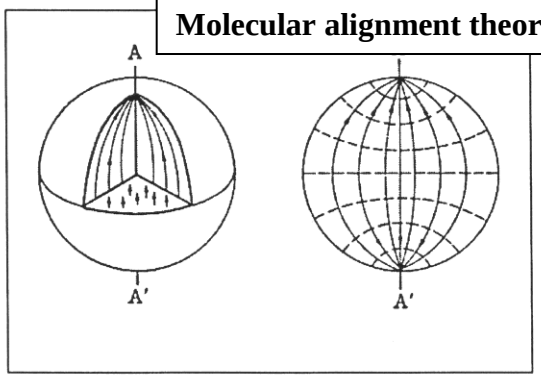

(a) Brooks-Taylor Type

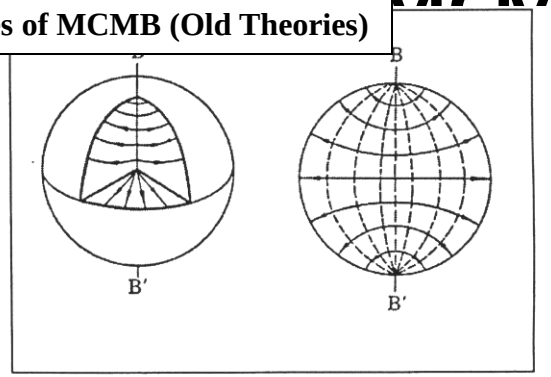

(b) Honda Type

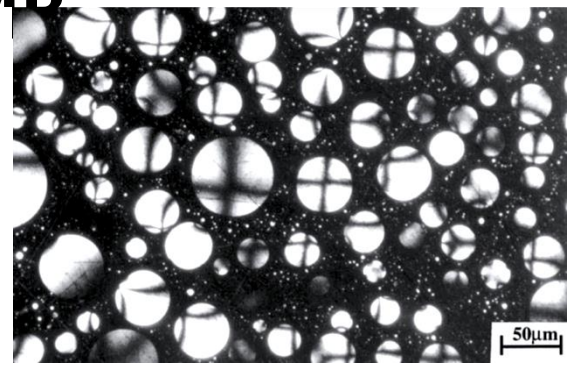

Optical Micrograph of MCMB in Isotropic Matrix

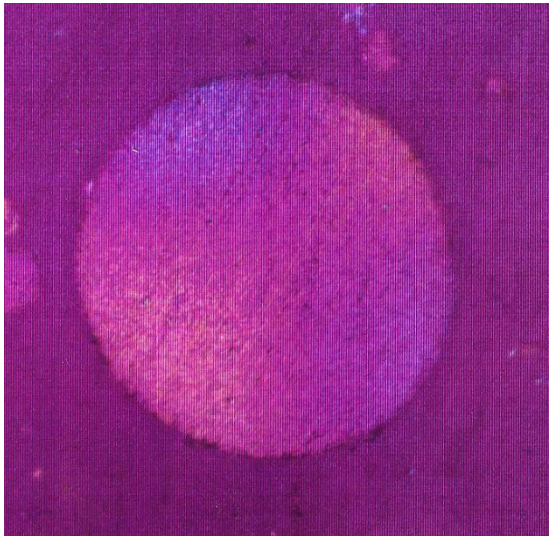

Optical Micrograph of PI
of AR pitch derived MCMB

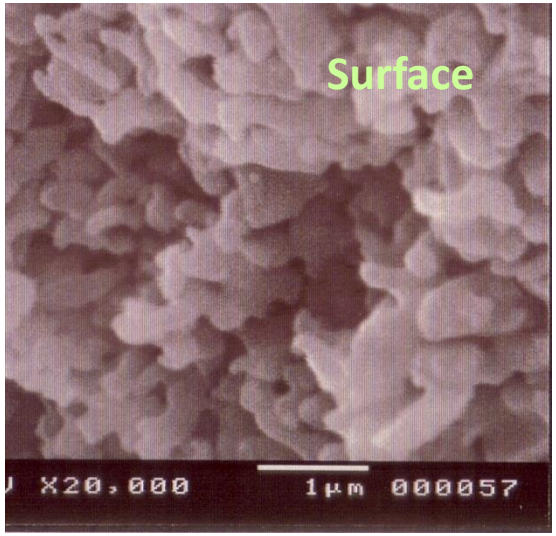

SEM Photograph of PI
of AR pitch derived MCMB

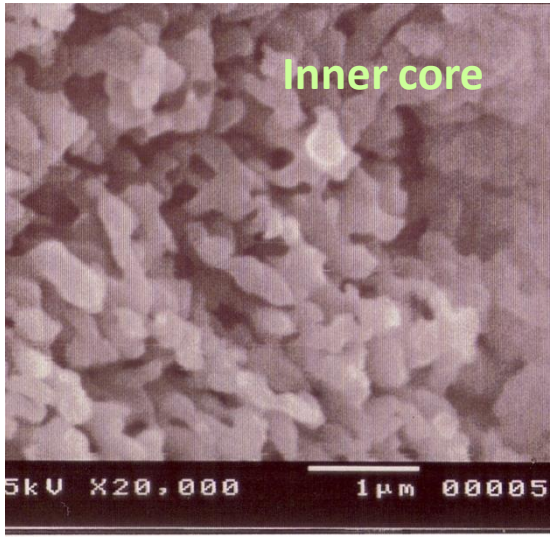

SEM Photograph of PI
of AR pitch derived MCMB

TEM Images of Hongye Anthracites Heat Treated at Various Temperatures

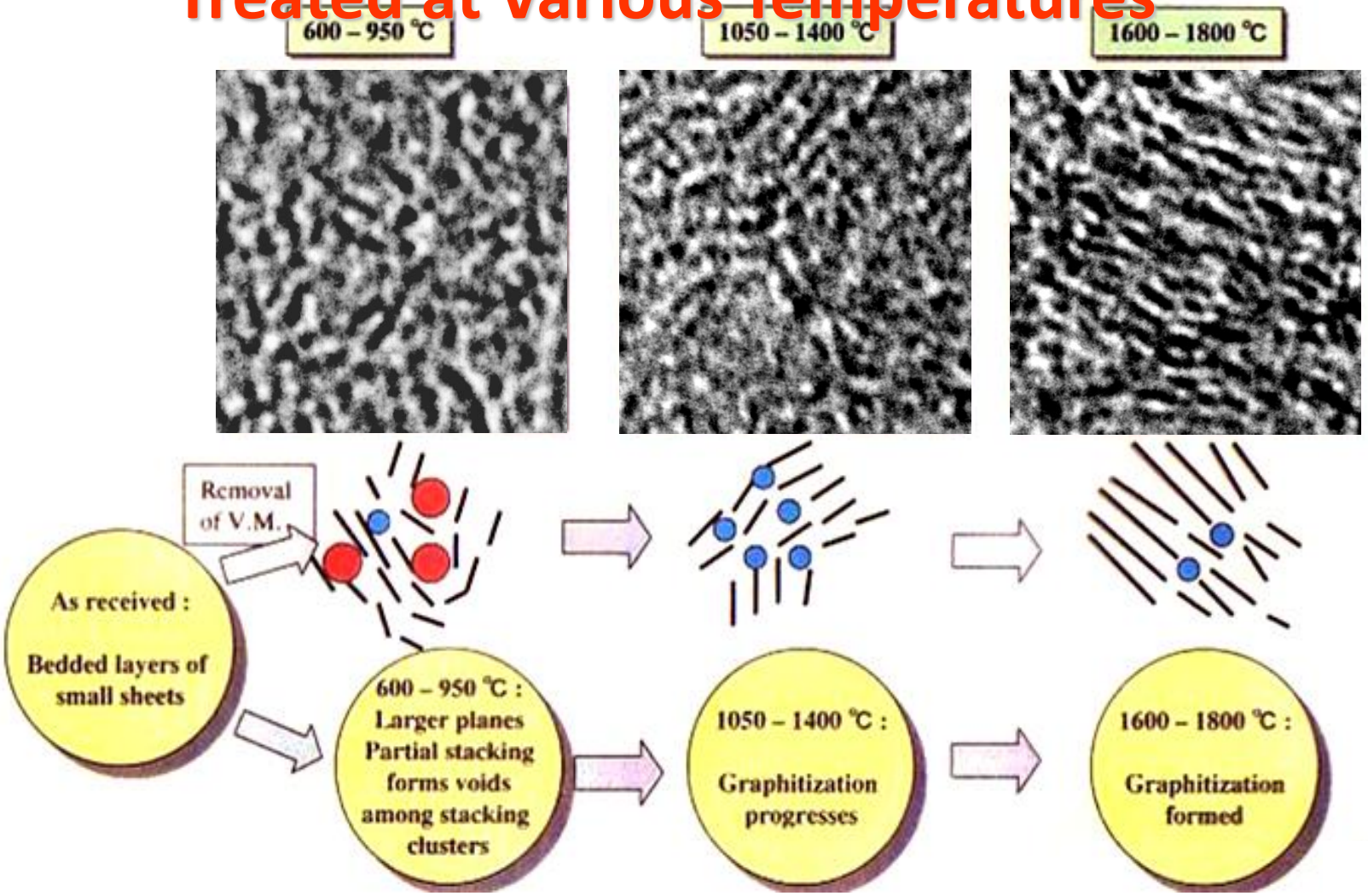

Structure of Activated Carbon

- **Surface Area, Pore: Depth Volume**

  Surface Structure
  Surface Chemistry
  Based and Edge Plane, Substituents
  Hetero atoms in Hexagon

- **Carbon Structure of Wall**

  Nano, Micro, Macro Structure of Carbon Wall
  -Graphitization Extent
  -Domain Structure

  → Density, Reactivity (Activated Surface)
  Precursor : Structure and Reactivity

Franklin's Models of Carbon Structures

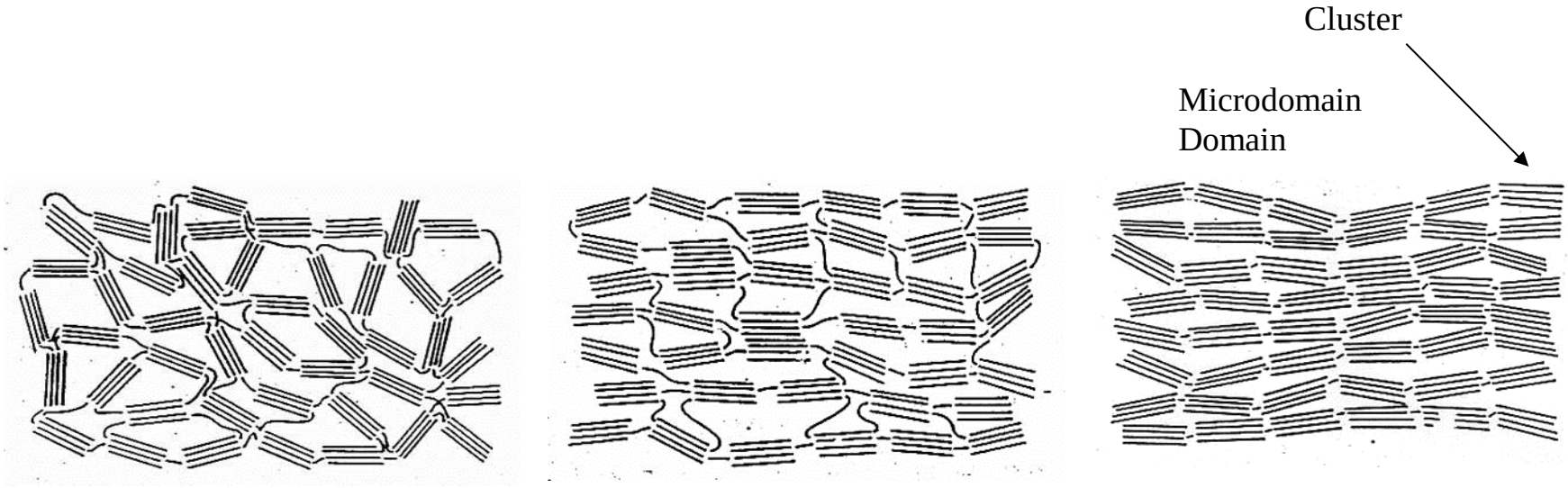

(a) Non-Graphitizing (Isotopic)

(b) Partially Graphitizing

(c) Graphitizing

Structural Models of Glassy Carbon Heated at High Temperature

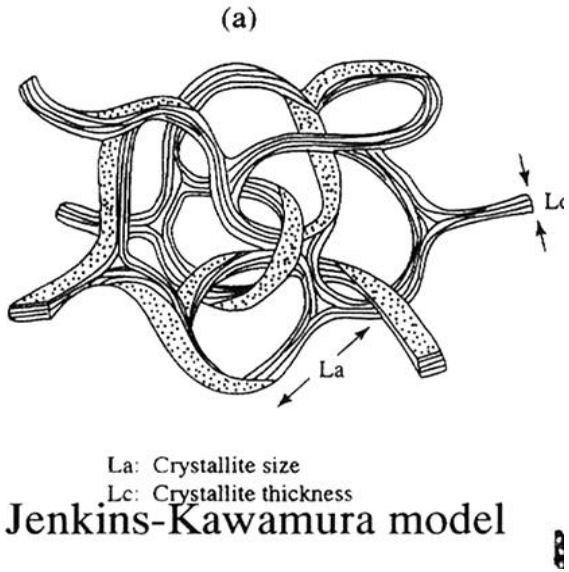

Jenkins-Kawamura model

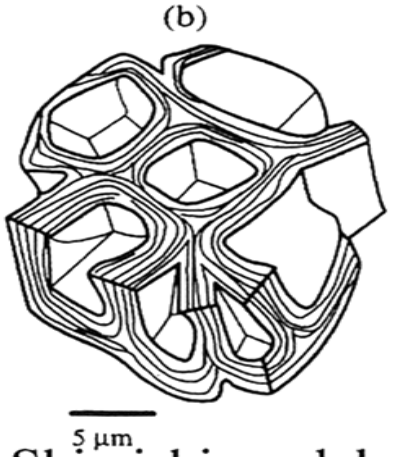

Shiraishi model

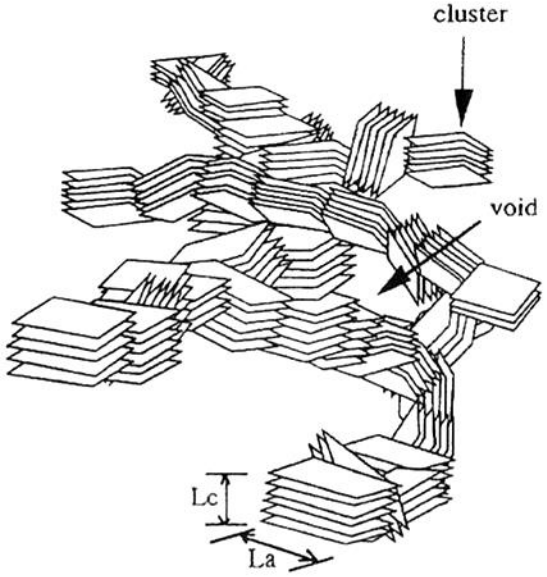

Mochida model

Structural Hierarchy in Mesophase Pitch

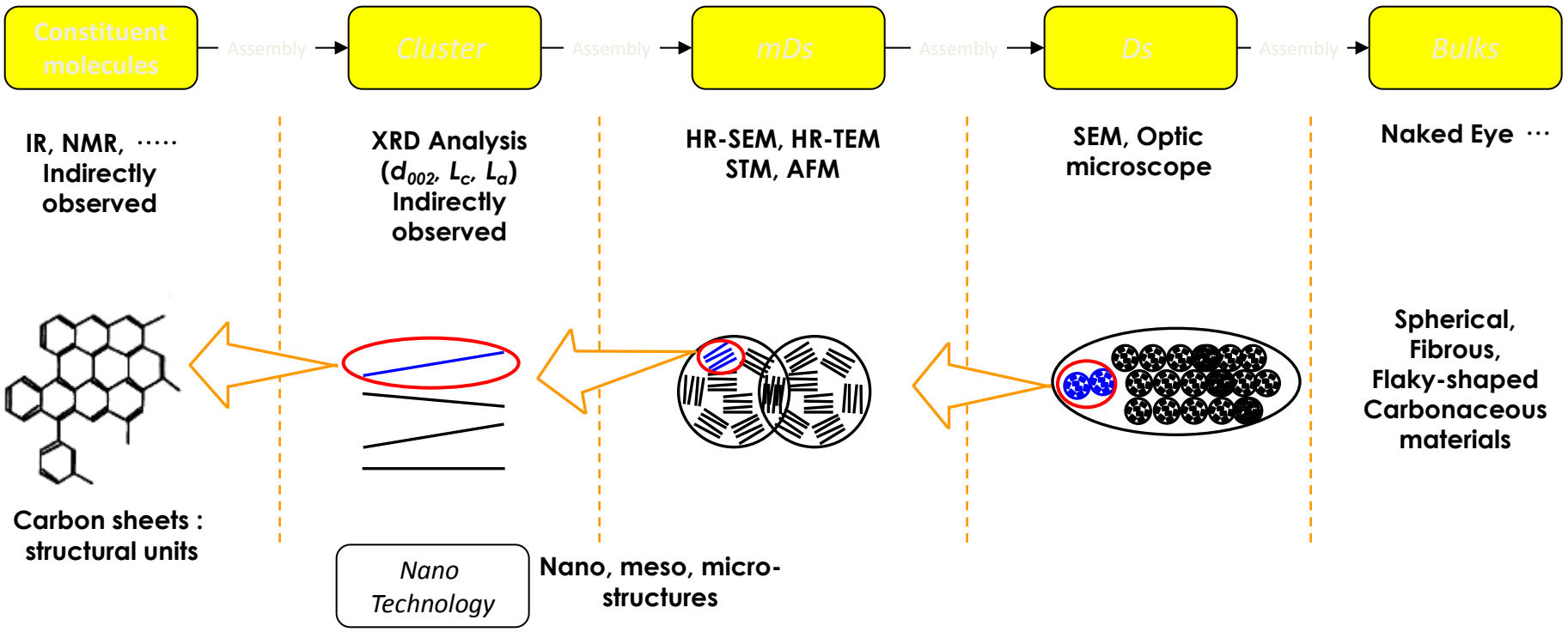

MCMB

Lot		容量(mAh/g, 0~1.5V)			Dcap. (0~0.5V)	低電圧特性 (0.5V/1.5V)(%)
		1cy	2cy	3cy		
600℃ 熱処理	ch	1497	440	368	124	**38.5**
	dis	396	342	321		
	効率(%)	26.5	77.6	87.2		
1200℃ 熱処理	ch	393	308	303	197	**67.1**
	dis	303	299	294		
	効率(%)	77.2	96.9	97.1		
1400℃ 熱処理	ch	359	295	289	198	**69.7**
	dis	291	288	284		
	効率(%)	81.1	97.6	98.3		
2000℃ 熱処理	ch	227	198	194	159	**83.0**
	dis	196	193	191		
	効率(%)	86.1	97.6	98.4		
2400℃ 熱処理	ch	298	262	259	238	**93.2**
	dis	258	258	256		
	効率(%)	86.6	98.5	98.8		
2800℃ 熱処理	ch	426	364	360	344	**96.5**

Previous study of Soft Carbon

Graphite has a limitation at capacity and power density, such reason enforced to develop other carbon materials like soft carbon and hard carbon

Ch-Dis Profile & SEM image

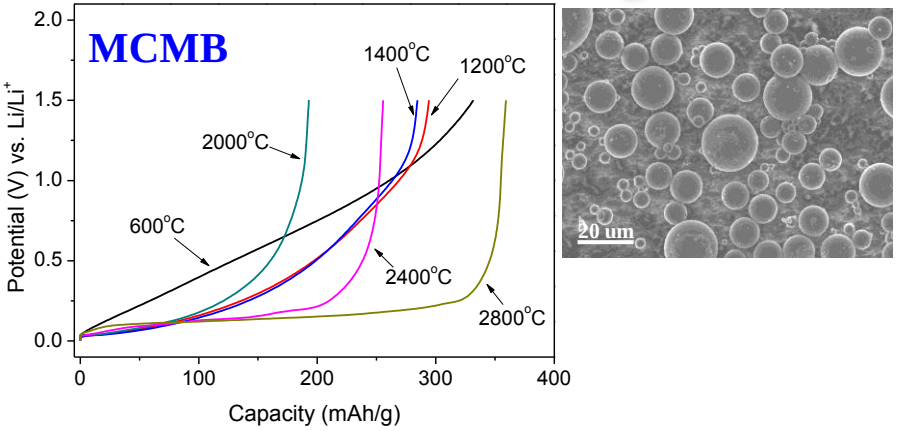

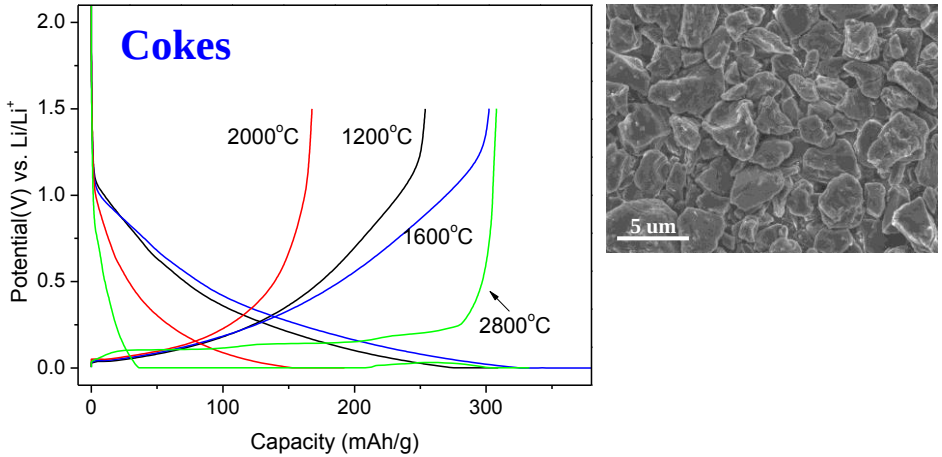

Structural change of Cokes

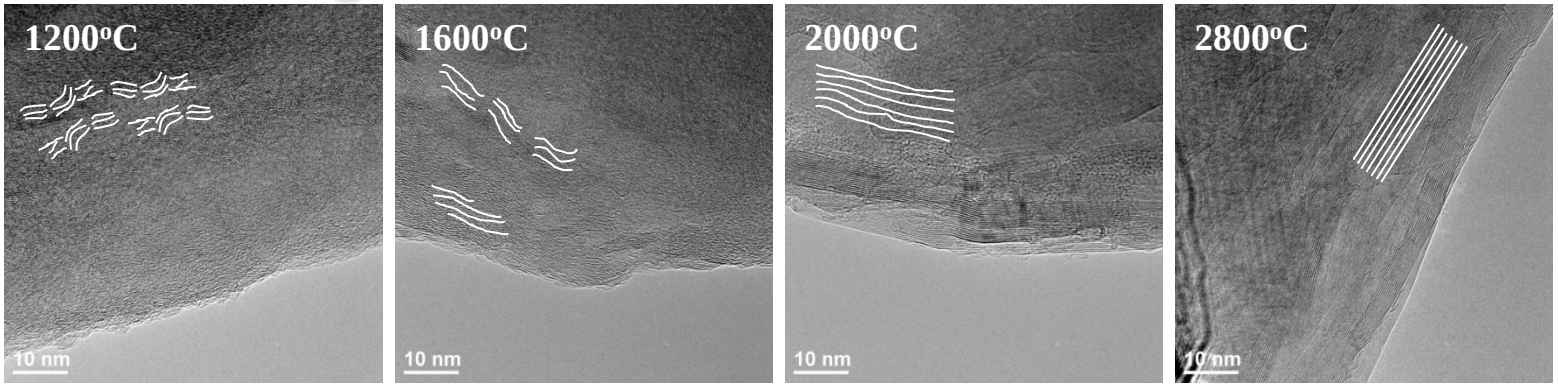

MCMB

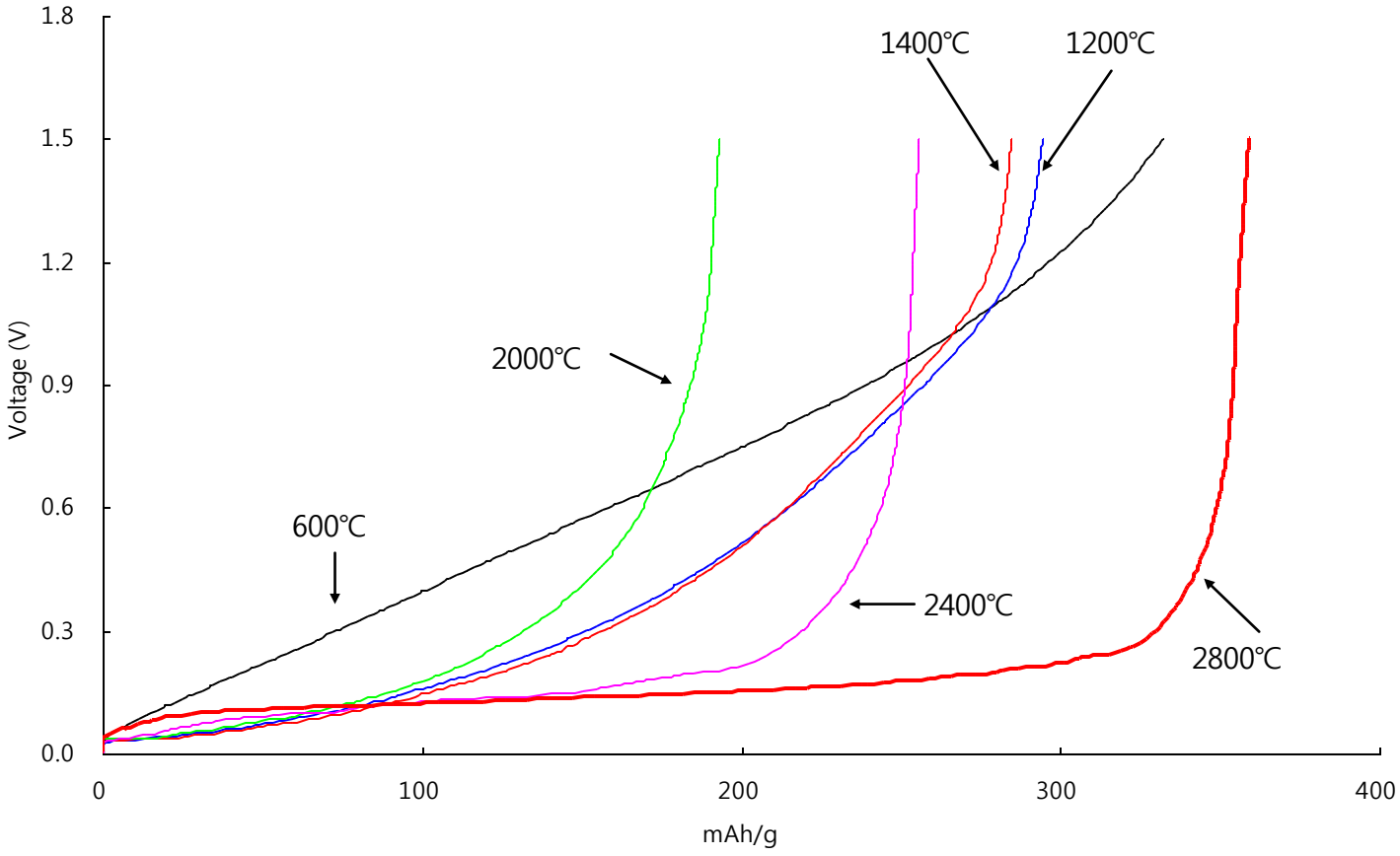
1.8
1.5
1.2
0.9
0.6
0.3
0.0
Voltage (V)
0
100
200
300
400
mAh/g
1400℃
1200℃
2000℃
600℃
2400℃
2800℃

MCMB

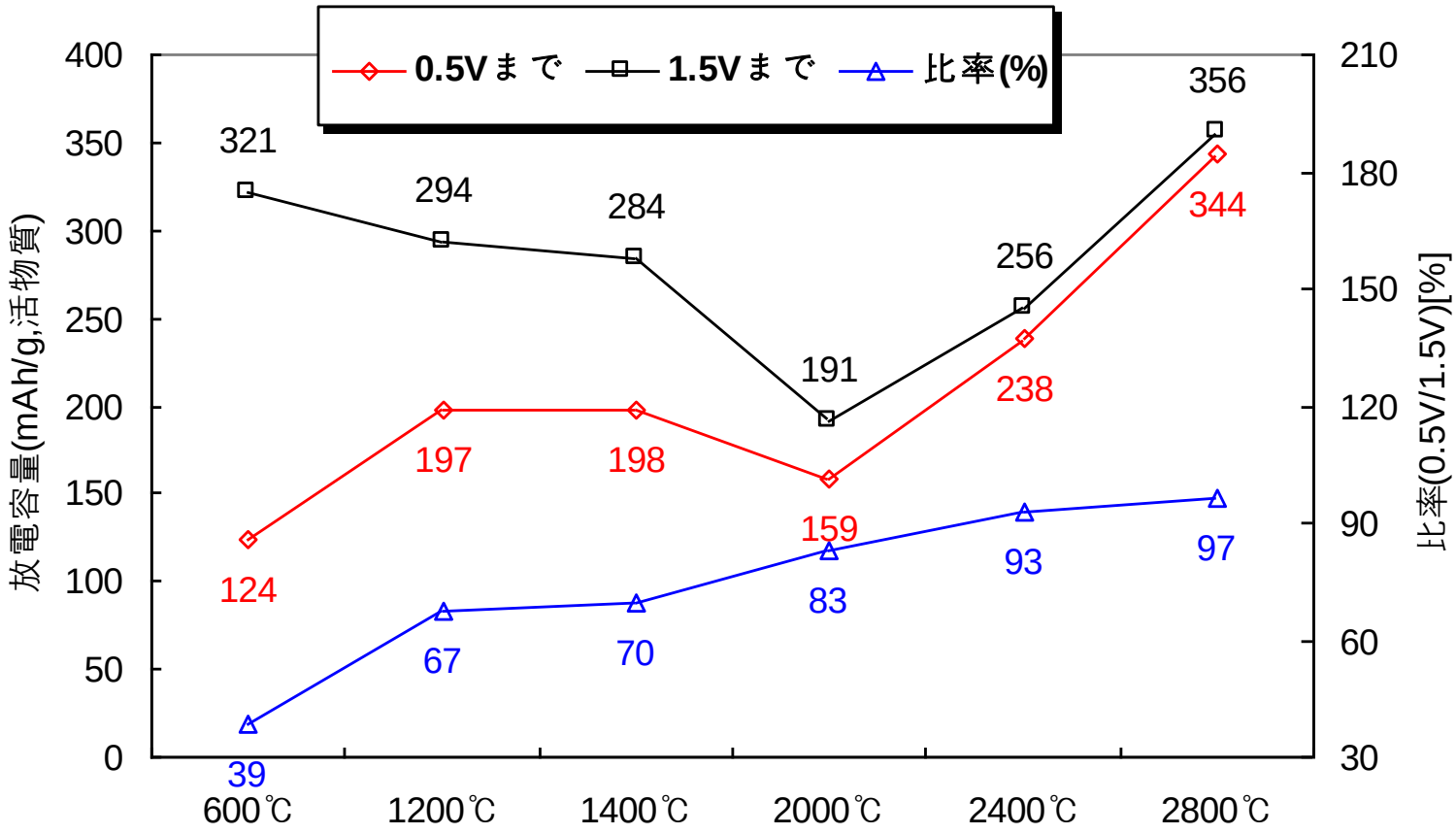
0.5Vまで
1.5Vまで
比率(%)
放電容量(mAh/g,活物質)
比率(0.5V/1.5V)[%]
400
350
300
250
200
150
100
50
0
210
180
150
120
90
60
30
321
294
284
191
256
356
124
197
198
159
238
344
39
67
70
83
93
97
600℃
1200℃
1400℃
2000℃
2400℃
2800℃

MCMB

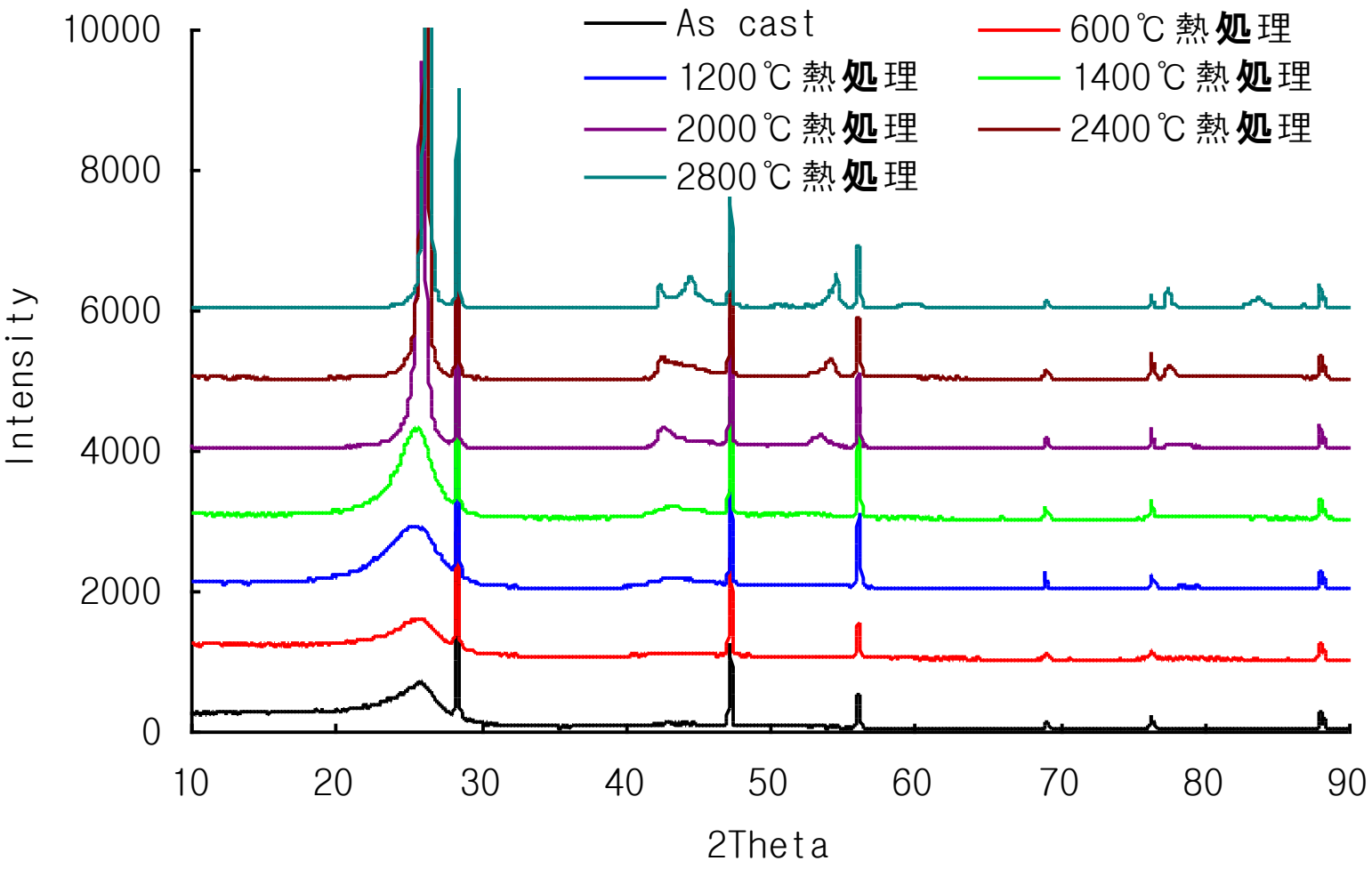
As cast
600℃ 熱処理
1200℃ 熱処理
1400℃ 熱処理
2000℃ 熱処理
2400℃ 熱処理
2800℃ 熱処理
Intensity
10000
8000
6000
4000
2000
0
10
20
30
40
50
60
70
80
90
2Theta

MCMB

	d_{002} (A)	Lc002 (nm)
As cast	3.4945	3.1
600℃ 熱処理	3.5138	3.1
1200℃ 熱処理	3.5278	4.1
1400℃ 熱処理	3.4876	6.8
2000℃ 熱処理	3.4280	35.44
2400℃ 熱処理	3.3887	53.70
2800℃ 熱処理	3.3628	122.0

MCMB

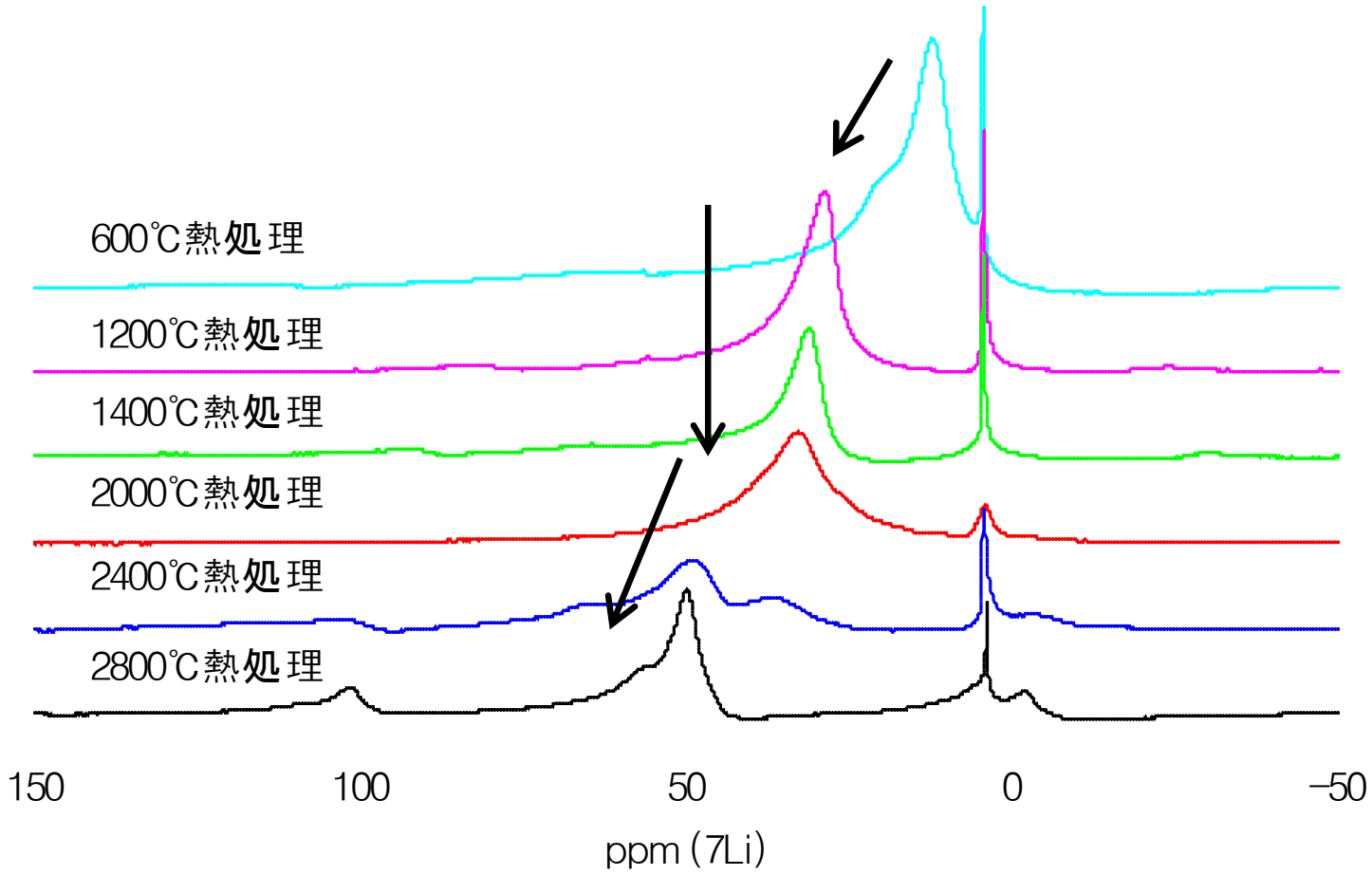
600℃熱処理
1200℃熱処理
1400℃熱処理
2000℃熱処理
2400℃熱処理
2800℃熱処理
150
100
50
0
−50
ppm (7Li)

Li-NMR of Various Carbons

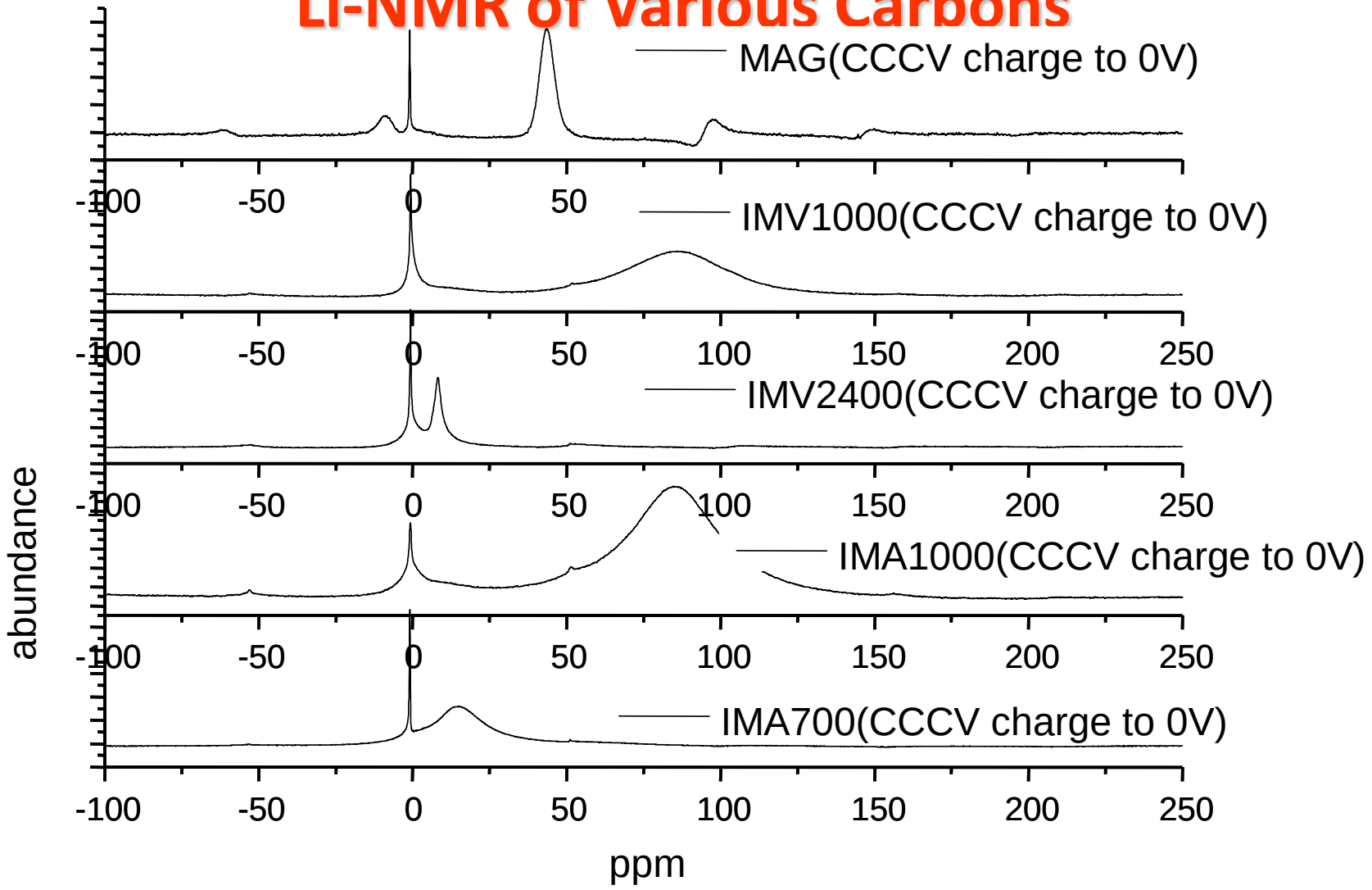

Discharging EVS Profiles of NC E Series

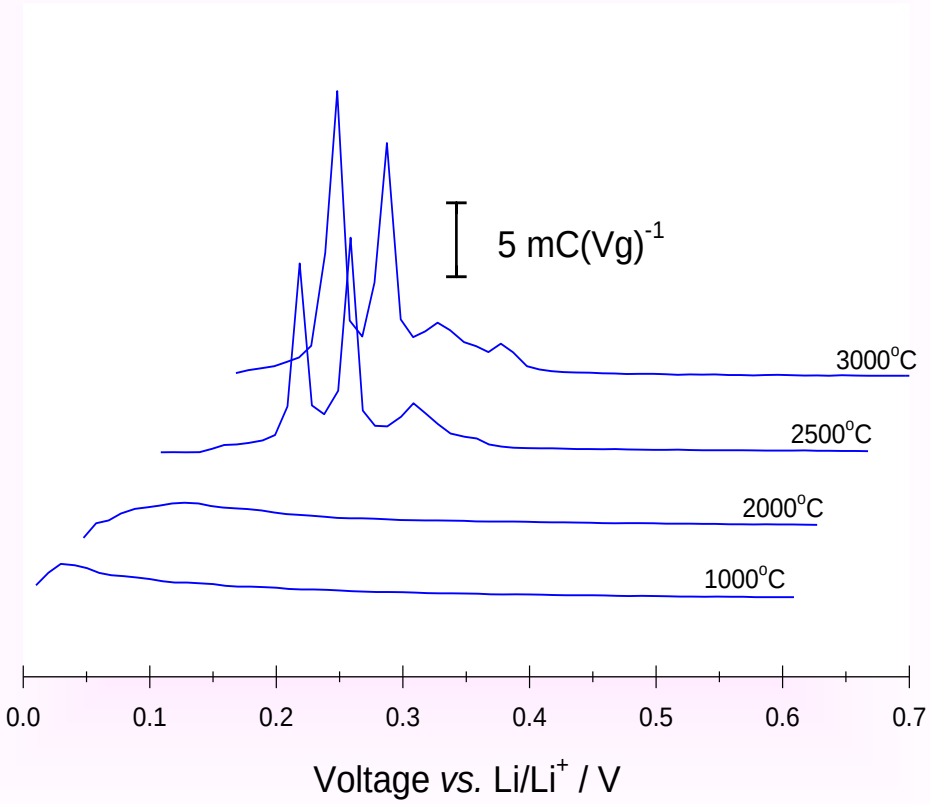

Discharging EVS Profiles of natural and synthetic graphites

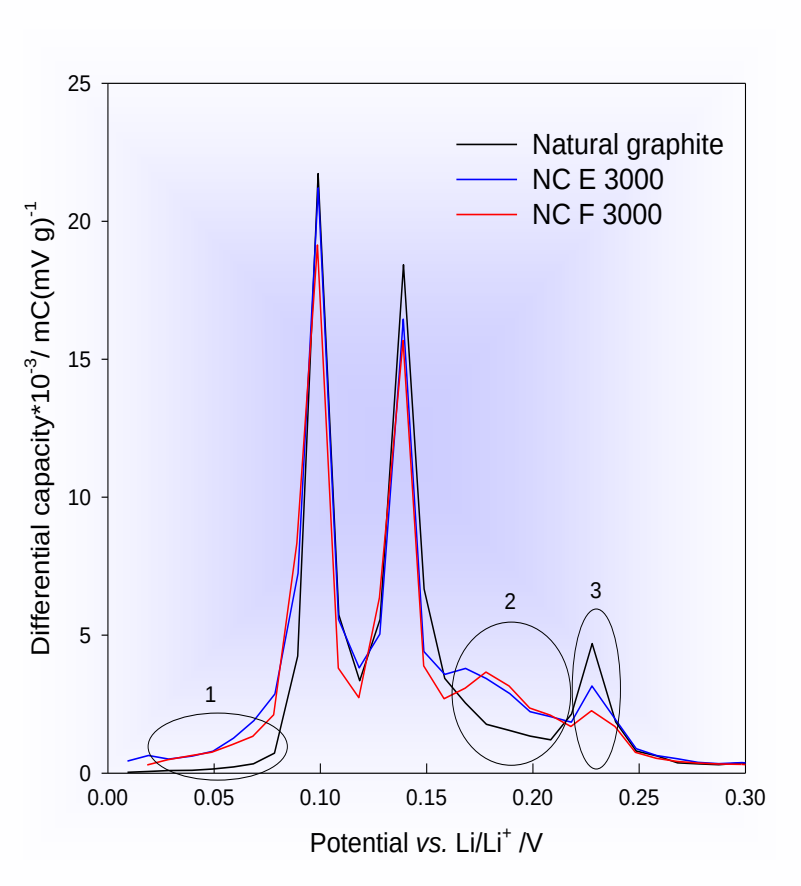

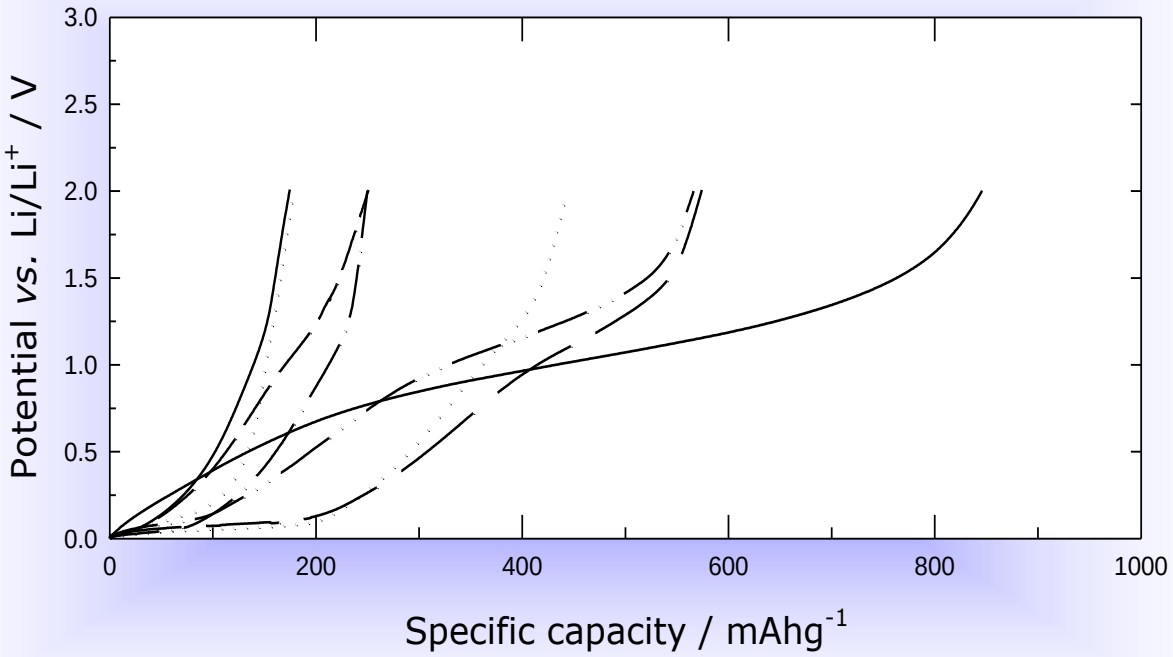
Potential vs. Li/Li+ / V
3.0
2.5
2.0
1.5
1.0
0.5
0.0
0
200
400
600
800
1000
Specific capacity / mAhg-1

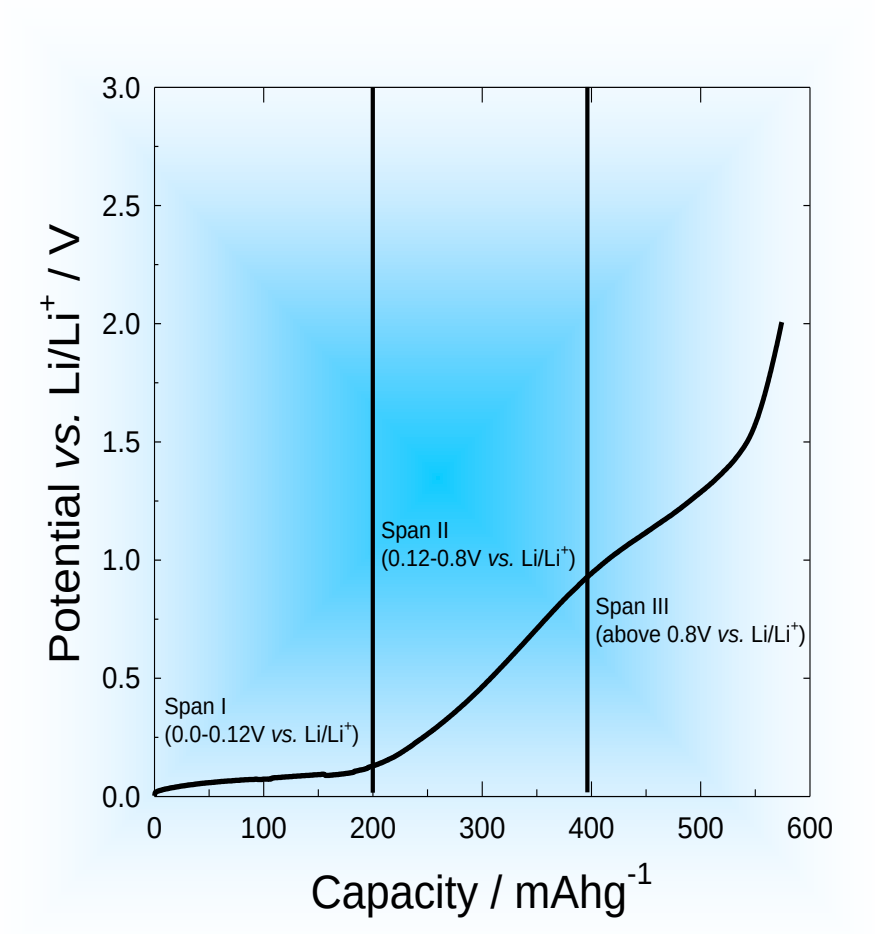
3.0
2.5
2.0
1.5
1.0
0.5
0.0
0
100
200
300
400
500
600
Potential vs. Li/Li+ / V
Capacity / mAhg-1
Span I
(0.0-0.12V vs. Li/Li+)
Span II
(0.12-0.8V vs. Li/Li+)
Span III
(above 0.8V vs. Li/Li+)

^{7}Li NMR MAS of MNIP 1000: fully-lithiated. RT

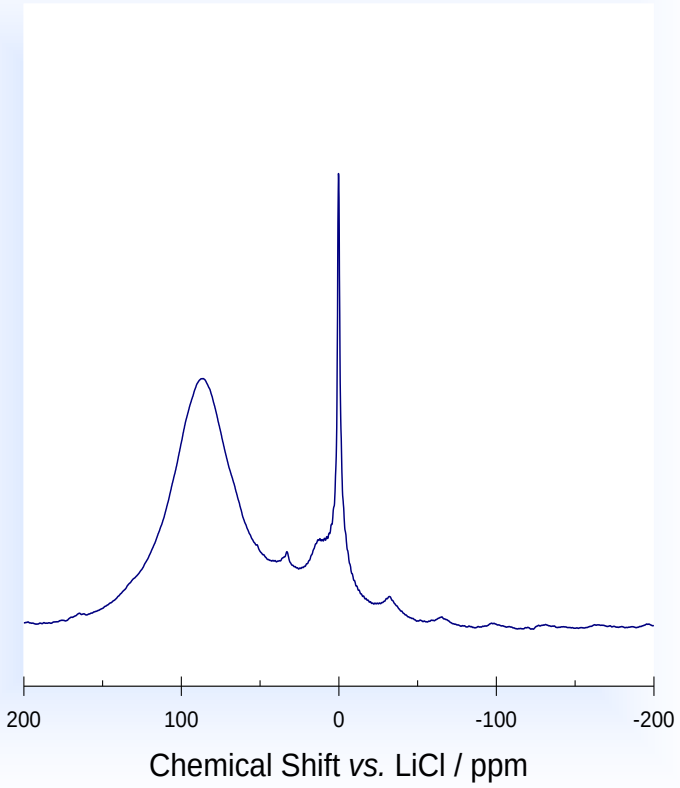

Four Li's

I. 0 ppm (Ionic): Electrolyte, decomposition product, etc.
II. 6 ppm (Ionic): Site III (ultra-micropores
III. 12 ppm (Ionic): Site II (carbonaceous interlayers)
IV. 82 ppm (Semi-metallic): Site I

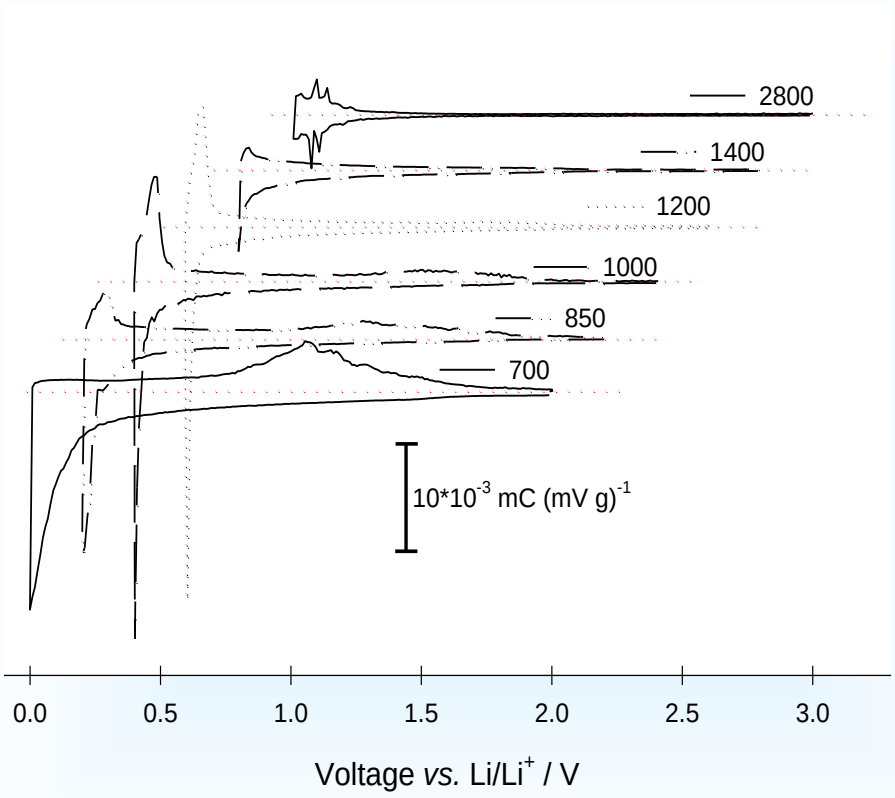
2800
1400
1200
1000
850
700
10*10-3 mC (mV g)-1
0.0
0.5
1.0
1.5
2.0
2.5
3.0
Voltage vs. Li/Li+ / V

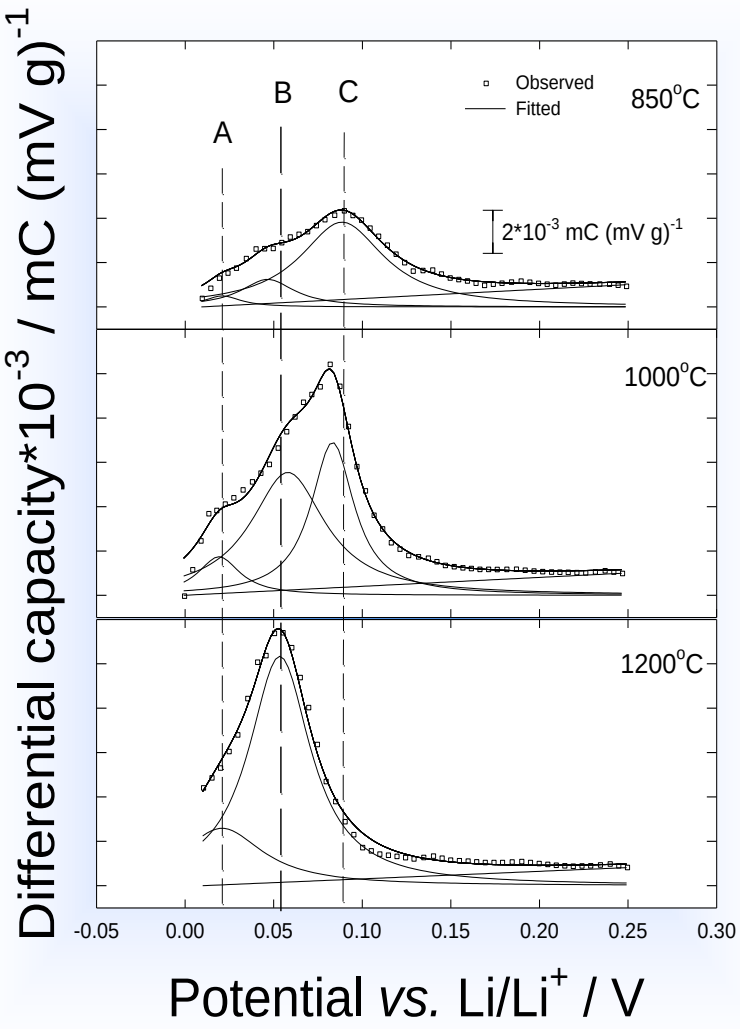
Differential capacity*10-3 / mC (mV g)-1
A
B
C
Observed
Fitted
850°C
2*10-3 mC (mV g)-1
1000°C
1200°C
-0.05
0.00
0.05
0.10
0.15
0.20
0.25
0.30
Potential vs. Li/Li+ / V

Roles of Carbon for Anode of Li-ion Batteries

- Anodic Electrode to Hold Reduced Li-ion

  Intercalation → Graphite

  Surface Electron Transfer into Sealed Void
  → Hard or Low Temperature
  Calcined Carbon

- Electron Conductive Material

  Anodic Carbon and Cathode Material

- Expansion Moderator

  Holding and Release of Ion Is Accompanied with Volumetric Charge

  Larger Capacity per Volume → Larger Expansion

- Moderation and Control of SEI

  Irreversible Charge → Surface Coating, Composite Structure

Charge/Discharge Profiles of MCMB

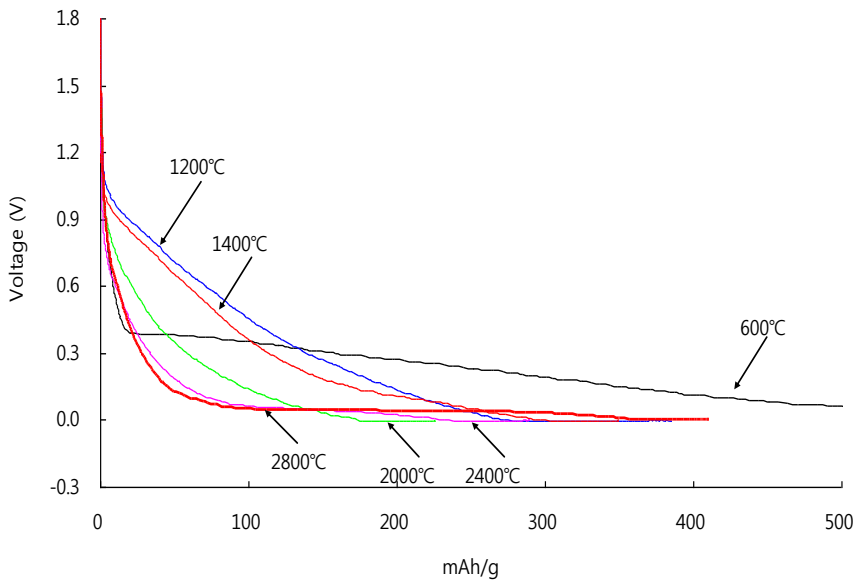

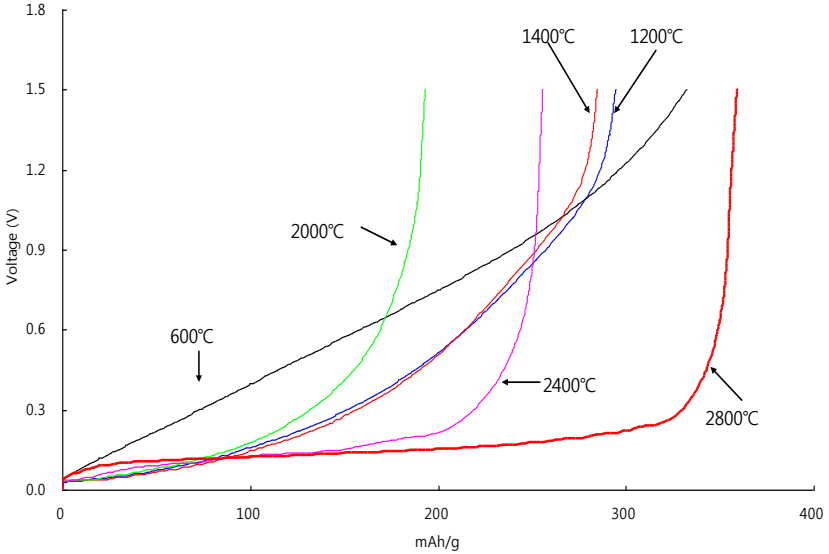

Li-NMR of Charged Li-ion in Heat Treated MCMB

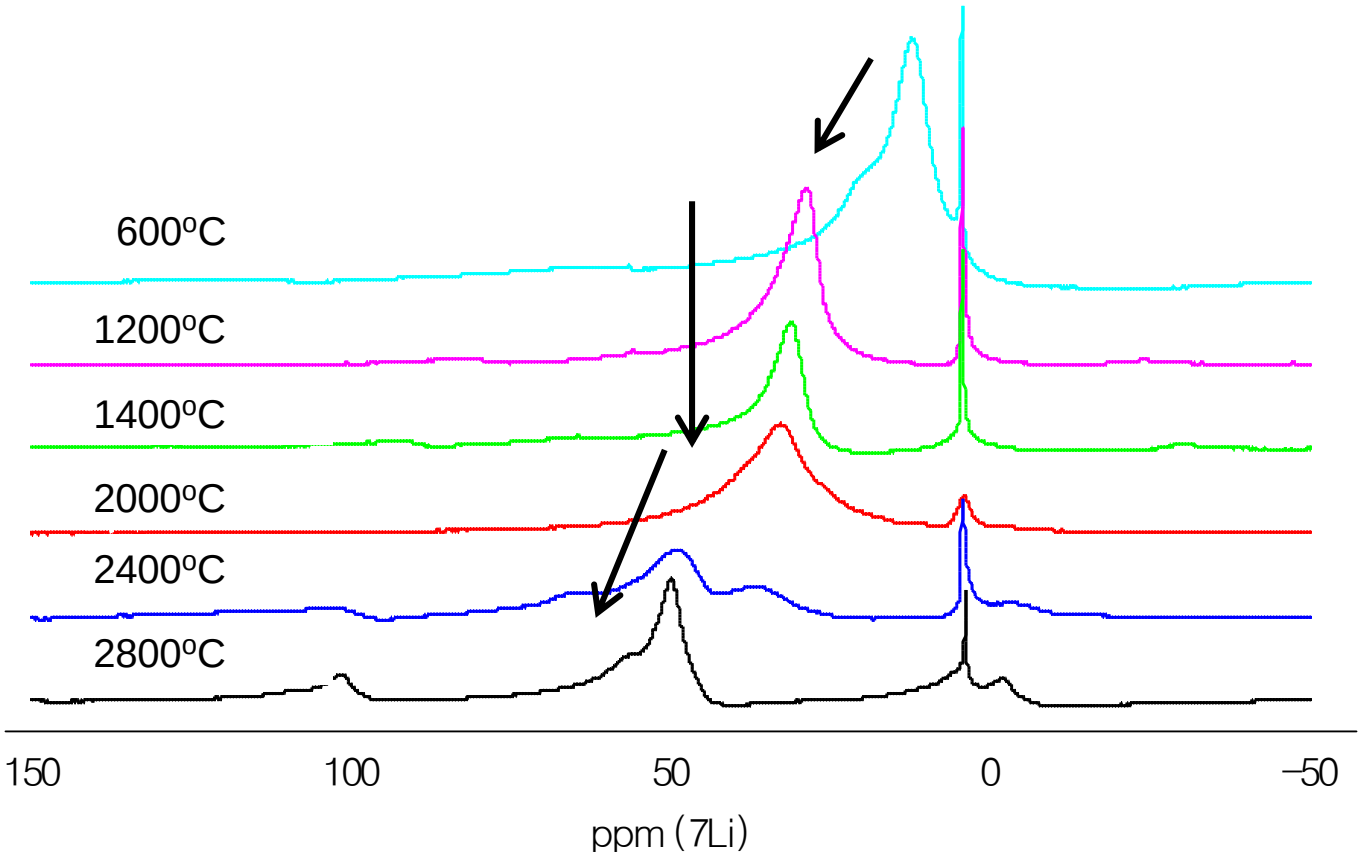

Discharge Profiles of Typical Graphites

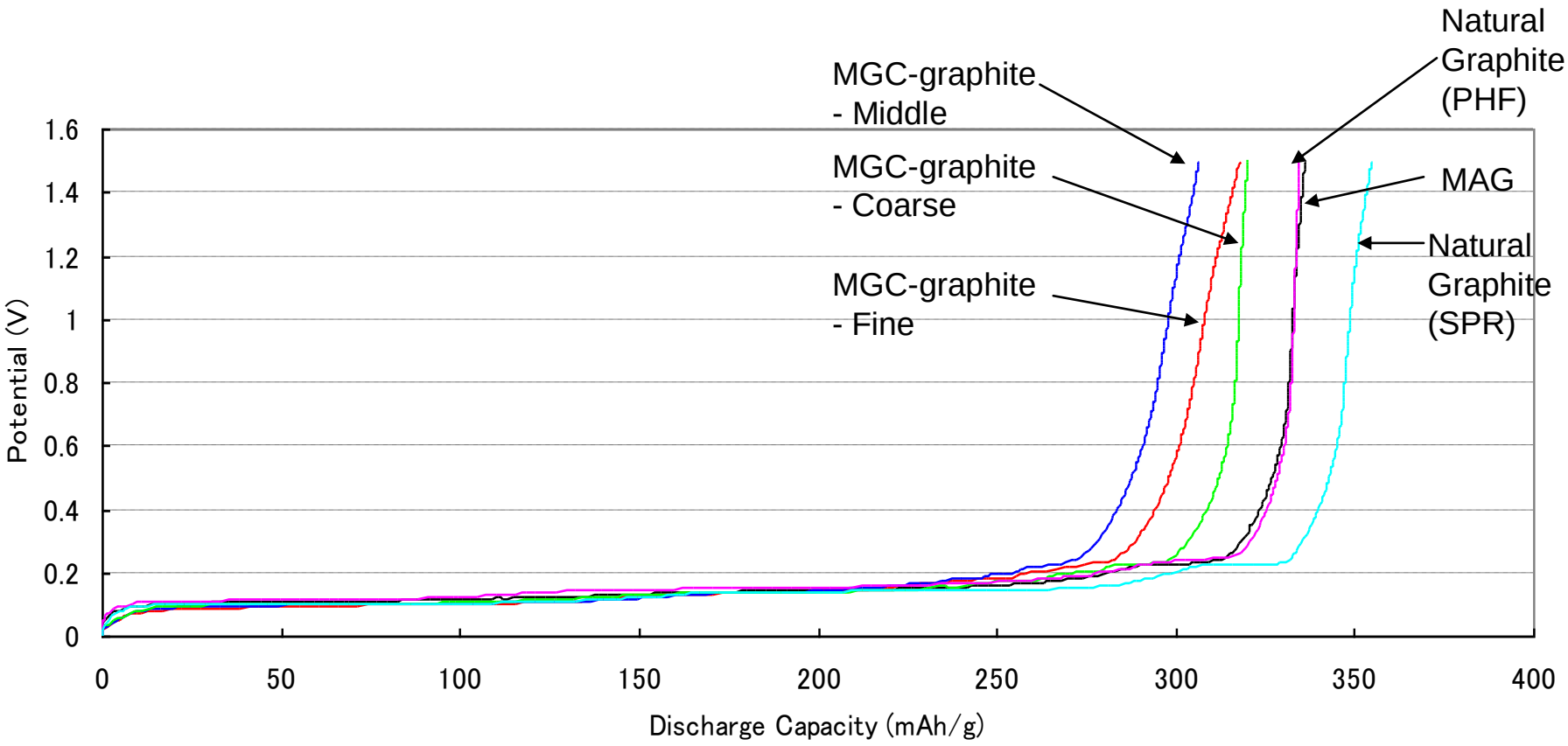

Charge/Discharge Profiles of Synthetic Graphite

(MAG; Hitachi Chemical Co.)

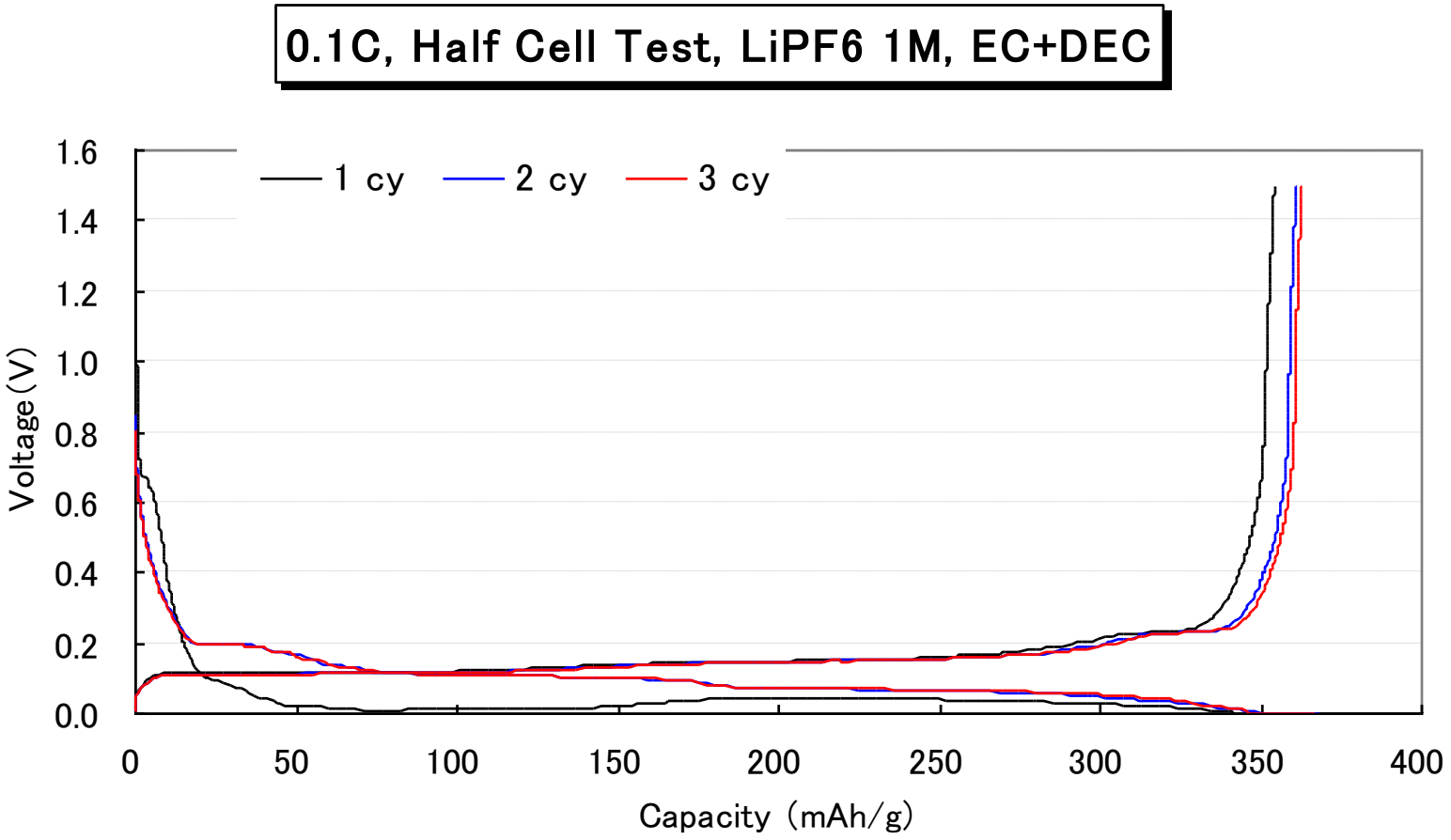

Typical Graphites

Natural Graphites

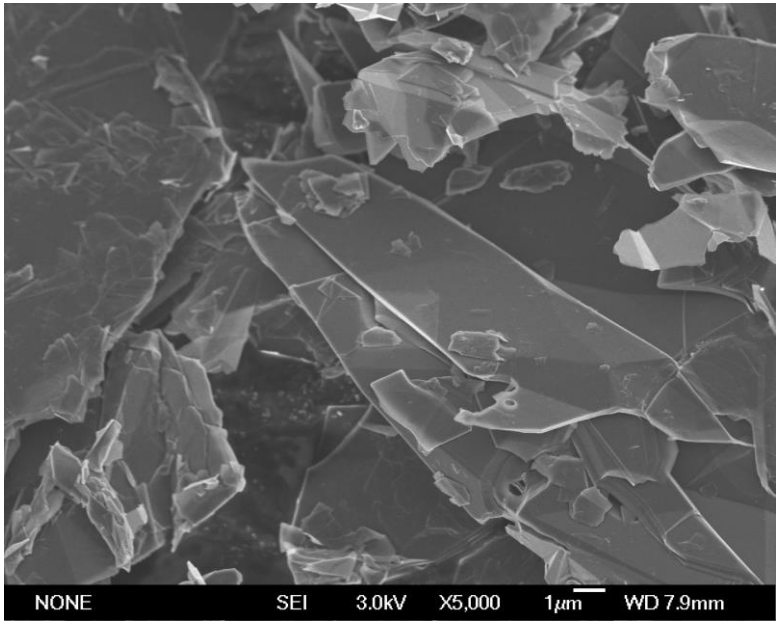

- Cheap
- High graphitization degree
- Large Irreversible Capacity
- Relatively poor Cycle Life
- Poor Rate Capability

Synthetic Graphites

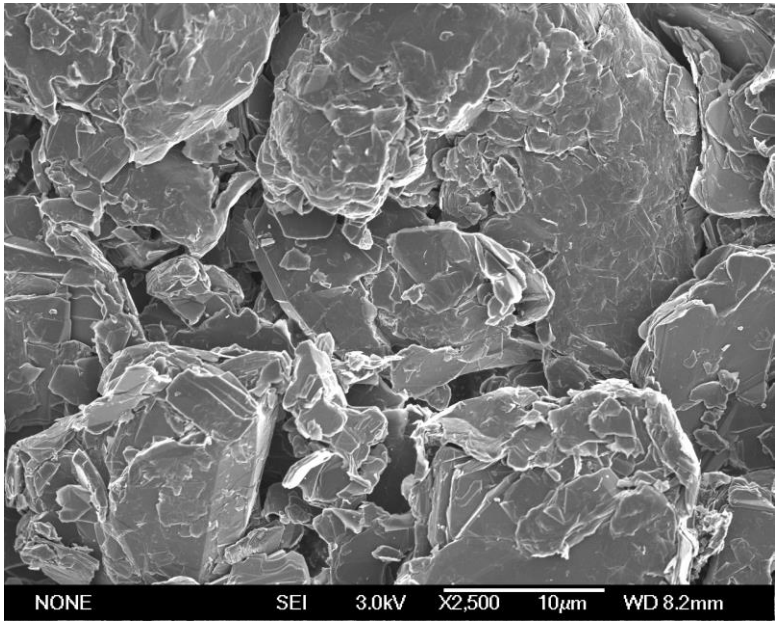

- Good 1st cycle efficiency & Cycle Life
- Relatively high graphitization degree
- Poor Rate Capability

(MAG; Hitachi Chemical Co.)

Surface Oxygen Functional Groups of AC

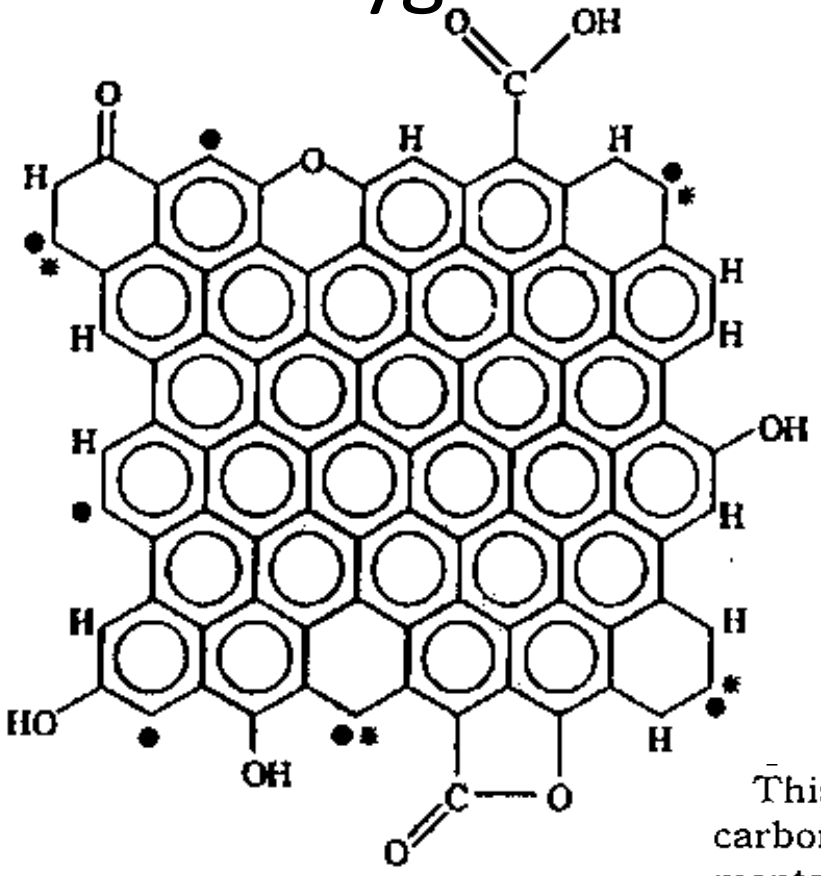

This structure is representative of an activated carbon with a crystallite width of 15 Å and an elemental analysis (by weight) of 87.5% C, 11.3% O, 1.2% H, ● represents an unpaired σ electron ; ●* represents an "in-plane σ pair" with * being a localized π electron, (Radovie)

SEM & TEM Images of PCNF Series

Ref.) S. Lim, et al.. *J. Phys. Chem. B* 108 (5), 1533 – 1536 (2004)

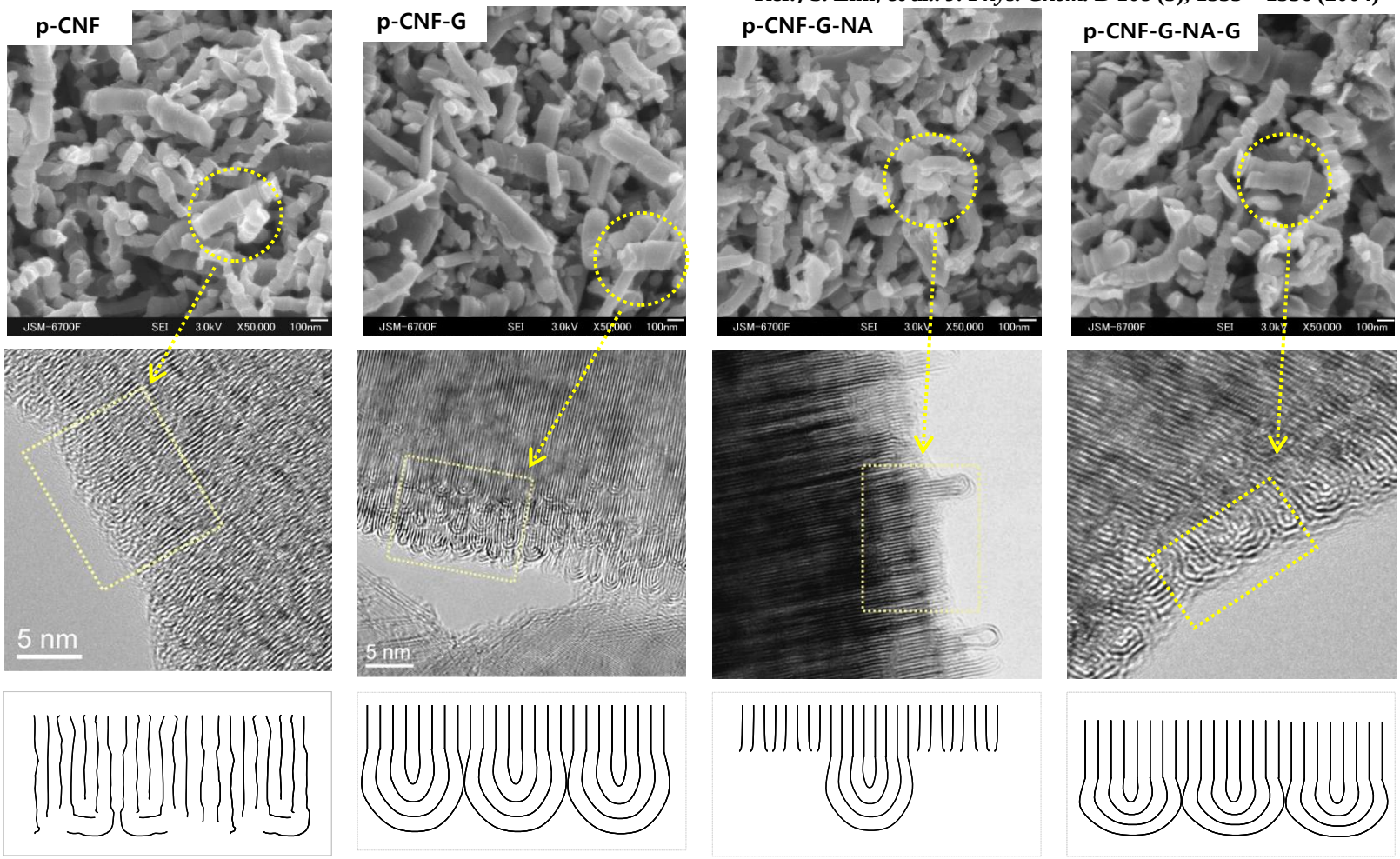

According to the graphitization degree,
we found some difference at edge plane by TEM analysis

Basic study of solid electrolyte interphase (SEI)

Characteristics of SEI

- Reduction of electrolyte components on anodes on initial charge
→ Irreversible capacity loss
→ Decrease of first-cycle coulombic efficiency
- Passage of Li-ion migration, but high electronic resistivity
- Essential to determine the electrochemical properties and safety of Li-ion battery

< Schematic model of SEI formed on anodes >

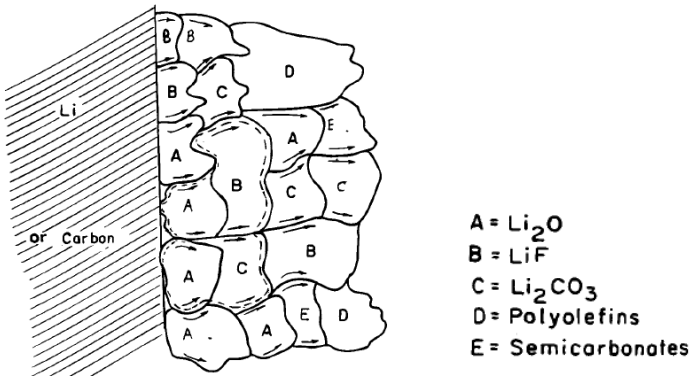

E. Peled et al., J. Electrochem. Soc. 144 (1997) L208

Previous researches on SEI

- Focused on SEI formation behavior of cross section of HOPG However, the cross section of HOPG was composed of edge planes and basal planes.

< Cross section of HOPG >

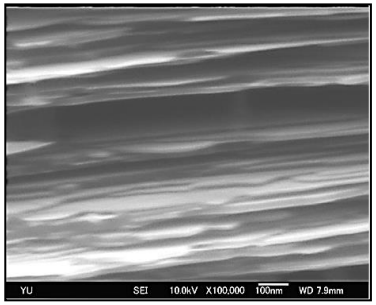

•T. Kim *et al.*, *Langmuir* 22 (2006) 9086.

Necessary to prepare well-defined edge and basal surfaces

Ch.2

Study on SEI formation behavior on well-defined edge and basal surfaces prepared by carbon nanofibers as a model material.

Chap.2 Solid electrolyte interphase formation behavior of well-defined carbon surfaces for Li-ion battery systems

✓ Objectives

- To track the SEI formation behavior on well-defined edge and basal surfaces of platelet carbon nanofibers (PCNF) by TEM and to study the effects of its boron-doped surfaces on SEI formation

✓ Contents

- Preparation of PCNF with well-defined edge and basal surfaces as a model material
- Effect of edge and basal surfaces on the SEI formation
- Effect of boron doping on the SEI formation

Preparation of PCNFs with well-defined surfaces

PCNF : Edge surface

- Fe catalyst
- $CO:H_2$ = 4:1 (total 2 L/min)
- 640˚C、4 h

PCNF-G : Basal

- 2800˚C, 10 min

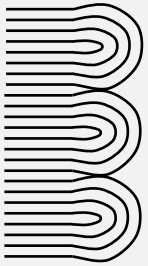

PCNF-G-NA : Edge

- 10 wt.% HNO_3
- 155˚C, 28 h

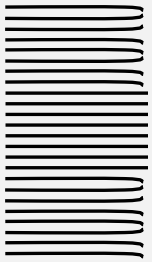

PCNF-B-G : Basal

- Ball-mill of PCNF with boric acid (5 wt% boron)
- 2800˚C, 10 min

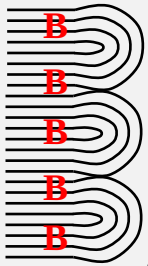

PCNF-B-G-NA : Edge

- 10 wt.% HNO_3
- 155˚C, 28 h

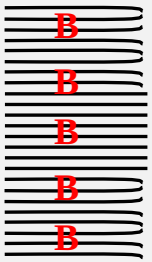

PCNF : Platelet carbon nanofibers

∗ **S. Lim *et al.*, *J. Phys. Chem. B* 108 (2004) 1533.**

TEM images of PCNFs with well-defined surfaces

PCNF : Edge

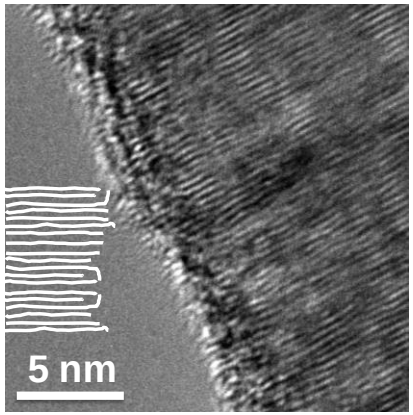

PCNF-G : Basal

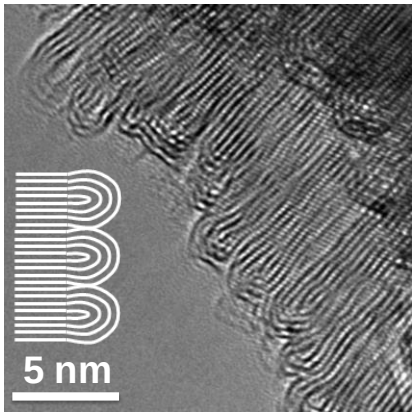

PCNF-G-NA : Edge

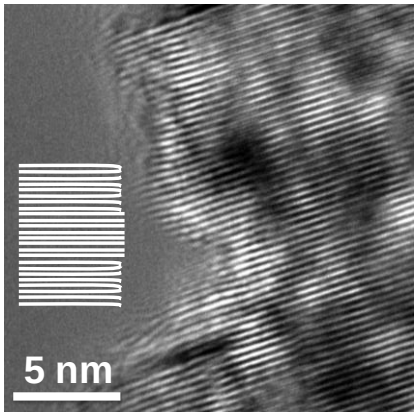

PCNF-B-G : Basal

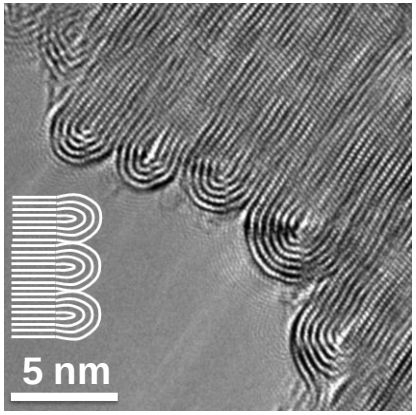

PCNF-B-G-NA : Edge

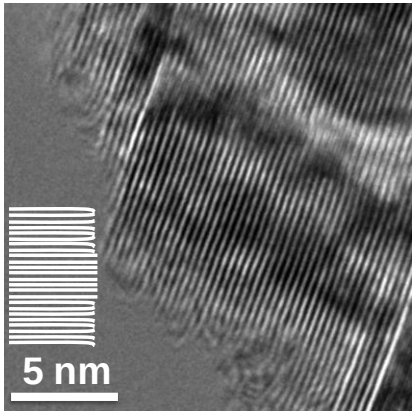

Effect of edge and basal surfaces on the SEI formation

< First cycle >

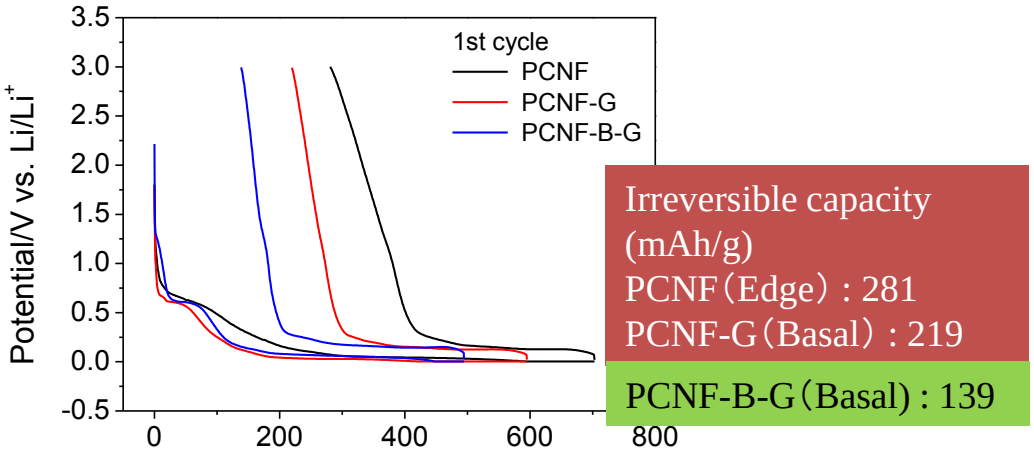

Irreversible capacity (mAh/g)
PCNF（Edge）: 281
PCNF-G（Basal）: 219

PCNF-B-G（Basal）: 139

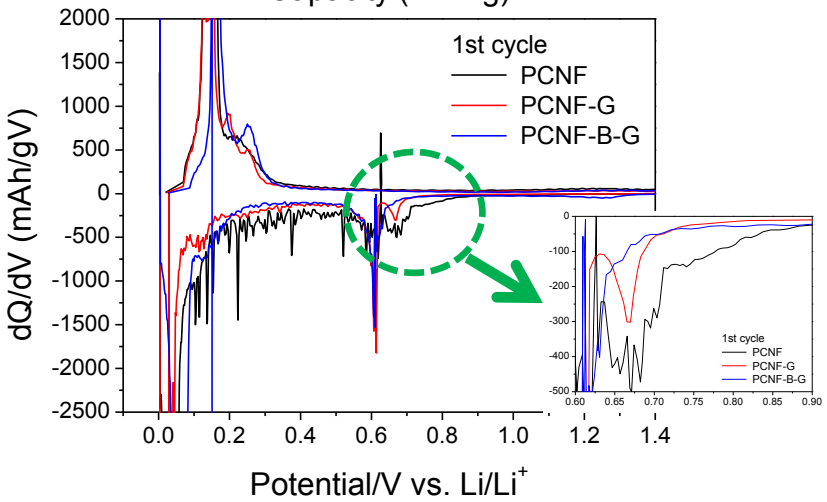

< Second cycle >

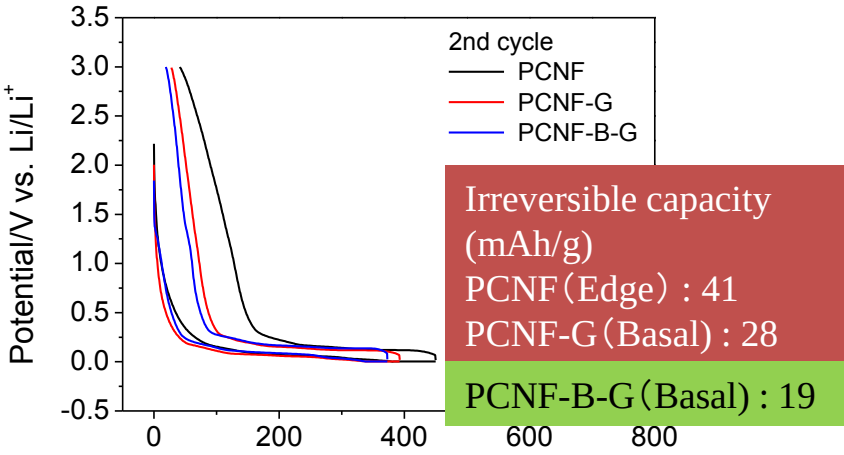

Irreversible capacity (mAh/g)
PCNF（Edge）: 41
PCNF-G（Basal）: 28

PCNF-B-G（Basal）: 19

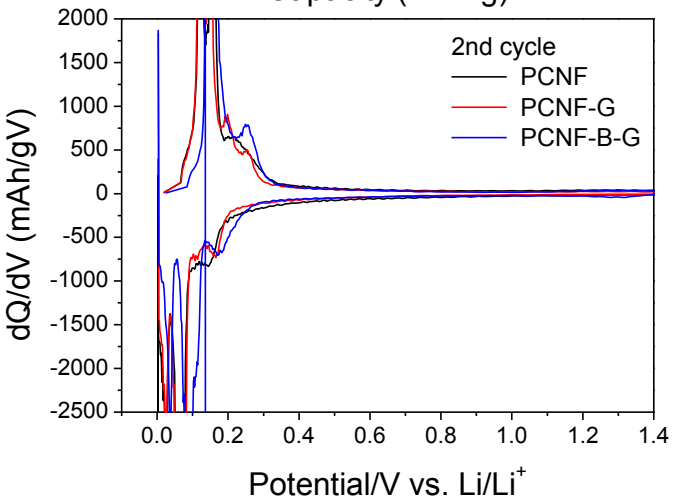

Electrolyte：1 M $LiClO_4$ in EC/DEC (1:1 vol%)、Binder：PVDF

Effect of edge and basal surfaces on the SEI formation

PCNF : Edge

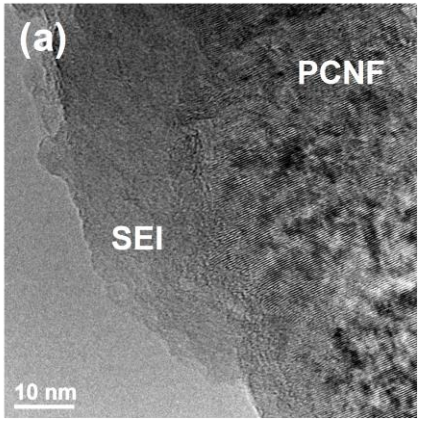

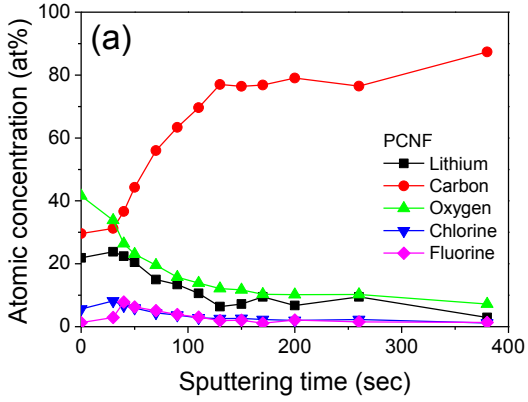

PCNF-G : Basal

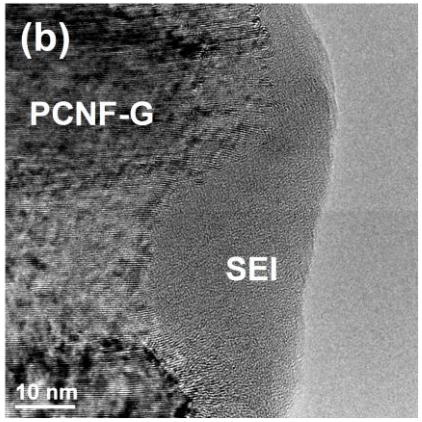

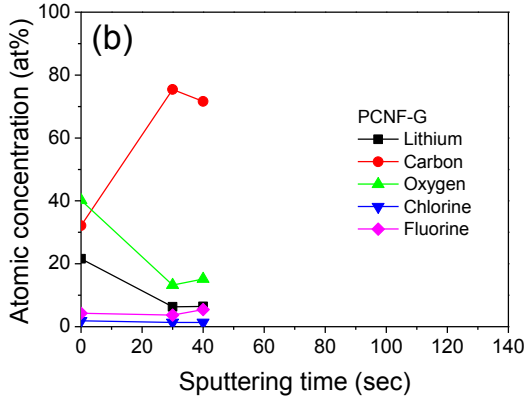

PCNF-B-G : Basal

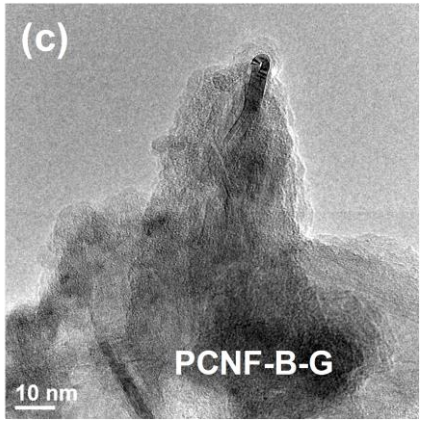

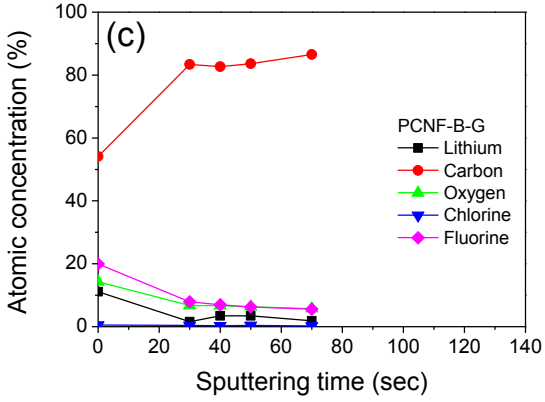

The XPS depth profiles indicated that the SEI of PCNF with edge surfaces was four times thicker than those of PCNF-G and PCNF-B-G with basal surfaces.

Effect of boron doping on the SEI formation

< First cycle >

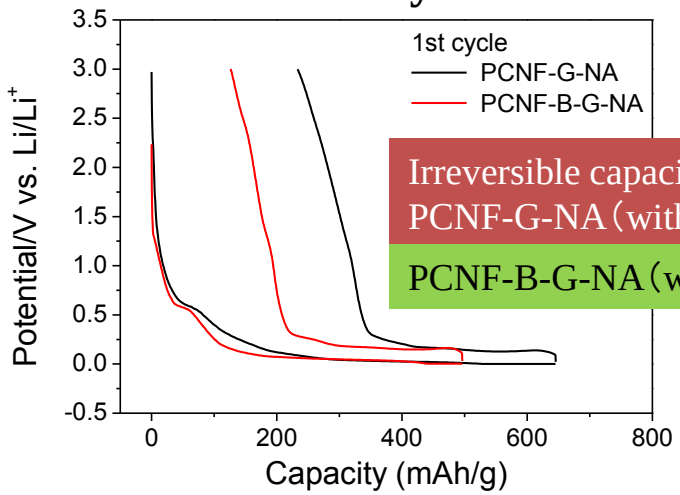

Irreversible capacity (mAh/g)
PCNF-G-NA（without boron）: 234

PCNF-B-G-NA（with boron）: 126

< Second cycle >

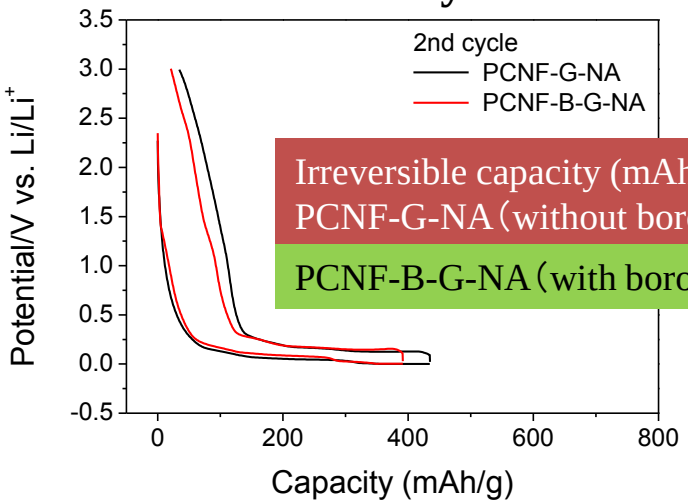

Irreversible capacity (mAh/g)
PCNF-G-NA（without boron）: 34

PCNF-B-G-NA（with boron）: 21

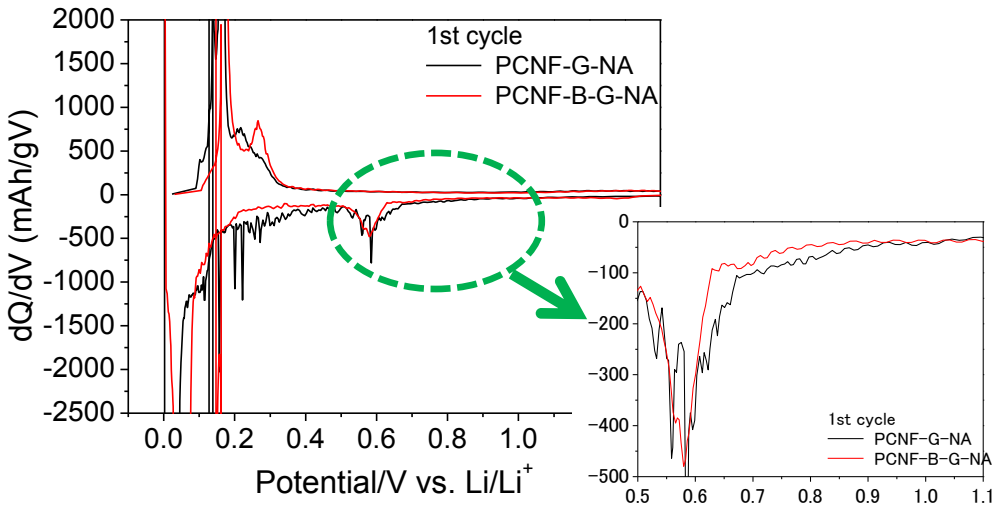

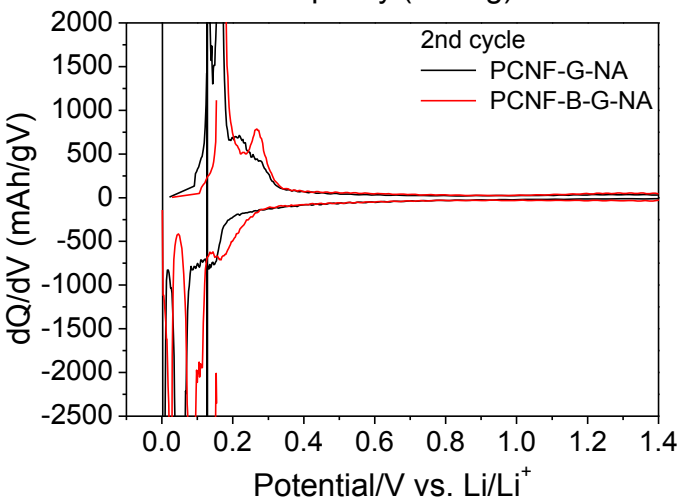

Effect of boron doping on the SEI formation

PCNF-G-NA : Edge

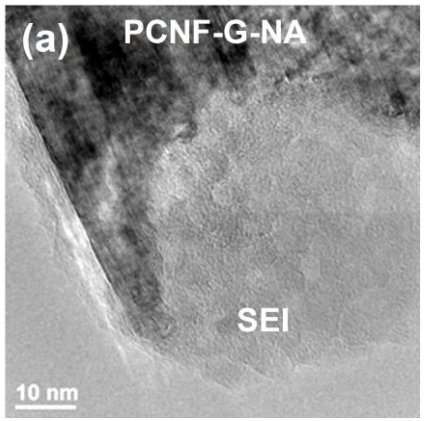

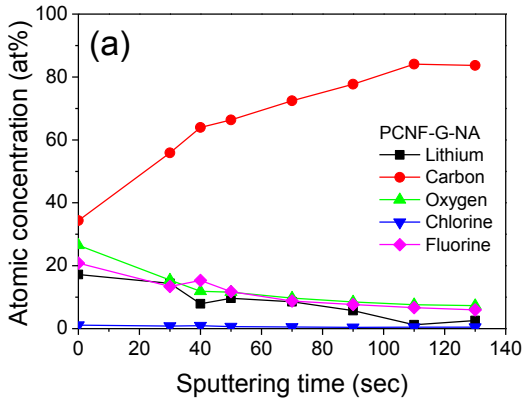

PCNF-B-G-NA : Edge

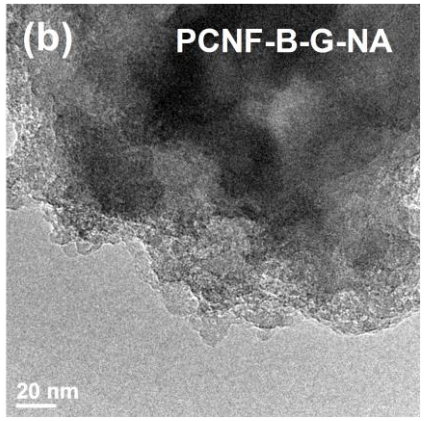

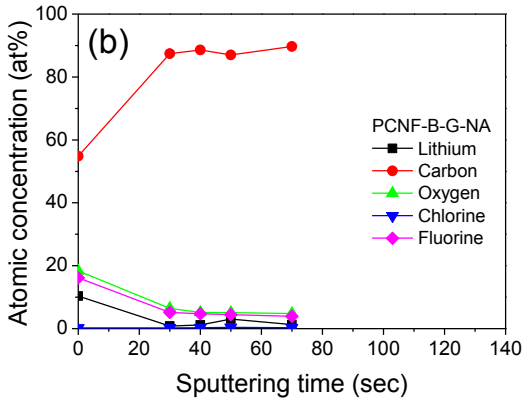

The SEI of PCNF-G-NA without boron doping was three times thicker than that of PCNF-B-G-NA with boron doping.

Explosion accident of Li-ion battery for EV (GM) 2012,04,12

GM Worker Injured After Lithium-Ion Battery Explodes